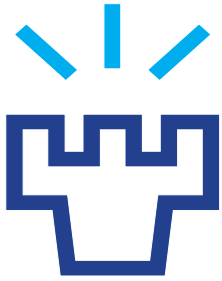

OULUN YLIOPISTO

FACULTY OF TECHNOLOGY

GEOCHEMISTRY AND MINERALOGY OF THE FELSIC PORPHYRIES AT HANHIMAA, KITTILÄ IN THE CENTRAL LAPLAND BELT, NORTHERN FINLAND

Viivi Ohvo

DEGREE PROGRAMME IN GEOSCIENCES

Master's Thesis

March 2020

ABSTRACT

FOR THESIS University of Oulu Faculty of Technology

Degree Programme (Bachelor's Thesis, Master's Thesis)	Major Subject (Licentiate Thesis)
Degree Programme in Geosciences	
Author	**Thesis Supervisor**
Ohvo, Viivi Henriikka	Ranta, J-P., PhD

Title of Thesis

Geochemistry and mineralogy of the felsic porphyries at Hanhimaa in the Central Lapland belt, Kittilä, northern Finland

Major Subject	Type of Thesis	Submission Date	Number of Pages
Geology and mineralogy	Master's Thesis	11.3.2020	54 p., 5 app.

Abstract

Several small gold occurrences are identified along the Hanhimaa shear zone, located in the Central Lapland belt, northern Finland. Gold occurrence are hosted by the mafic volcanites of the Kittilä suite. In addition, felsic porphyric rocks are common within these occurrences. However, their association to the gold mineralisation is not known.

In this thesis, petrography and geochemistry of the felsic porphyritic rocks occurring in the gold occurrences are used to characterize them and compare them appearance to the other known felsic porphyries within the Central Lapland belt.

55 samples are collected from the drill cores, representing eight exploration targets: Lisma, Kellolaki, Kiimalaki, Siskeli, Väli-Kiima, Kiimakuusikko, Kousa and Kapsa. Three of them; Kellolaki, Kiimalaki and Kiimakuusikko are identified gold mineralisation hosted by the Kittilä suite mafic volcanic rocks along the Hanhimaa shear zone. The rest are early stage exploration targets and cannot be called as gold occurrences at this stage. Methods used are geochemical whole rock assay, microscopical study of thin sections and electron microprobe study of selected, representative thin sections.

Results show that the felsic porphyries are ranging from rhyolitic to andesitic in composition. Based their textures in drill cores, petrographical studies and geochemical characteristics, they can be divided into the known felsic porphyry types, the Veikasenmaa (2.02-2.01 Ga) and the Nyssäkoski type (1.92 Ga). Locally, elevated gold is found from the felsic porphyric rocks belonging to the younger, Nyssäkoski type. This type is known to host gold in other occurrences within the Kittilä suite. The results may be used as an additional information at the exploration activities ongoing at the Hanhimaa area.

Keywords: orogenic gold, felsic porphyry, Kittilä, Hanhimaa, Central Lapland belt

Additional Information

TIIVISTELMÄ
OPINNÄYTETYÖSTÄ Oulun yliopisto Teknillinen tiedekunta

Koulutusohjelma (kandidaatintyö, diplomityö) Geotieteiden koulutusohjelma		Pääaineopintojen ala (lisensiaatintyö)	
Tekijä Ohvo, Viivi Henriikka		Työn ohjaaja yliopistolla Ranta, J.-P., FT	
Työn nimi Geochemistry and mineralogy of the felsic porphyries at Hanhimaa in the Central Lapland belt, Kittilä, northern Finland			
Opintosuunta Geologia ja mineralogia	Työn laji Pro Gradu	Aika Maaliskuu 2020	Sivumäärä 54 s., 5 liitettä

Tiivistelmä

Keski-Lapin vyöhykkeeltä, Kittilän alueelta Hanhimaan hiertovyöhykkeeltä tunnetaan useita kultaesiintymiä. Nämä esiintymät sijoittuvat geologisesti Kittilän sviitin mafisiin metavulkaniitteihin, joiden yhteydessä esiintyy kahdenikäisiä felsisiä porfyyrejä. Porfyyrien ja kultaesiintymien yhteyttä ei ole juurikaan tutkittu.

Tämän tutkimuksen tarkoituksena on selvittää Hanhimaan alueen felsisten porfyyrien mineralogiaa ja geokemiallista koostumusta ja vertailla niitä Kittilän sviitin tunnettuihin porfyyriyksiköihin, sekä selvittää mahdollista yhteyttä kultaesiintymiin.

55 näytettä kerättiin pääasiassa kairasydämistä; jotka edustavat kahdeksaa malminetsintäkohdetta; Lisma, Kellolaki, Kiimalaki, Siskeli, Väli-Kiima, Kiimakuusikko, Kousa sekä Kapsa. Kolme mainituista kohteista; Kellolaki, Kiimalaki ja Kiimakuusikko ovat tunnettuja kultamineralisaatioita Hanhimaan hiertovyöhykkeen läheisyydessä. Tutkimuksen menetelminä käytettiin kokokivigeokemiaa, mikroskooppitutkimuksia sekä elektronimikroanalysaattoria.

Tulosten perusteella felsisten porfyyrien geokemiallinen koostumus vaihtelee ryoliittisesta andesiittiseen. Kairasydännäytteiden ulkoasuun, petrografiaan ja geokemialliseen analyysiin perustuen porfyyrit voidaan jakaa kahteen ennalta tunnettuun ryhmään; Veikasenmaan porfyyrityyppiin (2.02-2.01 Ga) sekä Nyssäkosken porfyyrityyppiin (1.92 Ga). Kohonneita kultapitoisuuksia on löydetty nuorempaan Nyssäkosken tyyppiin kuuluvista porfyyreistä, jonka tiedetään olevan kultapitoisia muissa Kittilän sviitin kultaesiintymissä. Tutkimuksen tuloksia voidaan hyödyntää alueelle kohdistuvassa malminetsinnässä.

Asiasanat: orogeeniset kultamalmit, felsiset porfyyrit, Kittilä, Hanhimaa, Keski-Lapin vyöhyke

Muita tietoja

APPENDICES

APPENDIX 1. Thin section description

APPENDIX 2. Whole-rock Major- and trace element analyses

APPENDIX 3. Detection limits of whole-rock Major- and trace element analyses

APPENDIX 4. EPMA results

APPENDIX 5. EPMA standards

1. INTRODUCTION

The relationship of gold and felsic porphyric rocks in the Precambrian greenstone belts has been studied around the world (e.g. Groves et al. 2018; Goldfarb et al. 2005). Examples of rigid granitic bodies hosted by more ductile volcano-sedimentary sequence and related gold deposit can be found in greenstone belts worldwide e.g. Barberton, South Africa and Quadrilatero Ferrifrero, Brazil and in the Central Lapland belt, northern Finland (Groves et al. 2018). The suitability of such boundary zones for hosting gold deposits are due to the competence differences during deformation (Groves et al. 2018). This competence difference creates a pathways for gold-bearing hydrothermal fluids. According to Groves et al. (2018), any pre-existing structure may be mineralized. Groves et al. (2018) concluded that in orogenic gold exploration, the structural geometry seem to be more important parameter than structural history.

The Central Lapland belt is one of the exploration hotspots in Finland. There is more than 60 drilling-indicated gold occurrences in the greenstone belts of northern Finland, and 36 of these are located in the Central Lapland belt (Eilu 2007). The largest discovered deposit is the Suurikuusikko gold deposit, being the largest known gold deposit in Europe with proven and probable reserves of 4.4 million ounces gold in December 2018 (30,5 Mt at 4.50 g/t Au) (Agnico Eagle Mines Ltd.). It is hosted by the Kittilä suite metavolcanic rocks along the Kiistala shear zone (KSZ; Wyche et al. 2015). In addition, along the same structure, gold occurrences are closely associated with felsic porphyric rocks (e.g. Molnár et al., 2018)

This study focuses on the felsic porphyries located along one of the adjacent and parallel shear zone to KSZ, the Hanhimaa shear zone (HSZ). Currently, at least three gold occurrences have been identified related to the HSZ; Kiimakuusikko, Kiimalaki and Kellolaki. In addition to the known gold occurrence, five exploration target areas, Lisma, Siskeli, Väli-Kiima, Kousa and Kapsa, are included in this study (See Fig. 1 and Fig 7. for sample locations). Felsic porphyries are present in these areas, but their relationship to the gold has not been studied. The purpose of the study is to define geochemical composition and mineralogy of the felsic porphyry rocks in HSZ and their possible relationship to the gold mineralisation in the area.

The study area is located at Hanhimaa, in the municipality of Kittilä, northern Finland. The area is approximately 200 km^2 wide, located on the northeastern side of the Hanhimaa village (Fig. 1).

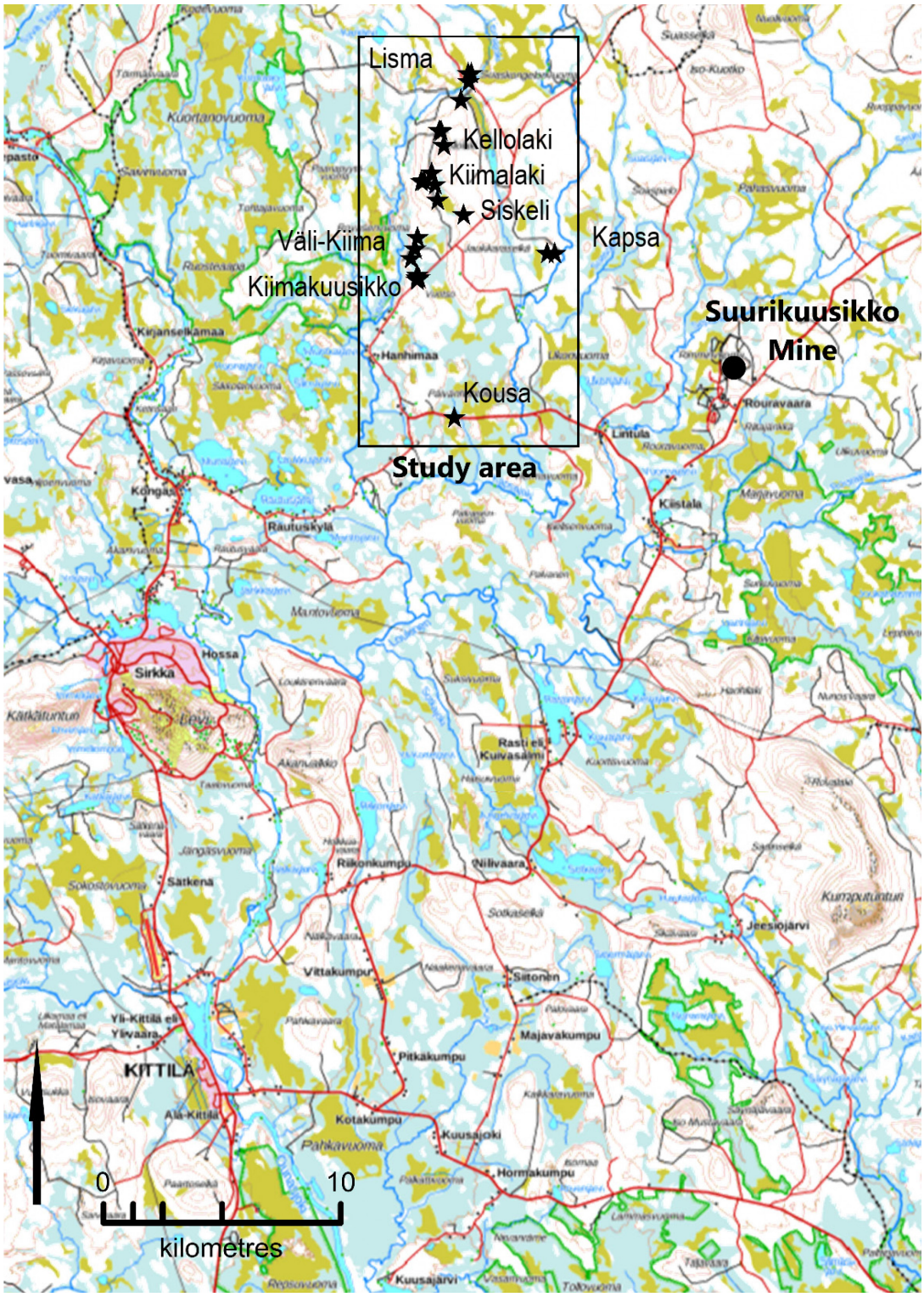

Figure 1. Location of the study area and sampling locations in Hanhimaa, Kittilä. Base map National Land Survey of Finland.

2. CLASSIFICATION OF FELSIC VOLCANIC ROCKS

Le Maitre (2002) defines volcanic rocks as igneous rocks with an aphanitic (grain size >1 mm) texture, as a result of a rapid cooling process. Felsic volcanic extrusive rocks are light-coloured, high-silica and low-specific gravity rocks, classified by their chemical composition and mineralogy; geochemically they are divided to rhyolites (SiO_2 ≤70 wt.%) and dacites (63-70 wt.%). The main distinctive feature between rhyolite and dacite is the ratio of plagioclase and alkali feldspar; rhyolites contain more alkali feldspars than plagioclase, and dacites have more plagioclase than alkali feldspar (Gill 2010). In addition to the felsic volcanic rock, the intermediate volcanic rock are named as andesite and has SiO_2 content of 52-63 wt.% (Haldar & Tisljar 2013). The formation of rhyolites and dacites is rather similar, and andesites follow the same process as well, but mix with surrounding mafic materials to form intermediate rocks (Frost & Frost 2014). Typical to felsic extrusive rocks is that they experience at least two-staged crystallisation, where single large crystals create phenocrysts in a aphanitic or even vitreous matrix, as a result of sudden cooling and solidification of the lava (Haldar & Tisljar 2013).

For classification of volcanic rocks, Le Maitre (2002) recommends the use of QAPF diagram (Fig. 2) if the modal mineralogy of the sample can be determined, and the TAS (total alkali silica) diagram (Fig. 2) if the modal mineralogy is not applicable and a geochemical analysis is available. They also point out that possible weathering and alteration of a volcanic rock may affect the results in geochemistry-based TAS diagram.

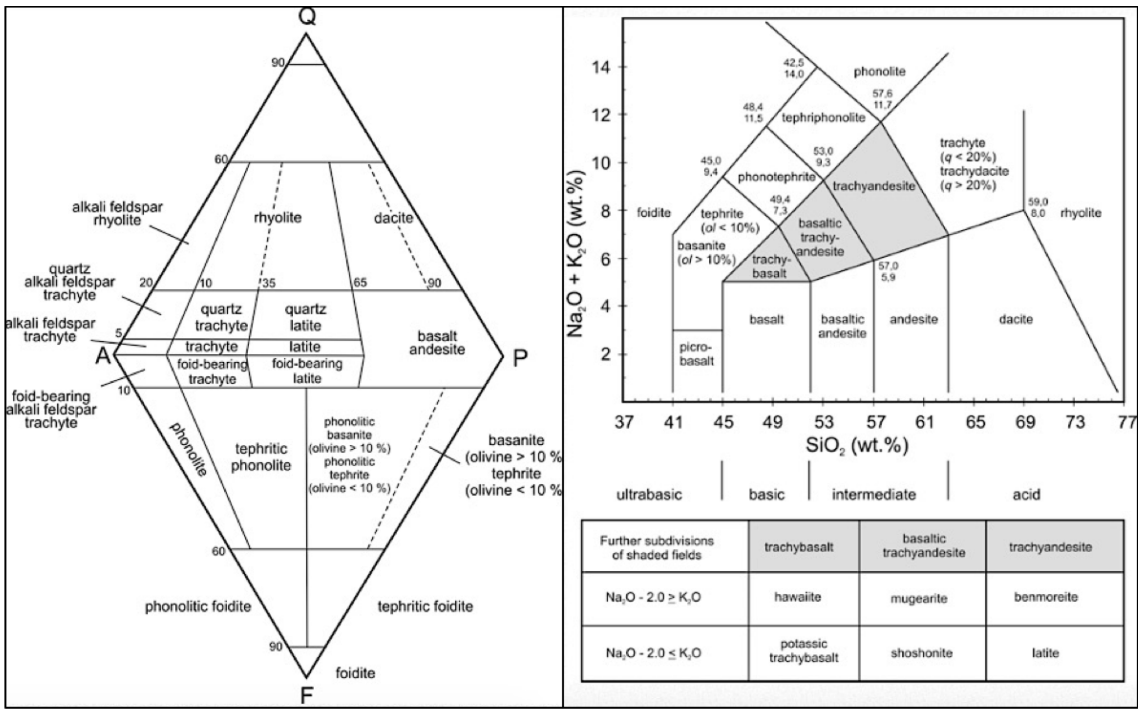

Figure 2. On left the QAPF diagram where Q=quartz, A=alkali feldspar, P=plagioclase, F=foids. (Le Maitre 2002 after Streckeisen 1978). On right the Total Alkali Silica (TAS) diagram (Le Maitre 2002 after Le Bas et al. 1986).

The Jensen Cation Plot (Fig. 3) is a method to discriminate the calc-alkalic and tholeiitic volcanic rocks based on FeO-Fe_2O_3-TiO_2, Al_2O_3 and MgO. The diagram is usable in metamorphosed rocks due to the stability of the elements plotted in lower metamorphosis conditions, where alteration processes may affect alkali, calcium and silica amounts (Jensen 1976; Rollinson 1993).

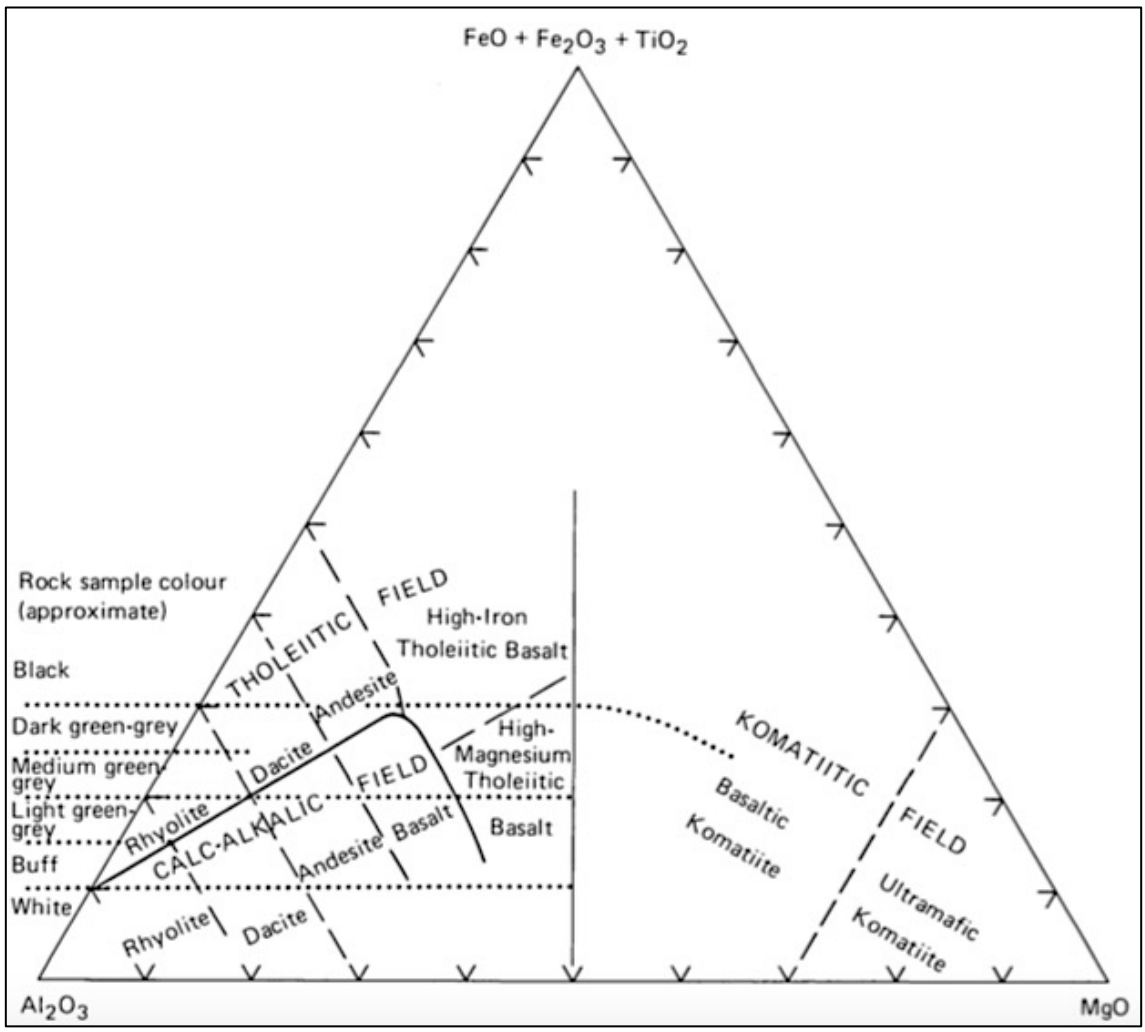

Figure 3. The Jensen Cation Plot with approximated colours in unaltered hand samples (Jensen 1976).

Mineralogically, rhyolite contains alkali feldspar, quartz and sodic plagioclase as main minerals, with possible accessory hornblende, biotite and pyroxene. Distinctive feature of rhyolite is glassy matrix, where individual minerals cannot be distinguished microscopically (Gill 2010). The colour of a rhyolite in hand sample varies greatly due to the glassy structure, even making them untypically dark to be highly felsic in geochemical composition. Rhyolite favours porphyric structure, which indicates first stage slow cooling and formation of phenocrysts, followed by second stage fast cooling of the rest of the melt leading to glassy matrix (Frost & Frost 2014). Rhyolite often contains sanidine as feldspar phenocryst (Gill 2010).

Dacite is light colored rock and is comprised of sodic plagioclase, quartz and alkali feldspar, and may contain hornblende, biotite, pyroxene and rarely garnet. Similar to rhyolite, dacite also favours porphyric texture indicating at least two-staged crystallisation, with abundant quartz and feldspar phenocrysts in microcrystalline matrix

(Gill 2010). Also oscillatory zonation texture in plagioclase phenocrysts is a typical feature of dacite (Gill 2010).

Andesite is an intermediate extrusive volcanic rock often presenting porphyric texture, where phenocrysts comprise of Na-Ca –plagioclases and hornblende; differing from rhyolite and dacite by containing at least one mafic mineral (Haldar & Tisljar 2013).

Hydrothermal alteration may affect the mineralogy and chemistry of the volcanites. One way to define hydrothermal alteration, is the use whole rock geochemical data in Molar Element Ratio diagrams (MER; Stanley 2017). The MER data evaluation is an useful tool when studying felsic porphyries, because it is able to discriminate specific alteration related differences between rhyolites, dacites and andesites with no distinguishable differences in hand samples or in microscopical view (Stanley 2017). Used parameters on MER diagrams are mobile elements Na, K, Ca and Si, and the relatively immobile Al is used as common denominator (Davies & Whitehead 2006). Generally, hydrothermal alteration leads to strong depletion of Na, and complete loss of K in rhyolites, when the alteration is pervasive (Davies & Whitehead 2006). In MER diagrams the mobility of Na, K and possible Mg is revealed, whereas the relatively immobile Al remains constant (Davies & Whitehead 2006 and references therein).

3. OROGENIC GOLD

Originally introduced by Böhlke (1982) and later defined by Groves (1993) and Groves et al. (1998), orogenic gold deposits are epigenetic, gold-only deposits, formed in orogenic settings from syn- to late-orogenic metamorphic fluids (e.g. Phillips et al. 2010). It is the most common deposit type in metamorphic terranes (Goldfarb et al. 2005). Orogenic gold deposits are formed in accretional and collisional orogenic settings, on the upthrusting continent, where compressional and shear-type deformations dominate (e.g. Groves et al. 1998). The common protoliths include volcanic or sedimentary rocks (Groves et al. 1998). However, host rock can potentially be any metamorphosed rock in the orogenic belt (Goldfarb et al. 2005). Orogenic gold deposits are strongly structurally controlled, with major first order structures acting as a fluid pathways and second- or third order structures representing the precipitation sites for the gold bearing hydrothermal fluids (Groves et al. 2018). These structures are generally faults, fractures and shear zones of brittle and brittle-ductile characters, in which orogenic gold favours the latter (Pirajno 2009).

Goldfarb and Groves (2015) summarize after Gebre-Mariam et al. (1995), Groves et al. (1998) and Goldfarb et al. (2001, 2005) five common features of orogenic gold deposits throughout the geological timescale. The features are 1) very late to post-peak metamorphic timing, 2) location in the metamorphosed fore-arc or back-arc setting, 3) forming in wide thermal equilibrium with country rocks containing typical alteration assemblages, and equivalent wall rocks, without telescoped zonation typical to deposits formed under higher geothermal gradients, 4) hydrothermal source of K, S, CO_2, H_2O, Si and Au, with variable elements As, B, Bi, Na, Sb, Te and W, yet low base metal content, and 5) supralithostatic H_2O-CO_2-CH_4-N_2-H_2S –solution, low to moderate salinity fluids, possibly phase separated in advection flow and gold deposition.

The crustal continuum model was presented by Groves (1993) and Groves et al. (1998), which defines the orogenic gold deposits to be formed in wide ranges of depths between 2 to 20 kilometres, divided into epizonal (2-6 km), mesozonal (6-12) and hypozonal (12-20 km) regimes with different types of metal associations reflecting the temperature and depth of deposit formation. Phillips & Powell (2009) reviewed and updated the continuum model (Fig. 4) with consideration of hydrothermal alteration related to orogenic gold deposits and orogenic gold deposits of amphibolite and granulite facies;

the original model of Groves (1993) and Groves et al. (1998) was based on studies of the greenschist facies orogenic gold deposits only.

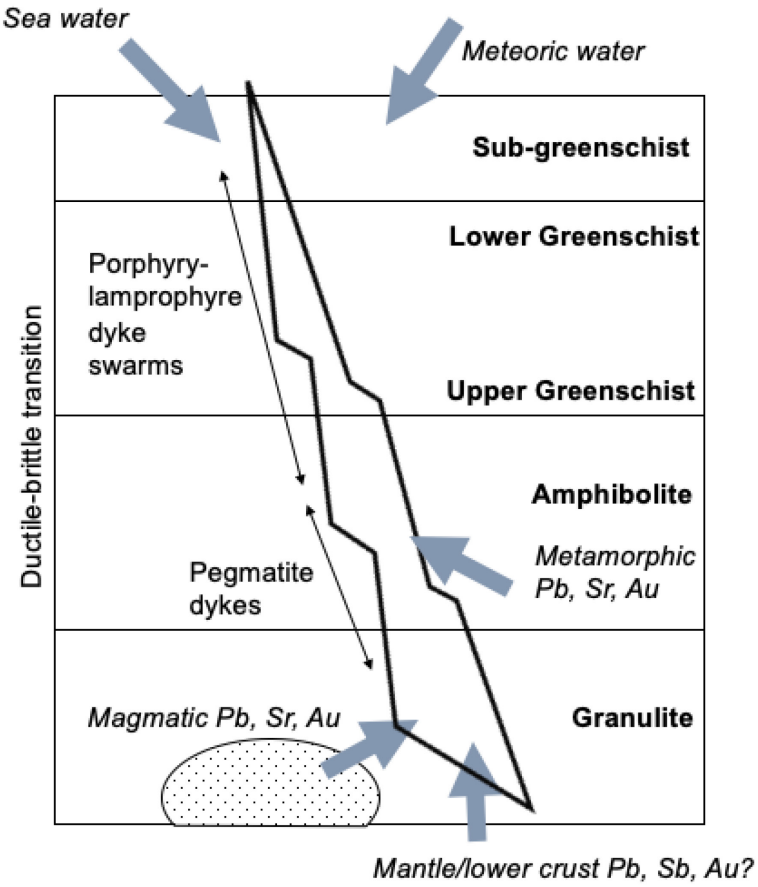

Figure 4. Crustal continuum -model, modified after Groves (1993), Phillips & Powell (2009) and Goldfarb & Groves (2015).

In terms of age, the orogenic gold deposits vary from mid-Archean to Tertiary (e.g. Goldfarb et al. 1998; Goldfarb et al. 2001; McCuaig & Kerrich 1998; Groves et al. 2018). Major part of the known orogenic gold deposits in the Precambrian have formed during late Archean between 2.8-2.55 Ga and during Paleoproterozoic between 2.1-1.8 Ga (Goldfarb et al. 2001). The formation of orogenic gold deposits correlates with the supercontinental cycle and the formation of new continental crust (op.cit.).

3.1 Hydrothermal alteration

Orogenic gold deposits display hydrothermal alteration zones, caused by the interaction of hydrothermal fluids with different host rocks at various temperatures. The intensity of alteration depends on various parameters, including composition of the protolith, depth of the mineralisation, pressure and chemical composition of the fluid, size of the deposit and duration of the hydrothermal process (Groves 1993; Eilu et al. 1999; Goldfarb et al. 2005). The hydrothermal alteration is commonly divided into three zones summarized in Table 1; distal alteration zone with weakest mineral alteration, intermediate alteration zone and intensively altered proximal alteration zone hosting the gold (e.g. Groves 1993, Eilu et al. 1999). In the greenschist facies conditions, the width of alteration haloes varies greatly from few centimetres up to kilometres, regulated by multiple parameters such as host rock type, structural bedding, metamorphic grade, permeability and porosity (Goldfarb et al. 2005). The proximal alteration zone is less than 50 meters wide, whereas the intermediate zone may reach up to 100 metres from the gold mineralisation, and the weakest alteration in distal zone can be as much as two kilometres (Goldfarb et al. 2005, Eilu et al. 1999).

General alteration assemblages in greenschist facies orogenic gold deposits include carbonates, sulphides, albite, muscovite, chlorite, feldspar, biotite and tourmaline, with an exception of high-temperature systems with skarn alteration assemblages (Goldfarb et al. 2005). In Table 1, typical alteration mineral assemblages for each alteration zones and the respective sulphides are presented as an example in lower and mid-greenschist facies metamorphic rocks. When progressing towards upper greenschist and lower amphibolite facies rocks, the main differences are occurrence of biotite over white micas and pyrrhotite occurring as abundant sulphide instead of pyrite (Goldfarb et al. 2005). Also, the width of the alteration halo narrows down to maximum of 10 metres (Eilu et al. 1999).

Table 1. Essential features of hydrothermal alteration zones in greenschist facies orogenic gold deposits after Goldfarb et al. 2005; Eilu et al. 1999.

	Alteration assemblage	Identifying features
Distal zone (1 mm to 2 km)	Chlorite + calcite + quartz ± albite ± rutile ± epidote	Abundance of quartz-calcite veins
Intermediate zone (1 mm to 100 m)	Calcite + dolomite/ankerite + chlorite + quartz + albite + rutile	
Proximal zone (1 mm to 50 m)	Dolomite/ankerite + quartz + muscovite ± paragonite ± albite	Strong bleaching, occurrence of sulphides

3.2 Precipitation of gold

Depending on the pressure and temperature conditions, mineralisation styles in orogenic gold deposits vary from disseminated gold in ductile shear zones to brittle stockworks and breccia in more shallow crustal settings (e.g. Groves et al. 1998; Goldfarb et al., 2005). Orogenic deposits have repetitive features such as location in major structures as faults and shear zones acting as fluid flow channels, but also the oblique fault arrays occurring at the second- or third-order structures, intersecting the first-order structures, are important to accommodate the strike changes within to create locations for gold precipitation (Groves et al. 2018). Precipitation is a result of multiple processes responsible of gold to precipitate from the hydrothermal solution. The fluid-wall rock reaction is the most prevailing precipitation mechanism where the mineralisation is disseminated or replacement style, whereas the quartz-vein hosted gold mineralisation are most likely precipitated as a reason of pressure fluctuation (Goldfarb et al. 2005). In high-arsenopyrite gold mineralisation types it is proposed that the dissolution reaction of the sulphide grains can generate a local redox trap, which can be effective in extracting gold from hydrothermal fluid and precipitating it along grain boundaries and fractures of arsenopyrite (Pokrovski et al. 2002).

The common ore minerals in orogenic gold deposits are pyrite, arsenopyrite, pyrrhotite, chalcopyrite, galena and sphalerite, which are either closely associated to gold or the host minerals in the mineral lattice as refractory gold (Groves et al. 1998). Depending on the origin and metamorphic grade of the host rock, generally the sulphide mineral assemblage varies from arsenopyrite in metasedimentary rocks to pyrite and pyrrhotite in greenschist- and amphibolite facies metavolcanites (Groves et al. 1998; Goldfarb et al. 2005). Stibnite is a common sulphide phase formed in late stage of the paragenesis of the deposit (Goldfarb et al. 2005).

4. GEOLOGICAL SETTING

4.1. Central Lapland belt

The Central Lapland belt (CLB; Fig. 5) (Köykkä et al. 2019), formerly known as the Central Lapland Greenstone Belt (CLGB) (Lehtonen et al. 1998; Hanski & Huhma 2005; Luukas et al. 2017) represents a Paleoproterozoic greenstone belt, located at northern Finland, reaching from Norway through Finland to northern Russia (Hanski & Huhma 2005). The is CLB divided into seven lithostratigraphic and lithodemic units deposited on top of the Archean basement (Fig. 6). The area is generally metamorphosed under upper greenschist facies (Hölttä et al. 2007).

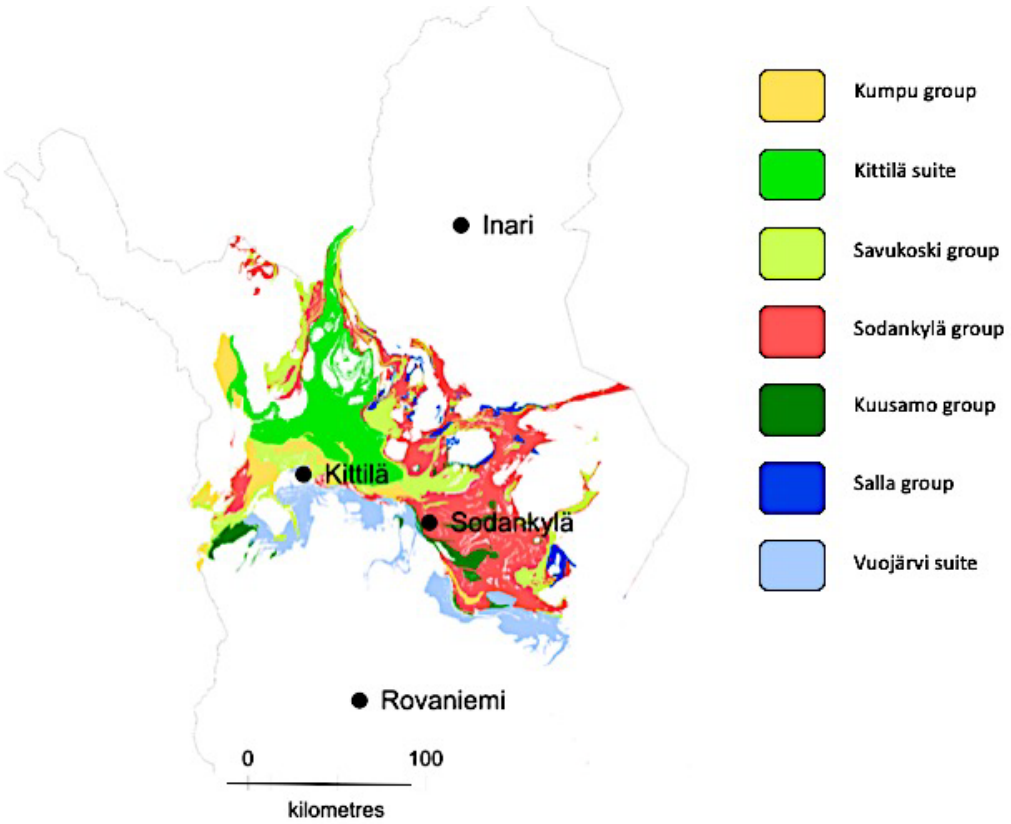

Figure 5. Geology of the Central Lapland belt in Finnish Lapland (modified after the DigiKP version 2.1. Base map National Land Survey of Finland)

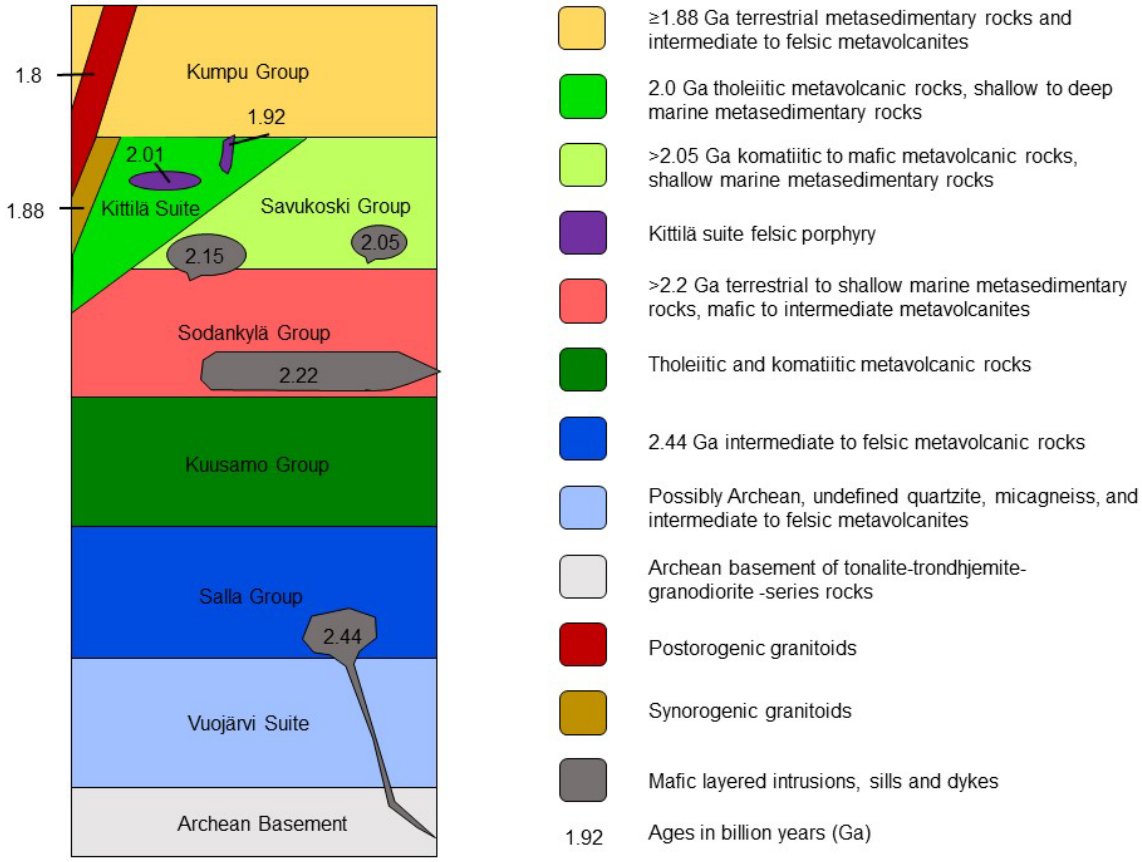

Figure 6. Lithostratigraphic and lithodemic units of Central Lapland belt (modified after Lehtonen et al. 1998; Niiranen et al. 2015 and Huhma et al. 2018).

4.1.1 Vuojärvi suite

The Vuojärvi suite quartzites, mica gneisses and intermediate to felsic metavolcanites are found only on the southern side of the CLB, in the margin to the bordering Central Lapland granitoid complex (Niiranen et al. 2015; Konnunaho et al. 2015). It is deposited on top of the Archean basement of tonalite-trondhjemite-granodiorite (TTG) –series rocks and proposed to be Neoarchean in age (Niiranen et al. 2015; Luukas et al. 2017).

4.1.2 Salla group

The Salla group consists of intermediate to felsic metavolcanic rocks, being the oldest and lowermost Paleoproterozoic unit of the CLB (Hanski & Huhma 2005). The rocks of the Salla group are divided into three formations; the type formation Rookkiaapa and formations Lohijoki and Kuortisaapa (Lehtonen et al. 1998). These formations comprise mainly of amygdaloidal andesites and dacites, with rhyolitic tuffs and agglomerates (Lehtonen et al. 1998; Hanski & Huhma 2005). Geographically the Salla group is exposed in the southeastern part of the CLB, with extensions to the Russian side of the national border (Hanski & Huhma 2005).

4.1.3 Kuusamo group

Previously named as Onkamo group, The Kuusamo group (Luukas et al. 2017) rocks are widely, but discontinuously distributed in the CLB in type formation of Möykkelmä in Sodankylä, as well as formations of Vajukoski, Keinoselkä, Vuollosvaara and Vaalajärvi in Sodankylä, Kaukonen formation in Kittilä, Nivunkijärvi formation in Muonio and Sahmisto formation in Pulju area (Lehtonen et al. 1998). The Kuusamo group rocks are mainly metavolcanites with tholeiitic and komatiitic composition. Basaltic andesites and andesites belong to the Kuusamo group rocks, being more primitive and variable in composition than the Salla group rocks due to interaction with the sialic crust and late hydrothermal processes (Lehtonen et al. 1998; Hanski & Huhma 2005).

4.1.4 Sodankylä group

The Sodankylä group consists of thick sedimentary sequence of quartzites, mica schists, dolomites and conglomerates deposited on a more stable environment after the active volcanism resulting in formation of Kuusamo group (Hanski & Huhma 2005; Niiranen et al. 2015). It is widely spread and well-exposed in the central Lapland area, forming several fell sequences in the western and southern areas (Lehtonen et al. 1998). The Sodankylä group metasediments comprise of major orthoquartzites, sericite quartzites and mica schists with minor carbonatites and mafic metavolcanites (Hanski & Huhma 2005). The metavolcanic rocks of Sodankylä group are mainly amygdaloidal, tholeiitic basalts and basaltic andesites.

The Sodankylä group is divided in two type formations by Lehtonen et al. (1998); Honkavaara formation consists of albitised metasedimentary rocks, mainly quartzite, siltstone and paraschists (Köykkä et al. 2019), and metavolcanites from felsic to mafic composition in formations of Vaalajärvi, Eksymäselkä, Hormakumpu and Vähäoja. The second type formation is the Virttiövaara formation, comprising of quartzites, mica schists and gneisses (Lehtonen et al. 1998; Hanski & Huhma 2005).

4.1.5 Savukoski group

The Savukoski group is a widely spread member of the CLB, comprising of fine-grained metasedimentary rocks and tholeiitic, komatiitic and picritic mafic metavolcanites (Lehtonen et al. 1998). Niiranen et al. (2015) suggest that the stage of the depositional basin has grown deeper in the formation of Savukoski group to form the fine-grained sedimentary rocks, followed by rifting of the basin and formation of volcanites and abundant mafic intrusions. The Savukoski group is divided to four type formations; Sattasvaara formation of komatiitic volcanites, Sotkaselkä formation of picritic volcanites, Linkupalo formation of iron-tholeiitic volcanites and Matarakoski formation of metasedimentary rocks including phyllite, black schist, dolomite, tuff and banded iron formations (Lehtonen et al. 1998; Köykkä et al. 2019). Savukoski group is in tectonic contact to Kittilä suite (Lehtonen et al. 1998), but has no proven discordance to the underlying Sodankylä group, expressing gradual deepening of the basin (Hanski & Huhma 2005).

4.1.6 Kittilä suite

The Kittilä group has been regarded as lithodemic and allochtonous unit (Hanski & Huhma 2005; Luukas et al. 2017; Köykkä et al. 2019). It consists mainly of mafic metavolcanic rocks with various types of sedimentary rocks. Lehtonen et al. (1998) divided the Kittilä group into four lithostratigraphic type formations: Vesmajärvi-, Kautoselkä-, Pyhäjärvi- and Porkonen formations. The Vesmajärvi formation consists of Mg-tholeiitic volcanic rocks, while the Kautoselkä formation is Fe-tholeiitic volcanic rocks (Hanski & Huhma 2005). Vesmajärvi and Kautoselkä formations do not originate from the same parental magma based on differences in their chemical compositions (Lehtonen et al. 1998). The Porkonen formation, which is thought to be located between Vesmajärvi and Kautoselkä formations, is comprised of banded iron formations and Fe-carbonate schists. The uppermost Pyhäjärvi formation comprises of mica schists and greywackes. In addition, these four type formations are divided to minor formations as presented on Table 2.

Table 2. Formations of Kittilä suite. Age data from Lehtonen et al. 1998.

Type formation	Lithology	Formations
Pyhäjärvi ~ 2.012 Ga	Micaschists, greywackes	Kirjaselkä
Vesmajärvi ~ 2.012 Ga	Mg-tholeiites	Veikasenmaa, Köngäs, Pokka, Pälkekero, Pallastunturi
Porkonen ~ 2.012 Ga	BIF, fe-sulphide schists	Suasselkä
Kautoselkä > 2.01 Ga	Fe-tholeiites	Karjakko-oja, Tarvasenvaara, Kulkuvuoma

Lehtonen et al. (1998) stated that the volcanites in the Vesmajärvi formation have greater variance in composition compared to the Kautoselkä formation volcanites, containing komatiites and local felsic metavolcanites and basalts. The Vesmajärvi formation represents the youngest mafic magmatism at the CLB, and the host unit of the Veikasenmaa formation, which comprises of the subvolcanic felsic porphyry. The Veikasenmaa porphyry is considered coeval and comagmatic with the Vesmajärvi formation, although the inner stratigraphy of the formation is poorly known and the age determination is solely based on the Veikasenmaa formation age studies and the stratigraphy of the Kittilä suite (Lehtonen et al. 1998). Despite that there is no specific age determination for Kautoselkä formation, the stratigraphy of the Kittilä suite formations indicates it to be older than the Vesmajärvi formation and its members (Table 2).

Kittilä suite is bordered by the Sodankylä and Savukoski group rocks in the east, and elsewhere by various types of granitoids, including Hetta complex in north, Haaparanta suite in the east and the Central Lapland granite complex in the south (Rastas et al. 2001).

4.1.7 Kumpu group

Kumpu group unifies the former groups of Lainio and Kumpu (Huhma et al. 2018; Hanski & Huhma 2005). The earlier division to Lainio and Kumpu groups in Lehtonen et al. (1998) is explained based on deformation; the Lainio group shows evidence of the

Svecokarelian orogeny, whereas the Kumpu group is lacking those features (Lehtonen et al. 1998).

Comprising of mainly metasedimentary rocks, including arkosites, quartzites, conglomerates and siltstones, with minor metavolcanic rocks with intermediate to felsic geochemical composition, the Kumpu group is the youngest member of CLB and shows stratigraphical disconformity to underlying units (Lehtonen et al. 1998; Hanski & Huhma 2005; Huhma et al. 2018). The type formations are Tuulijoki formation lamprophyric metavolcanites, Latvajärvi formation intermediate-felsic metavolcanites and Ylläs formation quartzites, conglomerates and mica schists, which were previously assigned to the Lainio group, and the Levi formation of quartzites, siltstones and conglomerates (Lehtonen et al. 2018; Hanski & Huhma 2005).

4.2. Felsic porphyry rocks in the Central Lapland belt

In the CLB, felsic porphyritic veins intrude the mafic metavolcanic rocks of the Kittilä suite, Sodankylä group and Savukoski group rocks (Lehtonen et al. 1998). Based on the U-Pb zircon dating, chemical composition and petrographical features, felsic porphyries are divided into two different generations, subvolcanic Veikasenmaa type (2.01-2.02 Ga) and Nyssäkoski type occurring as dykes (1.92 Ga; Rastas et al. 2001; Mikkola 2006). In addition to these two age groups, ca. 1.88 Ga old felsic porphyry veins are found to be cutting the Lainio group rocks (Rastas et al. 2001).

4.2.1 Veikasenmaa type (2.01-2.02 Ga)

These porphyries are geochemically ranging from dacites to rhyolites, and some with andesitic composition due to mixing of felsic and mafic magmas (Lehtonen et al. 1998). The Veikasenmaa type porphyry is determined to be coeval and co-magmatic with the Vesmajärvi and Kautoselkä mafic volcanite formations of the Kittilä suite (Lehtonen et al. 1998, Rastas et al. 2001). Typical mineralogical features of the Veikasenmaa type porphyries are quartz-feldspar-phenocrysts of varying size with groundmass of quartz, albite, and minor carbonates, chlorite, titanite, zircon and opaques (Rastas et al. 2001).

The chondrite normalized REE pattern of Veikasenmaa type are strongly enriched, and contain distinct negative europium anomaly (Rastas et al. 2001, Mikkola 2006). The LREE enrichment shows as 170 to 330 times the chondrite values, and the HREE values as 80-150 times the chondrite values (see Mikkola 2006).

4.2.2 Nyssäkoski type (1.92 Ga)

Geochemically, these quartz-plagioclase porphyries can be classified as dacites (Rastas et al. 2001, Mikkola 2006). Mineralogically, the Nyssäkoski type veins differ from the Veikasenmaa type by containing dark, lineated biotite and amphibole phenocrysts, in addition to quartz and plagioclase (Mikkola 2006). The veins cut the metavolcanites of the Kittilä suite sharply, which also indicates their latter formation in comparison to the host metavolcanites and the Veikasenmaa type porphyry generation (Mikkola 2006). The chondrite normalized REE pattern differ from the Veikasenmaa type veins distinctively with strong enrichment on LREEs in comparison to HREEs, and no distinctive anomalies of certain elements. The REE pattern of Nyssäkoski type is very descendent, showing HREE values only 5-10 times the chondrite values, whereas the LREE values are from 20 to 100 times the chondrite values (Mikkola 2006).

4.3. Geology of the Hanhimaa area

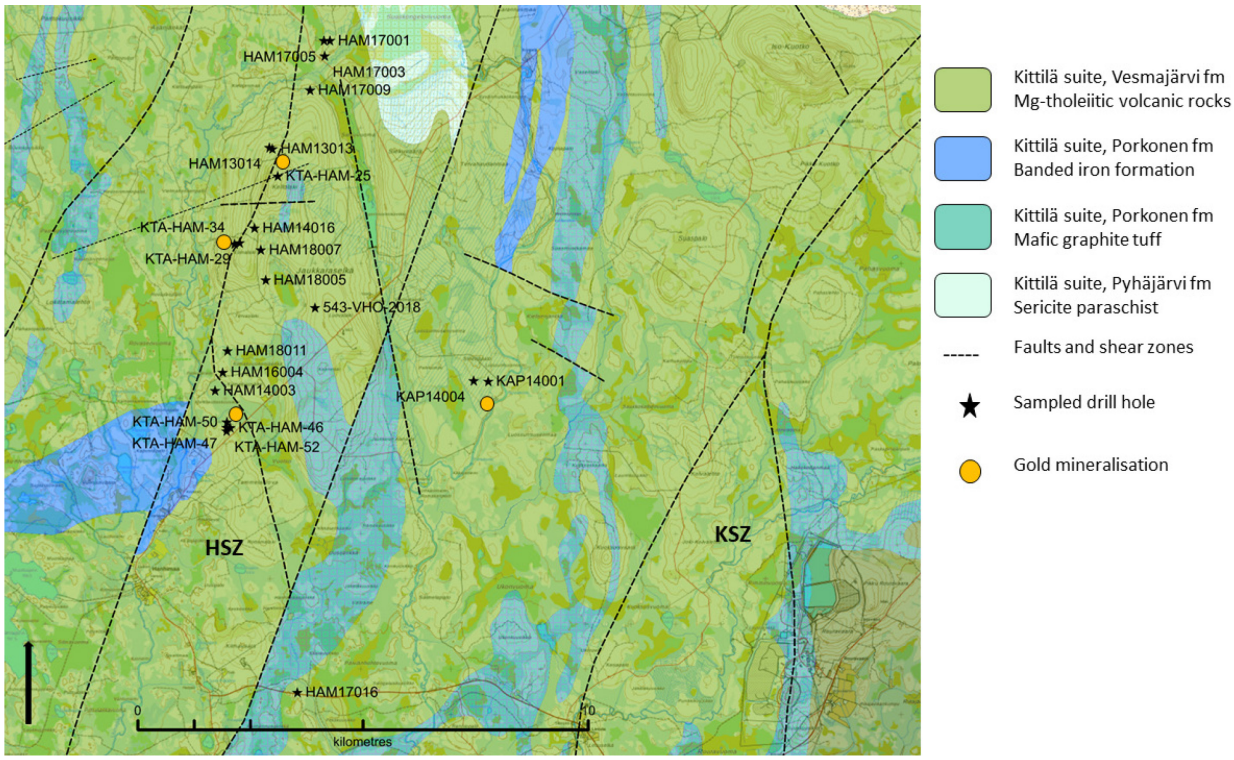

Figure 7. Major lithologies of the Kittilä suite in the Hanhimaa area, with major structures, gold mineralisation and sample locations. HSZ = Hanhimaa Shear Zone, KSZ = Kiistala Shear Zone. (modified after the DigiKP version 2.1. Base map National Land Survey of Finland)

Hanhimaa is located 30 kilometres NE from the city of Kittilä and 15 kilometres NW from the Suurikuusikko gold mine (Fig. 1). The rocks in the area are belonging to the Kittilä suite tholeiitic volcanic rocks, including mafic lavas and tuffs with cross-cutting felsic porphyry dykes (Lehtonen et al. 1998; Hanski & Huhma 2005). According to Saalmann and Niiranen (2010) volcanites at Hanhimaa belong to the Vesmajärvi-type Mg-tholeiites.

4.3.1 Structural geology and mineralisation of the Hanhimaa Au occurrences

The NS striking Hanhimaa shear zone cuts the volcanic rocks of the Hanhimaa area, parallel to the adjacent Kiistala shear zone (Fig. 7; Eilu 2007, Saalmann & Niiranen 2010). There are three known occurrences of Au mineralisation that are associated with the Hanhimaa shear zone (Fig. 7): Kellolaki, Kiimalaki and Kiimakuusikko (Eilu 2007, Kämäräinen 2014). All the known Au occurrences in HSZ have felsic porphyry rocks within the mafic metavolcanic host rocks or surrounding lithologies. The fourth gold

mineralisation in the area is the Kapsajoki mineralisation, located in between HSZ and KSZ (Fig. 7), and is hosted by an unspecified minor fault or shear (Eilu 2007, Kuronen 1980). In addition to these four Au mineralisation, there is samples in this study from five other targets in the proximity of the HSZ; Lisma, Siskeli, Kousa and Väli-Kiima. In the adjacent and parallel Kiistala shear zone, along which e.g. Suurikuusikko Au deposit (15 km SE of Hanhimaa) is located, Kittilä suite felsic porphyritic rocks of the younger Nyssäkoski type are one of the typical hosts of arsenopyrite-pyrite hosted gold (Molnár et al. 2018).

Saalmann and Niiranen (2010) identified six deformation stages from the Hanhimaa shear zone, based on the study conducted in the Kiimalaki occurrence. First deformation stage produced S1 layering after emplacement of the mafic volcanics. During this deformation stage, the first stage of alteration is represented by albitisation of the rocks. Second deformation stage produced tight, isoclinal folding with fold axes in SSE-NNW direction (Saalmann & Niiranen 2010). Third deformation stage is the major shearing event of the Kittilä area, resulting to formation of Hanhimaa shear zone and other major shear structures of the area, including the Kiistala shear zone. This deformation stage also led to the formation of the initial gold mineralisation (Saalmann & Niiranen 2010). Fourth deformation stage is represented by crenulation folding (F4), which has not been observed at the Hanhimaa area, but is indicated elsewhere in the parallel shear zones (Saalmann & Niiranen 2010). Fifth deformation stage consists of brecciation and fracturing, leading to the second stage of alteration, second stage of gold mineralisation and formation of the late quartz-carbonate veining. In this stage, the alteration is primarily pervasive sericite alteration of the felsic porphyries (Saalmann & Niiranen 2010). Sixth deformation stage is SSW-NNE faults dipping to east (Lehtonen et al. 1998; Saalmann & Niiranen 2010; Kämäräinen 2014). Geochronologically, the Kumpu group formation (<1.88 Ga) is located between the third and the fourth stage, and the post-orogenic ca. 1.77 Ga Nattanen-type granitic intrusions are between fourth and fifth stage (Lehtonen et al. 1998; Saalmann & Niiranen 2010).

5. ANALYTICAL METHODS AND SAMPLING

Total of 55 samples from the Hanhimaa area were collected for this study (Fig. 7). 54 are from diamond drill cores drilled by Agnico Eagle Finland Oy and Dragon/Polar Mining Oy. One sample is a grab sample from an exploration trench of the Siskeli target. The samples are listed in Table 3 and locations of the samples are shown in the Figure 7. All eight targets except Kapsa are located in proximity of the Hanhimaa Shear Zone or its predicted conjugate structures. The samples were collected from both Veikasenmaa and Nyssäkoski vein types, based on their known mineralogical features in the drill cores.

Table 3. Distribution of samples by sample locations in Hanhimaa

Location	Samples	Thin sections	Whole rock assays
Kiimakuusikko	14	14	13
Siskeli	4	4	4
Väli-Kiima	7	7	7
Kiimalaki	7	7	7
Kellolaki, Kello N	9	9	9
Lisma	4	4	4
Kapsa	7	7	7
Kousa	3	3	3
Total	**55**	**55**	**54**

Whole rock analysis was made from 54 samples. The assays were conducted by MS Analytical Inc. with laboratory package WRA-360. The analysed major elements included Al_2O_3, BaO, CaO, Cr_2O_3, Fe_2O_3, K_2O, MgO, MnO, Na_2O, P_2O_5, SiO_2, TiO_2. The analysed trace element included Ba, Ce, Cr, Cs, Dy, Er, Eu, Ga, Gd, Hf, Ho, La, Lu, Nb, Nd, Pr, Rb, Sm, Sn, Sr, Ta, Tb, Th, Tm, U, V, W, Y, Yb, Zr, As, Au, Bi, Hg, Sb, Se, Tl, Ag, Cd, Cu, Mo, Ni, Pb and Zn (MS Analytical Inc. 2019). Detailed assay results can be found in the Appendix 2 and detection limits of each element are presented in the Appendix 5.

55 polished thin sections were prepared at Vancouver Petrography Ltd. for petrographical studies. Geochemical diagrams are plotted using Imdex ioGAS v. 6.3.1.

Electron probe microanalyser (EPMA) studies were completed at the University of Oulu, Centre of Microscopy and Nanotechnology, with Jeol JXA-820 set on acceleration voltage of 15 kV and beam current of 15 nA. Spot size of 10µm was and analysed elements included Na_2O, F, V_2O_3, Cr_2O_3, P_2O_5, K_2O, MnO, MgO, CaO, Cl, Al_2O_3, FeO, BaO, SiO_2 and TiO_2. Detailed results of EPMA study can be found from the Appendix 4 and used standards in Appendix 5.

6. RESULTS

6.1 Petrography

Based on the drill core observations, 52 of the 55 samples are classified as felsic porphyries, porphyritic veins or altered porphyries. Samples vary in colour, appearance and abundance of phenocrysts, and in intensity of the hydrothermal alteration and metasomatism. Three of the 55 samples are logged to be hydrothermally altered mafic volcanic lavas, with alteration assemblage albite ± carbonate ± sericite. These mafic rocks are belonging to the Kittilä suite and is representing the host rocks for the felsic porphyries.

During drill core logging, tentative division was made, classifying the felsic porphyries into known two types, Nyssäkoski and Veikasenmaa, based on the macroscopical features. The Nyssäkoski type felsic porphyries exhibits vitreous matrix with relatively large phenocrysts (1-6 mm in diameter). They also show sharp contacts with the surrounding rocks. The subvolcanic Veikasenmaa type porphyries have more gradual contacts with elongated and deformed phenocrysts in an altered matrix comprising of hydrothermal albite and carbonates. The Kapsa samples were tentatively separated to their own group based on differences in appearance of drill core and microscopical features.

The felsic porphyry samples are in general aphanitic or even glassy, with euhedral plagioclase and quartz phenocrysts. Plagioclase twinning is visible in most of the thin sections.

Alteration minerals include chlorite, sericite, carbonate and albite in all hydrothermally altered samples. The colour of the rocks in drill core samples correlates well with the alteration intensity; light grey to dark grey samples are unaltered or display only minor alteration. Increasing amount of albite turns the rocks to more yellowish beige, whereas increasing sericite and chlorite alteration gives the colour a greenish tint. In thin sections, chlorite and sericite occur as banded alteration stripes, and albite occurs as fine grained, almost aphanitic in the matrix of the porphyries.

The detailed thin section description of the samples are shown in the Appendix 1. Sample list and their respective target areas, sample depth (drill core) and logged name are shown in Table 4. All the sample material are assumed to be metamorphic and thus, the prefix meta- is left out from the text.

Table 4. List of samples, their logged names and the porphyry types based on petrography.

Sample	Drill hole	Target	Depth (m)	Logged name	Porphyry type	EPMA
FIEXD117951	HAM18011	Väli-Kiima	40.45	altered mafic lava		no
FIEXD117952	HAM18011	Väli-Kiima	44.45	porphyry	Nyssäkoski	yes
FIEXD117953	HAM18011	Väli-Kiima	56.20	altered mafic lava		no
FIEXD117954	HAM18007	Siskeli	50.20	porphyry	Nyssäkoski	yes
FIEXD117955	M8HAM2018	Siskeli	trench	porphyry	Veikasenmaa	no
FIEXD117956	KTAHAM-50	Kiimakuusikko	30.60	altered mafic lava		no
FIEXD117957	KTAHAM-50	Kiimakuusikko	36.60	porphyry	Nyssäkoski	yes
FIEXD117958	KTAHAM-50	Kiimakuusikko	98.40	porphyry	Nyssäkoski	no
FIEXD117959	KTAHAM-46	Kiimakuusikko	54.30	porphyry	Nyssäkoski	yes
FIEXD117960	KTAHAM-46	Kiimakuusikko	97.95	porphyry	Nyssäkoski	no
FIEXD117961	KTAHAM-46	Kiimakuusikko	108.40	porphyry	Nyssäkoski	no
FIEXD117962	KTAHAM-46	Kiimakuusikko	114.40	porphyry	Nyssäkoski	no
FIEXD117963	KTAHAM-52	Kiimakuusikko	10.60	porphyry	Nyssäkoski	no
FIEXD117964	KTAHAM-52	Kiimakuusikko	83.70	porphyry	Nyssäkoski	no
FIEXD117965	KTAHAM-52	Kiimakuusikko	88.80	porphyry	Nyssäkoski	no
FIEXD117966	KTAHAM-52	Kiimakuusikko	104.40	porphyry	Nyssäkoski	no
only thin section	KTAHAM-47	Kiimakuusikko	81.80	sulphide-qtz vein	Nyssäkoski	no
FIEXD117967	KTAHAM-47	Kiimakuusikko	17.00	porphyry	Nyssäkoski	no
FIEXD117968	KTAHAM-47	Kiimakuusikko	85.60	porphyry	Nyssäkoski	no
FIEXD117969	HAM16004	Väli-Kiima	151.60	porphyry	Veikasenmaa	no
FIEXD117970	HAM16004	Väli-Kiima	158.00	porphyry	Veikasenmaa	no
FIEXD117971	HAM17005	Lisma	244.20	porphyry	Nyssäkoski	yes
FIEXD117972	HAM17005	Lisma	250.60	porphyry	Nyssäkoski	yes
FIEXD117973	KTAHAM-25	Kellolaki	22.90	porphyry	Nyssäkoski	no
FIEXD117974	KTAHAM-25	Kellolaki	33.00	porphyry	Veikasenmaa	yes
FIEXD117975	KTAHAM-34	Kiimalaki	12.80	porphyry	Veikasenmaa	yes
FIEXD117976	KTAHAM-34	Kiimalaki	69.50	porphyry	Veikasenmaa	no
FIEXD117977	KTAHAM-34	Kiimalaki	94.90	porphyry	Veikasenmaa	no
FIEXD117978	KTAHAM-29	Kiimalaki	79.40	porphyry	Nyssäkoski	no
FIEXD117979	KTAHAM-29	Kiimalaki	88.40	porphyry	Nyssäkoski	no
FIEXD117980	HAM13014	Kellolaki	48.20	porphyry	Veikasenmaa	yes
FIEXD117981	HAM13013	Kellolaki	68.00	porphyry	Nyssäkoski	no
FIEXD117982	HAM13013	Kellolaki	89.40	porphyry	Veikasenmaa	no
FIEXD117983	HAM13013	Kellolaki	96.00	porphyry	Veikasenmaa	no
FIEXD117984	HAM13013	Kellolaki	139.00	porphyry	Veikasenmaa	no
FIEXD117985	HAM17016	Kousa	114.20	porphyry	Nyssäkoski	no
FIEXD117986	HAM17016	Kousa	122.50	porphyry	Nyssäkoski	yes
FIEXD117987	HAM17016	Kousa	136.05	porphyry	Nyssäkoski	yes
FIEXD117988	HAM17009	Kello N	91.00	porphyry	Veikasenmaa	yes
FIEXD117989	HAM17009	Kello N	142.80	porphyry	Veikasenmaa	no
FIEXD117990	HAM17003	Lisma	78.80	porphyry	Nyssäkoski	no
FIEXD117991	HAM14016	Kiimalaki	268.50	porphyry	Veikasenmaa	yes
FIEXD117992	HAM14016	Kiimalaki	333.00	porphyry	Veikasenmaa	no

FIEXD117993	HAM17001	Lisma	141.80	porphyry	Nyssäkoski	no
FIEXD117994	KAP14001	Kapsa	85.90	porphyry	neither	yes
FIEXD117995	KAP14001	Kapsa	159.10	porphyry	neither	yes
FIEXD117996	KAP14001	Kapsa	175.50	porphyry	neither	no
FIEXD117997	KAP14004	Kapsa	62.30	porphyry	neither	no
FIEXD117998	KAP14004	Kapsa	67.00	porphyry	neither	yes
FIEXD117999	KAP14004	Kapsa	91.10	porphyry	neither	no
FIEXD118000	KAP14004	Kapsa	220.80	porphyry	neither	no
FIEXD143571	HAM14003	Väli-Kiima	155.70	porphyry	Veikasenmaa	yes
FIEXD143572	HAM14003	Väli-Kiima	200.80	porphyry	Veikasenmaa	no
FIEXD143573	HAM18005	Siskeli	12.60	porphyry	Nyssäkoski	yes
FIEXD143574	HAM18005	Siskeli	10.20	porphyry	Nyssäkoski	no

6.1.1 Division of the target to groups by common features

Kellolaki, Kello North and Kiimalaki

Samples taken from the Kellolaki, Kello North and Kiimalaki targets display felsic porphyries which are classified as both Nyssäkoski and Veikasenmaa type. Typical examples of both Nyssäkoski and Veikasenmaa types are shown in Figure 8, where both types are occurring within the same drill core. Both samples are fine-grained and darkish in colour, with highly varying plagioclase and quartz phenocryst size; Nyssäkoski type samples have finer phenocrysts whereas the Veikasenmaa type contains larger phenocrysts which are shattered in the alteration process. The main minerals include quartz and plagioclase in both matrix (aphanitic to 0.2 mm) and phenocrysts (0.1-0.5mm). Accessory minerals are biotite, hornblende, carbonate and local sulphides; mainly pyrite, arsenopyrite in few samples. In general, the samples have very aphanitic matrix and hydrothermal alteration is strong, occurring as albitisation and sericitation. Plagioclase phenocrysts show clear twinning in several samples, following Albite Law and Carlsbad twinning. Plagioclase crystals are often replaced by saussurite preserving the primary twinning appearance.

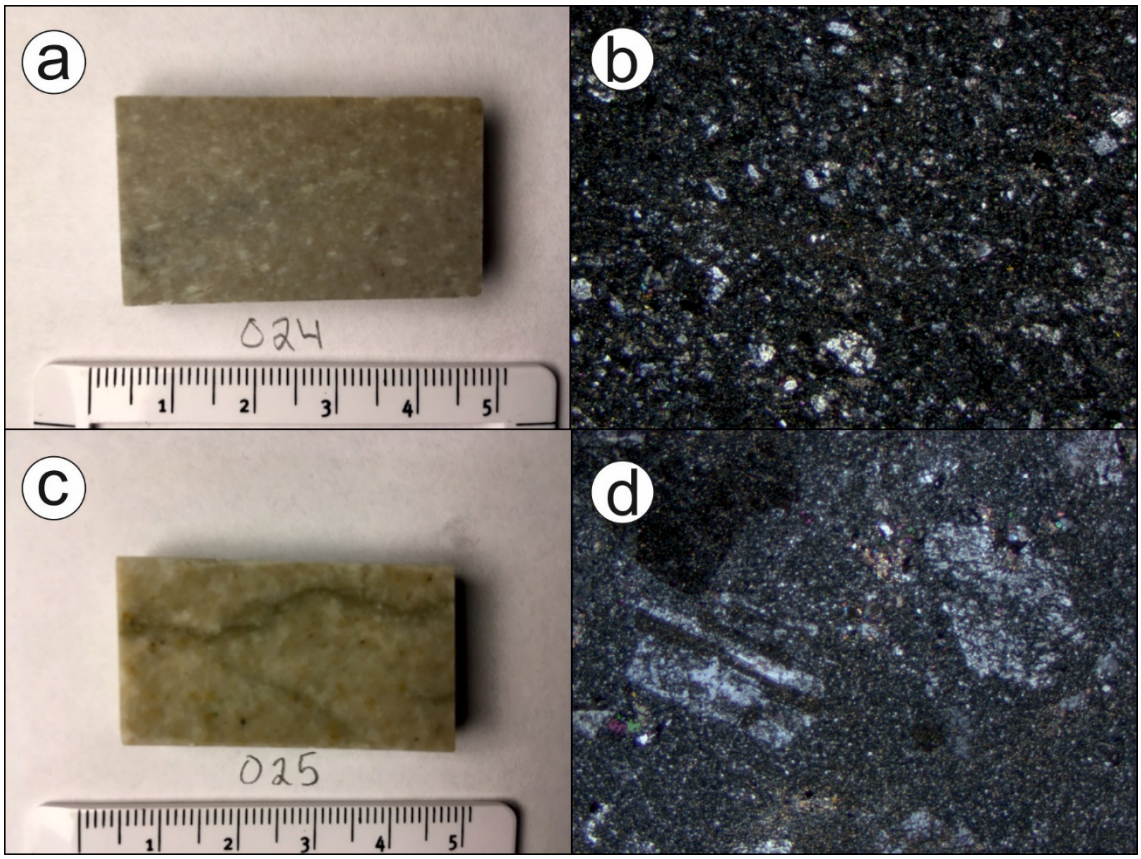

Figure 8. Type examples of the Nyssäkoski and Veikasenmaa type felsic porphyries (drill hole KTAHAM-25). a) Nyssäkoski type, Kellolaki target, 024 FIEXD117973 hand sample, b) microphotograph of 024, c) Veikasenmaa type, Kellolaki target, 025 FIEXD117974 hand sample and d) microphotograph of 025. 1.25x XPL, width of image in microphotographs is 4.5 mm.

Siskeli, Kousa and Lisma

The samples from Siskeli, Kousa and Lisma targets are all logged as being the Nyssäkoski type rhyolites. Figure 9 a-d presents typical examples of variation in phenocryst abundance and appearance in the Nyssäkoski type porphyry, as well as typical greenish beige alteration colour of the porphyry in hand sample. Main minerals are plagioclase and quartz in both matrix (aphanitic) and phenocrysts (0.1-0.4 mm). Plagioclase phenocrysts are broken. Accessory minerals include biotite, hornblende and sulphides; pyrite occurs as large (0.1-0.3 mm) euhedral grains. In Lisma, arsenopyrite occurs locally as very fine dissemination. Alteration is strong, including albitisation and strong, almost pervasive sericitation. Figure 10 displays occurrences of arsenopyrite and pyrite in in totally sericite altered phenocryst, hosted by albite-sericite altered quartz-bearing matrix at Kousa target.

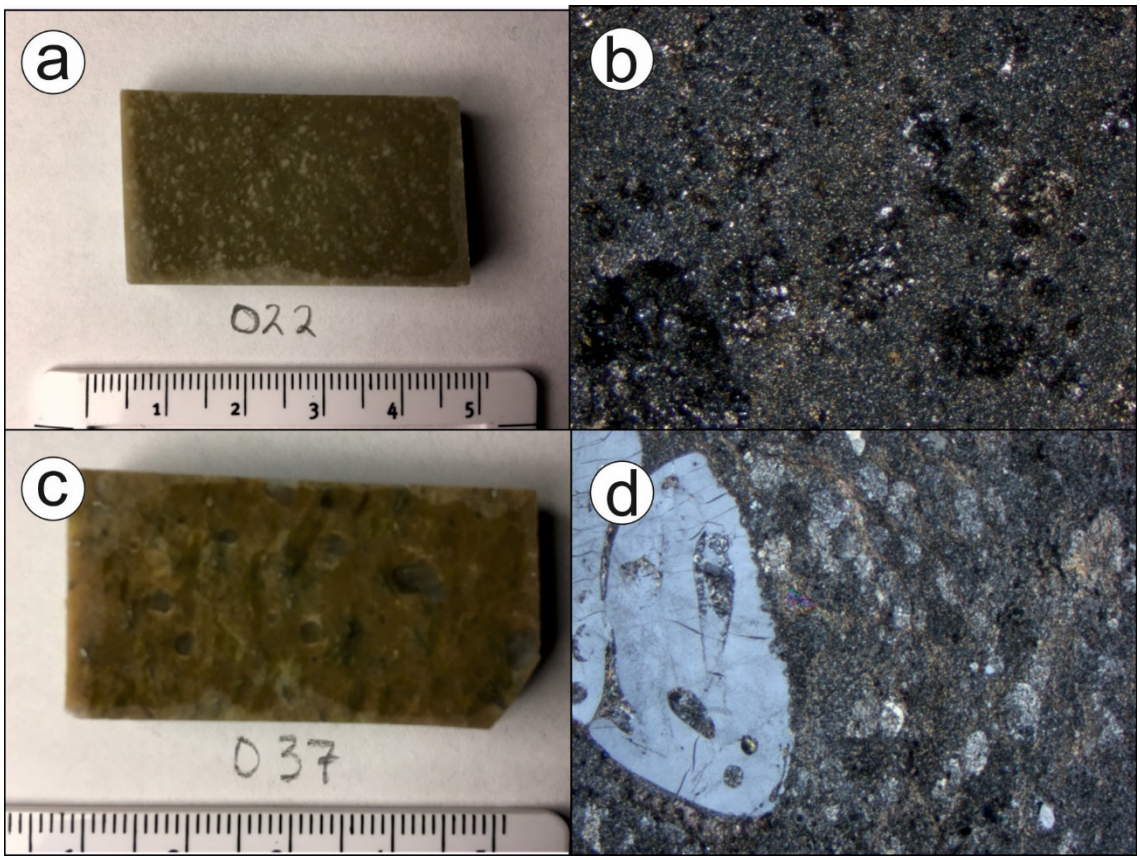

Figure 9. Type examples of the Nyssäkoski type felsic porphyries. a) Lisma target, 022 FIEXD117971 b) microphotograph of 022, c) Kousa target, 037 FIEXD117986 hand sample and d) microphotograph of 037. 1.25x XPL, width of image in microphotographs is 4.5 mm.

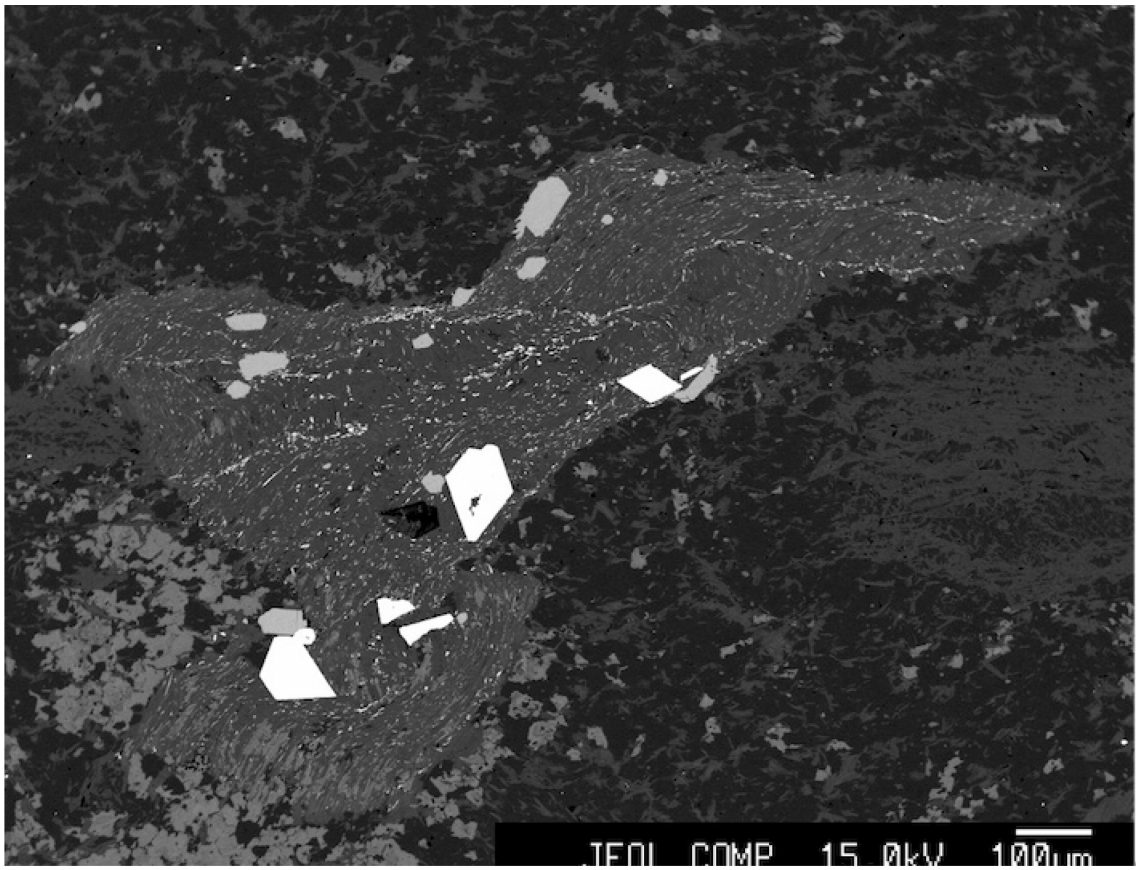

Figure 10. Pyrite as fracture filling and arsenopyrite as euhedral grains. Sample 038 FIEXD117987, Kousa target, Nyssäkoski type.

Kiimakuusikko

All the Kiimakuusikko samples belong to the Nyssäkoski type. They are distinguished from the Siskeli-Kousa-Lisma group based on differences in sulphidisation; Kiimakuusikko contains polymetallic sulphides and the Siskeli-Kousa-Lisma group only arsenopyrite. Figure 11 shows examples of Nyssäkoski type porphyry in Kiimakuusikko target, with strongly varying alteration from highly altered (Fig. 11a and b) to weakly altered (Fig. 11c and d) sample with quartz rich matrix. These two samples are close to each other (Fig. 7; 20 m distance between drill holes) and the azimuth of the drill core is same. Main minerals are quartz and plagioclase in matrix (aphanitic to 0.1 mm) and as phenocrysts (0.2-0.7 mm), accessory minerals are mainly sulphides; pyrite, stibnite, chalcopyrite and arsenopyrite occurring in the matrix of the porphyry. Alteration is intensive in most of the samples and alteration assemblages are abundant, including albite, sericite, chlorite and carbonates as accessory minerals. Samples are aphanitic and more quartz-bearing than the other targets.

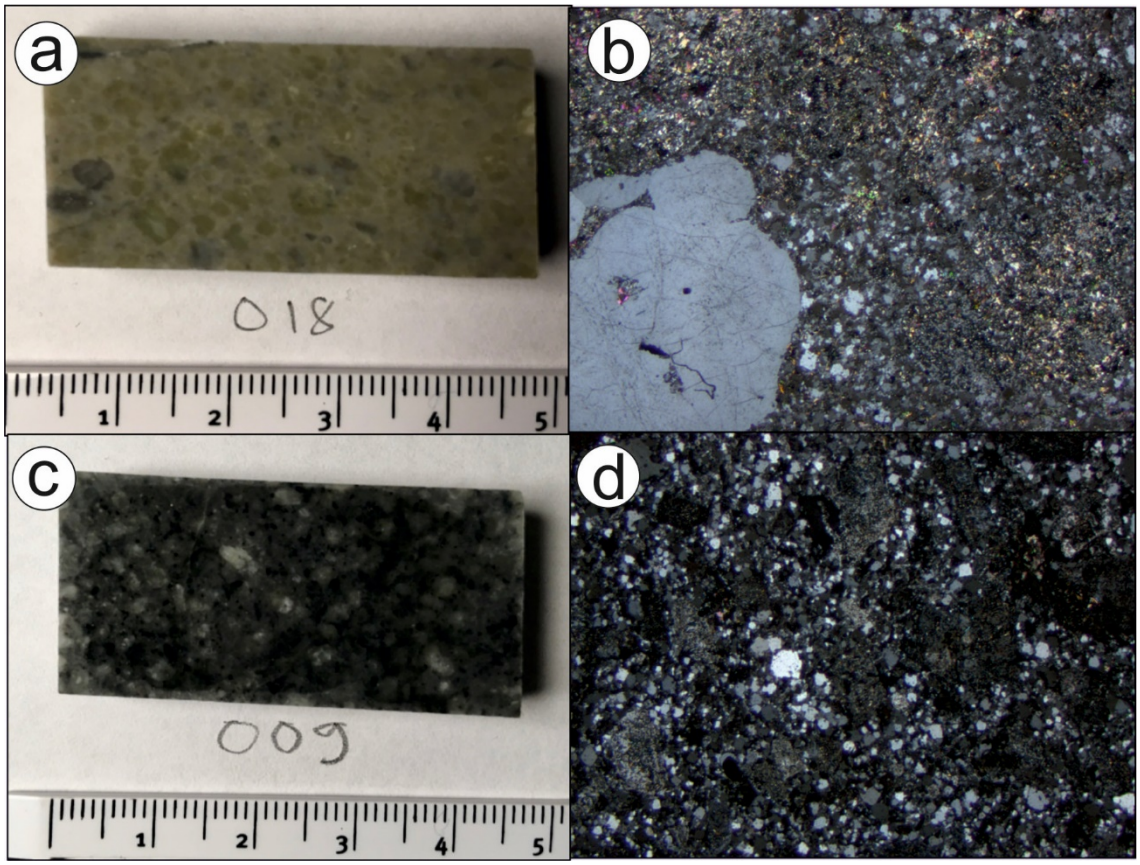

Figure 11. Type examples of the Nyssäkoski type felsic porphyries in Kiimakuusikko target. a) 018 FIEXD117967 hand sample, b) microphotograph of 018, c) 009 FIEXD117959 hand sample and d) microphotograph of 009. 1.25x XPL, width of image in microphotographs is 4.5 mm.

Examples of hydrothermal alteration intensity and resulting texture in Fig. 12, where typical alteration textures of phenocrysts is presented from targets of Kiimakuusikko (Fig. 12a) and Kellolaki (Fig. 12b), respectively Nyssäkoski and Veikasenmaa type. In thin section sample 017, microscopically visible gold detected in stibnite (Fig. 13)

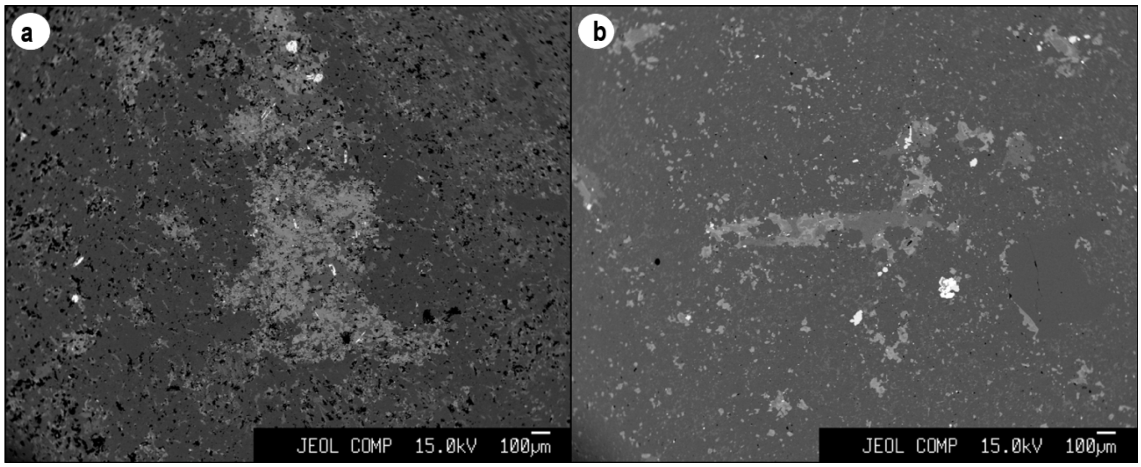

Figure 12. Resulting texture of hydrothermal alteration in plagioclase phenocrysts. A sample 007 FIEXD117957 Kiimakuusikko target, Nyssäkoski type porphyry. B sample 025 FIEXD117974 Kellolaki target, Veikasenmaa type porphyry.

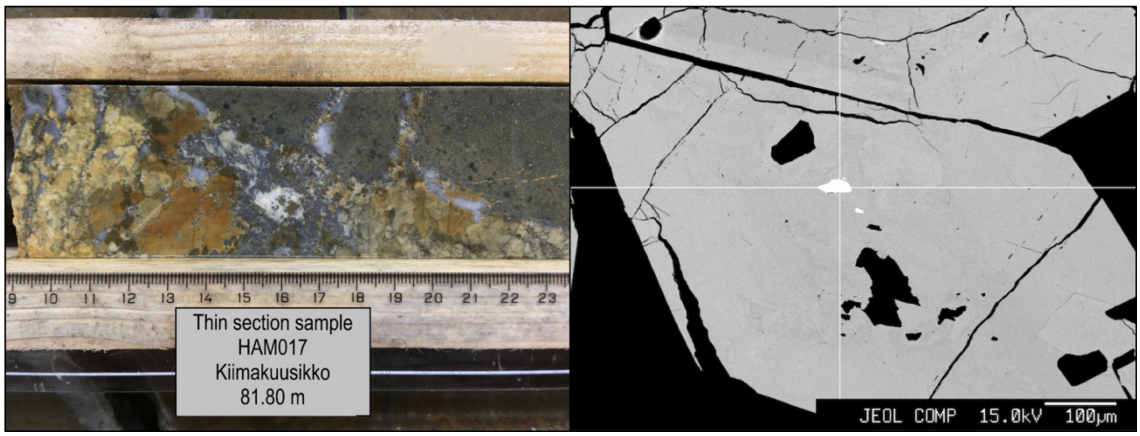

Figure 13. Coarse auriferous arsenopyrite-stibnite vein in Nyssäkoski type felsic porphyry, thin section sample 017. On right, same sample in EPMA analysis; Au in stibnite.

Väli-Kiima

The Väli-Kiima samples belong to the Veikasenmaa type porphyries. Main minerals are plagioclase, quartz and biotite, in which quartz and plagioclase in matrix (0.1-0.3 mm), and plagioclase (0.5-5.0 mm) and biotite as phenocrysts. Alteration minerals are sericite, albite, biotite and carbonates. Plagioclase forms relatively large phenocrysts (Fig. 14 a and c), and biotite occurs as bands and schist accumulation, most likely as an alteration product (Fig. 14b and d). In comparison, quartz is rarely present as large phenocrysts in Veikasenmaa type as it is in Nyssäkoski type. Accessory minerals include euhedral pyrite.

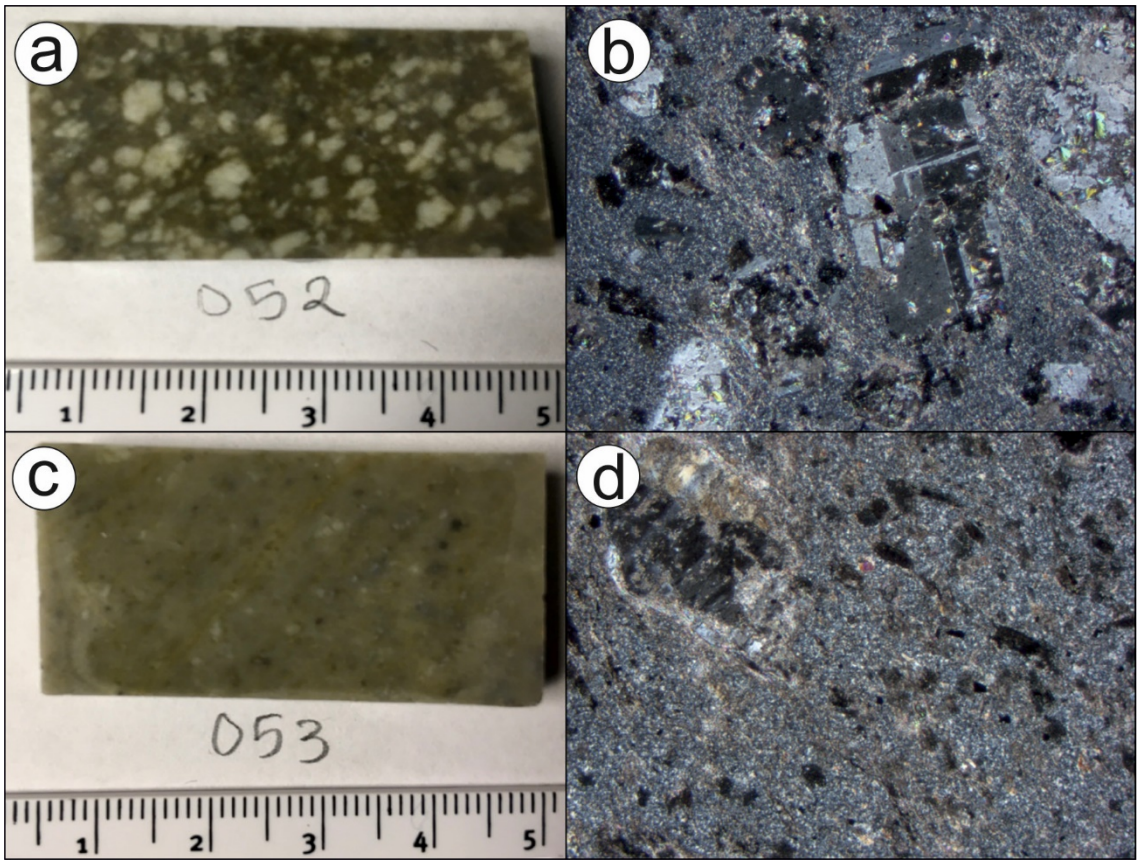

Figure 14. Type examples of the Veikasenmaa type felsic porphyries in Väli-Kiima target. a) 052 FIEXD143571 hand sample, b) microphotograph of 052, c) 053 FIEXD143572 hand sample and d) microphotograph of 053. 1.25x XPL, width of image in microphotographs is 4.5 mm.

Kapsa

Based on logging of the drill cores and samples therein, the Kapsa type differs strongly from the other porphyries of the area by colour and appearance. The samples from Kapsa target (FIEXD117994 to FIEXD118000) show plagioclase occurring as distinctly zonated phenocrysts, which is visible also in the hand samples (Fig. 15 a-d). The Kapsa target samples are classified as plagioclase porphyry rocks due to lack of quartz phenocrysts. Kapsa type porphyry has black, vitreous matrix with whitish-green, strongly zonated plagioclase phenocrysts. Interestingly, the Kapsa samples are only ones in this study containing bluish colored chlorite as an alteration mineral in phenocrysts (Fig. 15b).

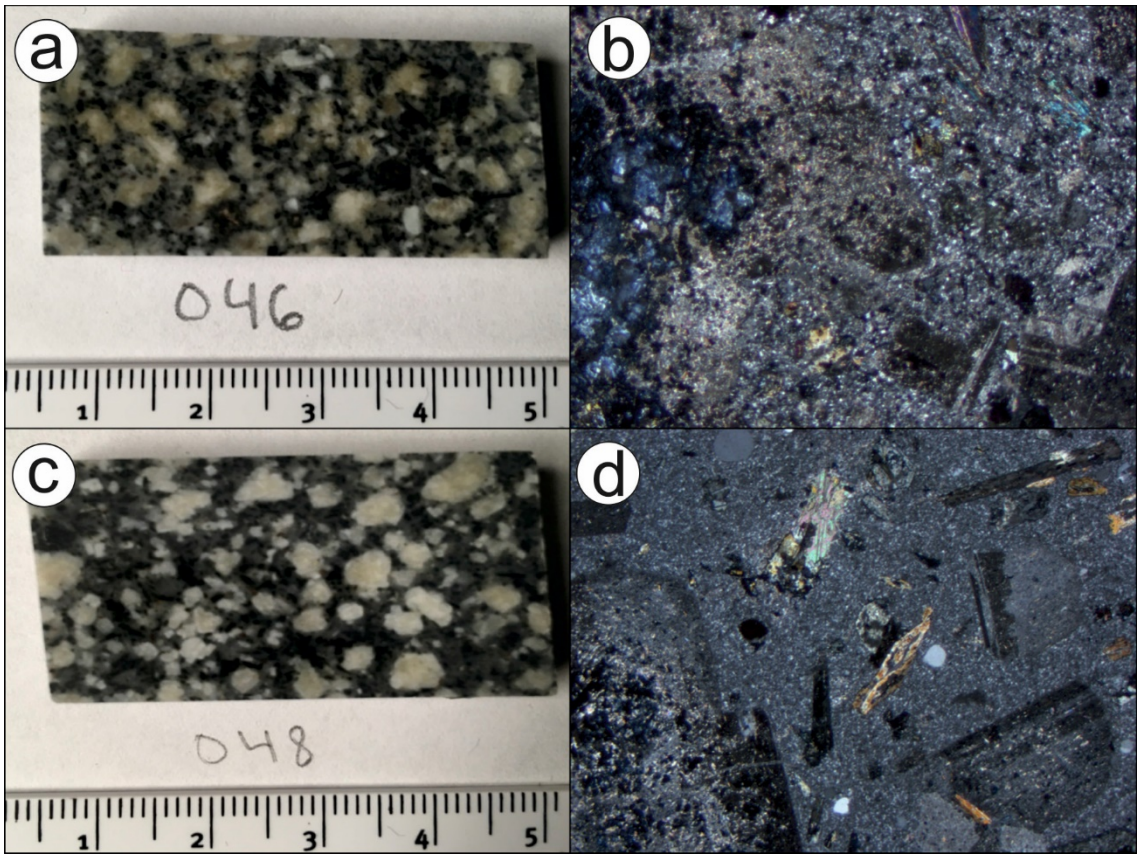

Figure 15. Type examples of the Kapsa type plagioclase porphyry. a) 046 FIEXD117995 hand sample, b) microphotograph of 046, c) 048 FIEXD117997 hand sample and d) microphotograph of 048. 1.25x XPL, width of image in microphotographs is 4.5 mm.

6.2 Whole-rock geochemistry

Whole-rock geochemical data was used in order to determine the composition of the felsic porphyries, identify possible differences and similarities in geochemistry between the target locations, and to see if the samples display characteristics of the two different known felsic porphyry generations, the Nyssäkoski- and Veikasenmaa type. Furthermore, the intensity of hydrothermal alteration in the felsic porphyry samples are evaluated.

Due to the greenschist facies metamorphism and hydrothermal albitisation of the rocks in the Hanhimaa area, the total alkali silica diagram TAS (Le Bas et al. 1986) is not suitable for this study. The greenschist facies metamorphic minerals e.g. amphiboles of actinolite-tremolite series and the sodium content of the albitic plagioclase distorts the diagram making the samples plot in the trachytic field, whereas there are no clinopyroxene or olivine in the samples. The Yb/Th plot used in Hanski & Huhma (2005) to discriminate the Nyssäkoski and Veikasenmaa types based on the ytterbium-thorium ratio of the

samples is not applicable in the Hanhimaa area due to abundance of hydrothermal monazite containing thorium, thus lowering the Yb/Th ratio from the actual.

6.2.1 Major elements

All the felsic porphyries are calc-alkaline and form a series from rhyolite to andesite (Fig, 16 and 17).

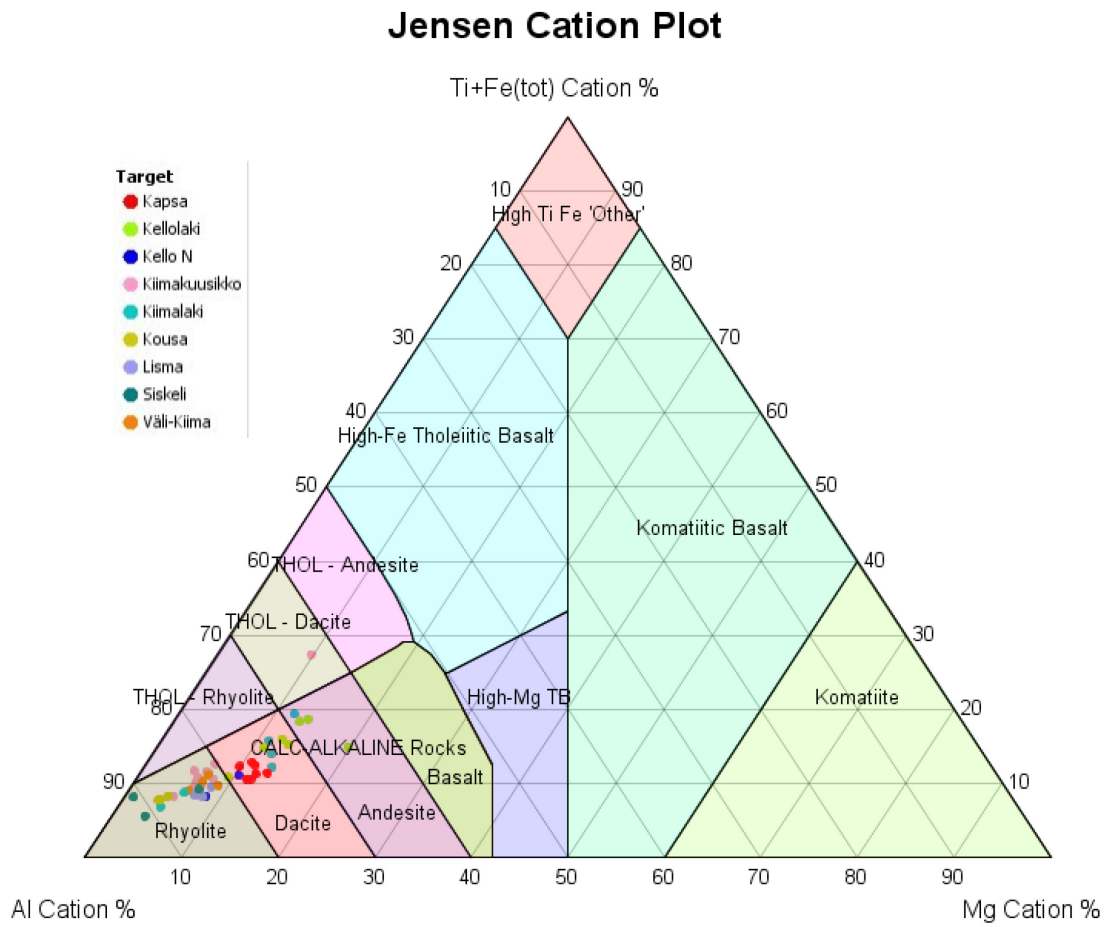

Figure 16. Samples divided by target in Jensen cation plot (Jensen 1976).

In the Jensen Cation Plot (Fig. 16), the samples form a series in the calc-alkaline rhyolite-dacite-andesite fields, where major of the samples plot into rhyolitic and dacitic field and few in the andesitic.

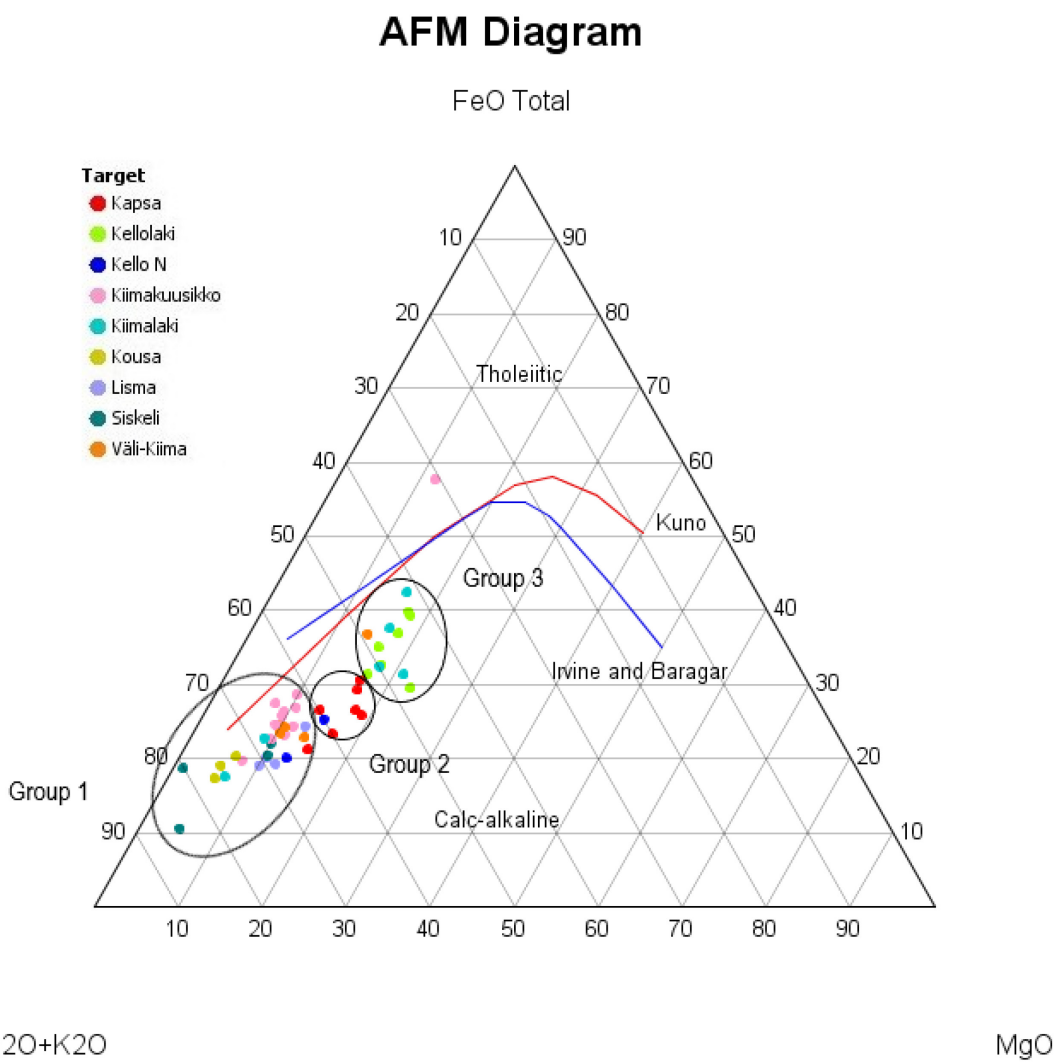

Figure 17. Samples in AFM diagram with division to three groups (Irvine and Baragar 1971).

Based on the geochemical similarities between the target areas, three groups can be inferred;

1) Siskeli – Kousa – Lisma – Kello N – Kiimakuusikko – Väli-Kiima (Group 1)
2) Kellolaki – Kiimalaki group (Group 2)
3) Kapsa type group (Group 3)

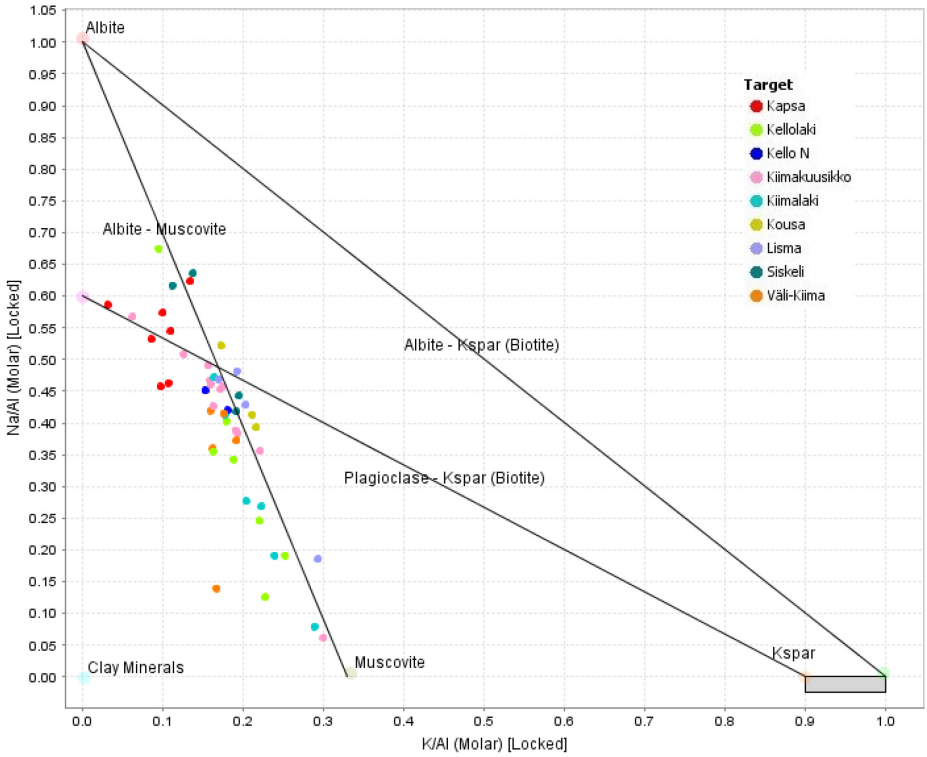

Figure 18. Na/Al to K/Al molar ratio diagram (modified from Davies and Whitehead 2006).

The Na/Al vs. K/Al diagram (Fig. 18) shows the differences of hydrothermal alteration intensity. The albitisation and sericitisation of the samples are evident in the petrography and is shown also in the geochemistry with samples going towards the muscovite end with variable intensities (Fig. 18 and 19). Samples from Kellolaki and Kiimalaki occurrences are showing the strongest effect of the alteration, plotting towards the muscovite in the diagram. The same group 2 from AFM diagram (Fig. 17) forms a group in the middle of the albite-muscovite trend. Kapsa target distinguishes slightly from the others, plotting to the plagioclase trend line.

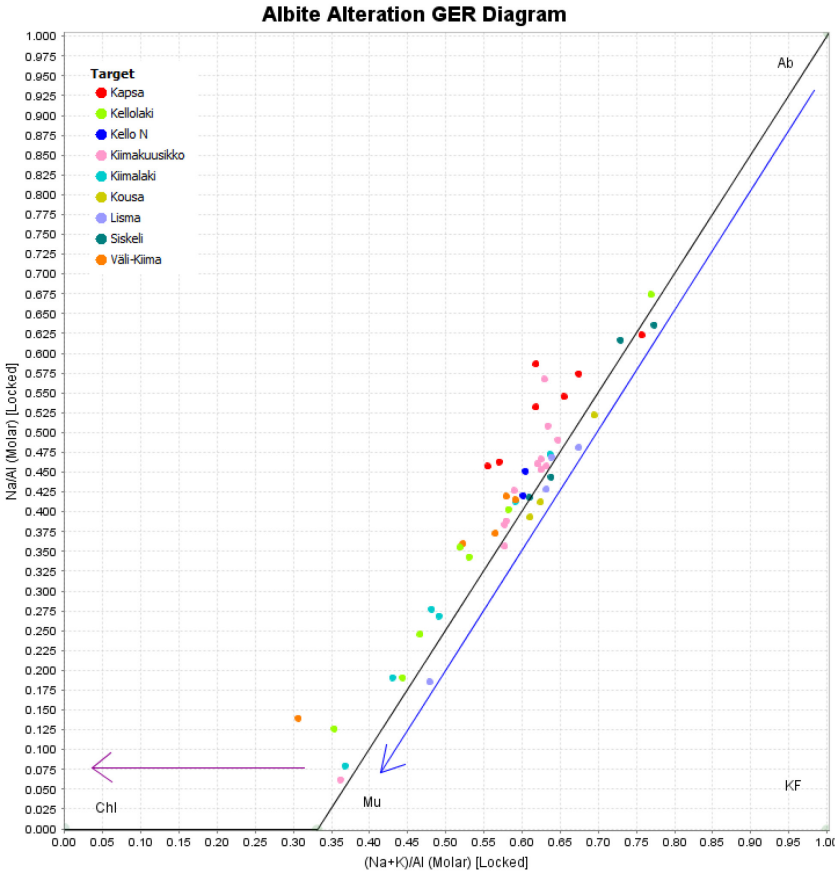

Figure 19. (Na+K)/Al vs. Na/Al diagram after Stanley (2017). Abbreviations: Mu=Muscovite, Ab=Albite, Chl=Chlorite.

6.2.2 Trace elements

Chondrite normalised REE pattern of the samples show uniform enriched LREE trend with more fractionated trend in HREE where the samples divide into two distinct groups (Fig. 20). Few samples with clearly different LREE-trend is caused most probably by alteration. In comparison to Mikkola (2006), the porphyrites divide similarly to two clusters in the HREE side, separating the Veikasenmaa type with higher values of the HREE, from the lower HREE values of the Nyssäkoski type. The REE-patterns correlate with the division to groups by petrographic study; Kellolaki-Kiimalaki samples are located in both HREE-enriched and not enriched; containing both Nyssäkoski and Veikasenmaa type. Kapsa forms a trend on the lower part of HREE-enriched, being Veikasenmaa type based on this diagram. Siskeli-Kousa-Lisma samples are in the lower HREE section representing Nyssäkoski type, and Väli-Kiima with Kiimakuusikko the lowest of HREE end in the pattern, also representing Nyssäkoski type.

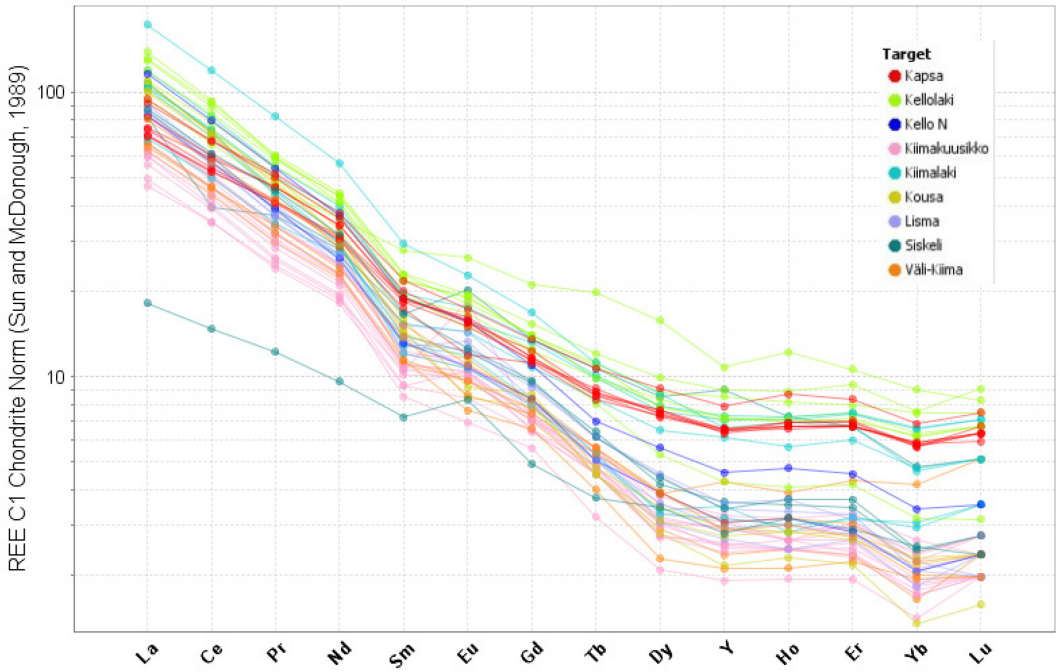

Figure 20. Chondrite normalised REE patterns for the felsic porphyries. Chondritic values after Sun and McDonough (1989)

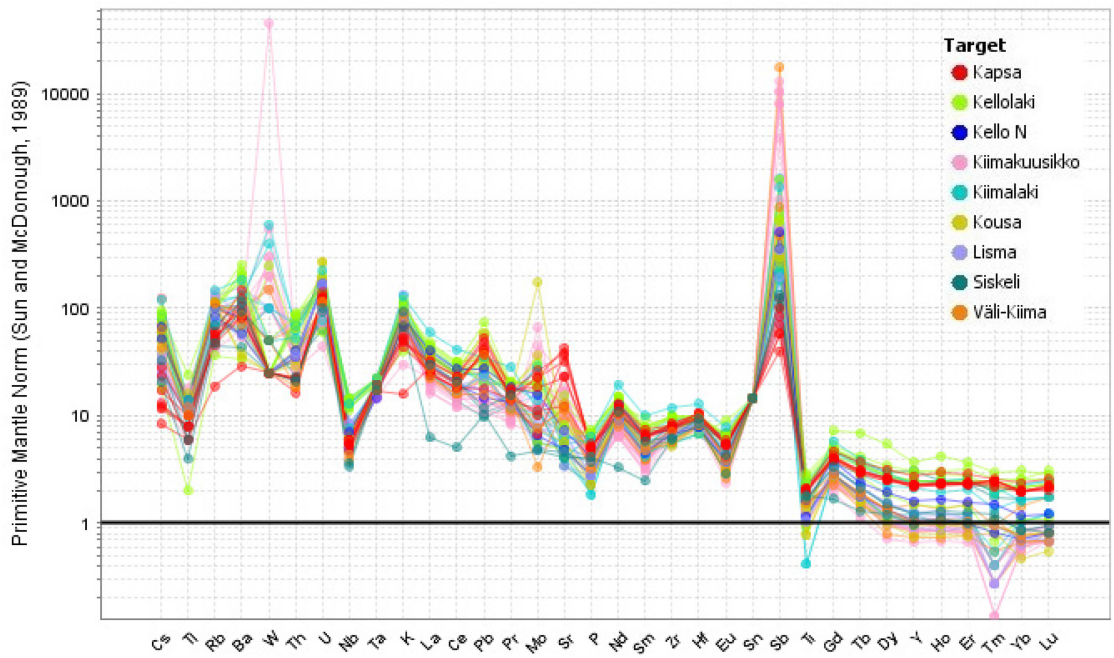

Figure 21. Primitive mantle normalised spidergrams for the felsic porphyries. Normalisation values after Sun and McDonough 1989)

The normalised primitive mantle diagram (Fig. 21) plots all the samples in relatively uniform pattern, with few exceptions on enrichment of W and Sb, most strongest in the Kiimakuusikko samples.

6.2.3 Correlation of selected elements

The Spearman correlation coefficients (Table 5), calculated from the whole rock analysis data of Nyssäkoski and Veikasenmaa porphyry types combined, shows significant correlations for Au-As and Au-Bi; also Ag-Bi and Cu-Sb correlate rather strongly. The correlation coefficient can range from -1 to 1, where 1 indicate perfect positive correlation and -1 perfect negative correlation. The Au values of the porphyry samples are not anomalously high. The Kapsa type plagioclase porphyry assays were excluded to determine specific Nyssäkoski and Veikasenmaa type correlations only.

Table 5. Spearman correlation coefficients for selected elements.

Spearman - 43 rows - Pair	Au_ppm	Ag_ppm	As_ppm	Bi_ppm	Cu_ppm	Sb_ppm
Au_ppm	1	0.64	0.75	0.75	0.33	0.51
Ag_ppm	0.64	1	0.63	0.82	0.72	0.71
As_ppm	0.75	0.63	1	0.69	0.43	0.51
Bi_ppm	0.75	0.82	0.69	1	0.68	0.66
Cu_ppm	0.33	0.72	0.43	0.68	1	0.78
Sb_ppm	0.51	0.71	0.51	0.66	0.78	1

6.3. Plagioclase composition

The electron microprobe studies were concentrated to the compositional differences of the plagioclase phenocrysts. Samples selected represent both the Nyssäkoski (009 and 022) and Veikasenmaa (025 and 026), as well as the Kapsa plagioclase porphyry (045) (Table 6). In other samples, phenocrysts were to intensely altered and thus, proper chemical analyses were not possible.

The composition of plagioclase varies from labradorite to albite (Fig. 22). The compositional variability does not seem to be related specifically to either target areas nor to felsic porphyry type. Kapsa target area (Thin section ID 045) display plagioclase composition of labradorite (An_{57}). Samples from the Kellolaki (Thin section ID 025) and Kiimalaki target areas (Thin section ID 026) show plagioclase composition from oligoclase (An_{23-25}) to albite composition of plagioclase ($An_{0.4-1}$). Lisma target area (Thin section ID 022) show albitic composition of plagioclase (An_{2}).

Table 6. Calculated anorthite components of plagioclase phenocrysts in EPMA analyses

Thin section ID	An%	Felsic porphyry type
009	46	Nyssäkoski
009	42	Nyssäkoski
009	47	Nyssäkoski
022	2	Nyssäkoski
025	23	Veikasenmaa
025	0.4	Veikasenmaa
026	1	Veikasenmaa
045	57	Kapsa

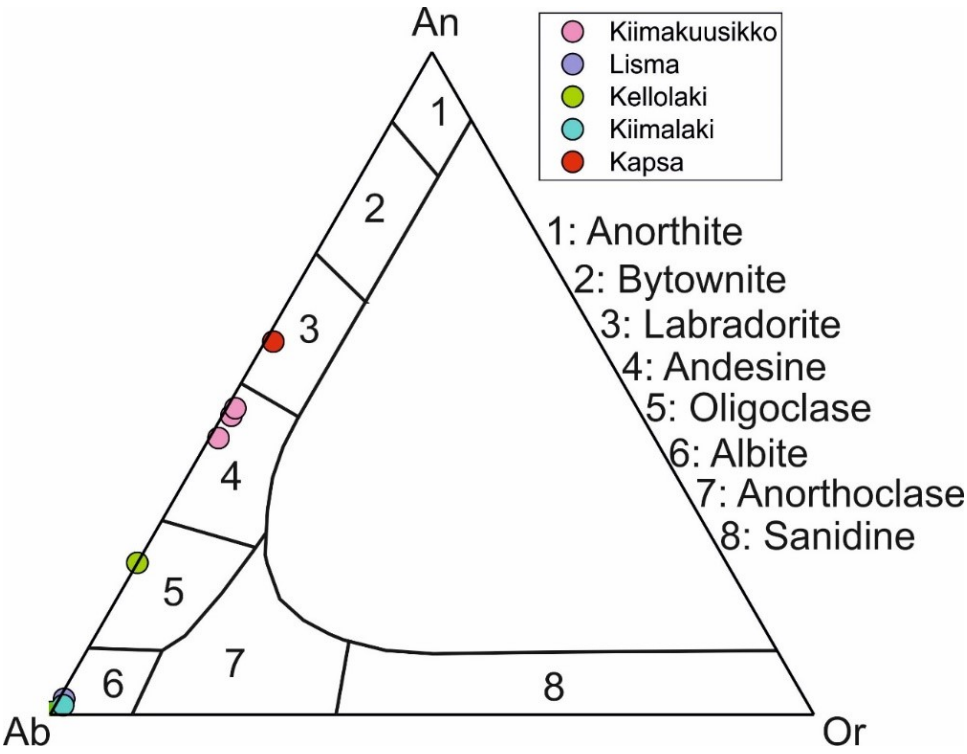

Figure 22. Ternary diagram for feldspars of the analysed thin sections.

7. DISCUSSION

7.1 Felsic porphyry types in the Hanhimaa area

The initial classification of the felsic porphyries was based on macroscopical features during drill core logging. The initial classification of the quartz phenocryst bearing felsic porphyries in the Hanhimaa drill cores is supported by the whole-rock geochemical major- and trace element data, which show similarities with the earlier studies of the Nyssäkoski and Veikasenmaa felsic rocks (Mikkola 2006). The appearance of the quartz phenocrysts allows the identification of these felsic rocks even though they locally show intense hydrothermal alteration, destructing the primary features of the rocks. The abundance of quartz reflects to the higher SiO_2 content of the rocks and thus making them rhyolitic to dacitic in composition.

Plagioclase occurs as phenocrysts as well as in matrix in both types, varying geochemically from sodic to calcic plagioclases, which leads to no distinguishable differences in either macroscopical, petrographical or geochemical view. Although the number of unaltered analyses in microprobe studies of plagioclase phenocrysts are low, it can be detected that certain porphyry type does not favour any specific composition of plagioclase.

Spatially, the most distinguishable feature in geochemistry is that samples from Kellolaki and Kiimalaki form their own trend apart from other targets in both Jensen and AFM diagrams (Figs. 16 and 17). Samples plot in two groups based on their geochemical composition, major of them plotting to the dacite-andesite field and few in the rhyolitic field. Also, the REE patterns of Kellolaki, Kello N and Kiimalaki are heterogeneous, implying these targets contain both rhyolitic Nyssäkoski dykes and dacitic Veikasenmaa subvolcanic porphyries (Fig. 20). The targets of Kellolaki and Kiimalaki contain both Nyssäkoski and Veikasenmaa type porphyries in a relatively small area.

Siskeli, Kousa and Lisma targets have similar geochemistry and are classified rhyolites. Based on the REE pattern, felsic rocks of these three targets can be classified belonging to the Nyssäkoski type porphyry. The Veikasenmaa type felsic porphyries seem to be missing in these areas.

All samples of Kiimakuusikko target are classified to the Nyssäkoski type porphyry based on geochemical assay, having the least REE-enriched nature in both LREE and HREE. As the number of samples shows (table 3), the Nyssäkoski porphyry dyke is very abundant in the target, with long intersections in drill core from the surface to drilled depths of 110 meters. In drill core, the Nyssäkoski porphyry occurs as network hosted by pervasively altered mafic volcanic rocks. Geochemically, all Kiimakuusikko samples plot to the rhyolite field in Jensen Cation diagram and AFM diagram (Figs. 16 and 17).

The samples from Väli-Kiima target are rhyolites. They can be classified to belong to the Veikasenmaa type by their REE-patterns. In comparison to Kiimakuusikko target, where felsic porphyries are classified as Nyssäkoski type and plots to the same location in the Jensen and AFM diagrams with the Väli-Kiima target, the difference is in the REE patterns distinguishing the samples of Väli-Kiima as older Veikasenmaa type. Also there is variation in the alkali-alumina ratio diagram (Fig. 18), indicating the Väli-Kiima samples are showing more intense sericitisation compared to the samples from Kiimakuusikko.

Kapsa target porphyry rocks can not be determined to be belonging to either of the known porphyry types of Kittilä suite, due to limited amount of drill cores. Further studies and determining the Kapsa type porphyry would require more extensive sampling and possibly zircon age determination study to see the relation to known porphyries of the area. With the acquired petrographical and geochemical data of this study, the porphyry at Kapsa target is named as plagioclase porphyry rock. The AFM diagram (Fig. 16) is the only geochemical diagram which divides the Kapsa samples in a distinct place between two major groups, including samples in both groups. In the petrographical studies, the Kapsa samples have more quartz-bearing, aphanitic matrix than other locations, which explains the geochemical separation from other groups and also the darkish, even black colour in hand sample. This indicates that the Kapsa type porphyry does not belong to either Veikasenmaa or Nyssäkoski type porphyry. The only common feature is the REE pattern (Fig. 20), where the Kapsa samples plot into the HREE-enriched Veikasenmaa group. The untypical features and narrow extent of the porphyry in Kapsa target makes it impossible to place in either known porphyry type; the samples could be a mix of porphyry and surrounding metavolcanic rocks, or a result of a deviant hydrothermal alteration, possibly due to the unspecified shear structure nearby, as Fig. 7 presents.

7.2 Hydrothermal alteration

Differences in alteration between targets are represented in alkali-alumina ratio diagram (Fig. 18), which suggests that albitisation and sericitisation are the two main alteration types in the felsic porphyries. Varying intensity and mineral assemblages of hydrothermal alteration makes macroscopical identification of the Nyssäkoski and Veikasenmaa porphyry types difficult.

Albitisation of the felsic porphyries and the hosting mafic volcanites occurred in D1-stage, followed by shearing and first gold mineralisation as arsenopyrite-hosted Au in D3 (Saalmann & Niiranen 2010). Final alteration in felsic rocks occurs as pervasive sericitation formed in deformation stage D5, with minor gold mineralisation as mineralised quartz veins (Saalmann & Niiranen 2010; Kämäräinen 2014). In the felsic porphyry samples of Hanhimaa area, all are altered with varying intensity of albitisation and sericitation, with gold in some samples in correlation with arsenic. This indicates that Au in the felsic rocks are hosted by arsenopyrite, and probably formed in the D3 stage major shear phase, after peak metamorphism in D2 (Saalmann & Niiranen 2010), which is typical to orogenic gold deposits (Goldfarb & Groves 2015).

7.3 Association of felsic porphyries and gold

In the felsic porphyries, sulphides occur locally in all target areas, and are mostly euhedral and undeformed pyrite with local arsenopyrite and stibnite. The most abundant arsenopyrite and As-bearing pyrite have been found in the targets located further from the Hanhimaa shear zone (Lisma, Siskeli and Kousa), with few anomalous high-As samples in the Kiimakuusikko and Kiimalaki targets.

Considering the proximity of the sampling locations to the shear, the prevailing theory of contacts from porphyry to greenstone belt mafic volcanic rocks acting as fluid flow channels and precipitation places (Groves et al. 2018) can be adapted to Kiimakuusikko target. Regularly occurring sulphidisation occurs in all samples at Kiimakuusikko and Siskeli-Kousa-Lisma, where the latter targets are so scarcely drilled and sampled that the true As-Au anomalies cannot be defined.

Table 5 presents the relations of arsenic and gold in the porphyry samples based on geochemistry. Most of the samples do not carry anomalous gold and arsenopyrite with exceptions to few samples from the Kiimakuusikko (0.1-0.3 ppm) and Kiimalaki mineralisation (0.7 ppm), indicating that the gold in felsic porphyries is probably refractory or closely linked to arsenopyrite, as gold in known mineralisation in Hanhimaa area generally occurs. The samples with higher Au and As belong to both Nyssäkoski and Veikasenmaa groups, indicating that there is no connection between gold and specific porphyry type.

Antimony is found in auriferous coarse-grained arsenopyrite-stibnite veins in the Nyssäkoski-type felsic porphyry dyke (Fig. 13) in Kiimakuusikko target, indicating later remobilization of sulphides and precipitation in younger generation felsic porphyries. Stibnite occurs as inclusions in euhedral, diamond-shaped arsenopyrite grains. As samples from other targets in proximity of the Hanhimaa shear zone (Kiimalaki, Kellolaki, Kello N and Väli-Kiima), the Kiimakuusikko samples have one of the highest enrichment of W and Sb (Fig. 21). The enrichment is due to proximity of the HSZ and caused the hydrothermal fluids flowed through the structure, creating remobilization of the elements into the porphyries as late, coarse-grained veins and vein networks.

However, the Kiimakuusikko target proves to be the most interesting location when considering the relation between possible Au mineralisation and the occurrence of felsic porphyrites. All the Kiimakuusikko samples can be classified as Nyssäkoski type, and they are rhyolitic in composition. In microscopical studies, most of the sulphides detected were pyrites, but the geochemical assay shows there is arsenic throughout the samples in all four Kiimakuusikko drill holes. These features make the Kiimakuusikko porphyries rather similar to the gold-bearing porphyrite dyke of Iso-Kuotko Au mineralisation, where common features are both being Nyssäkoski type porphyrites, chemically high-silica rhyolites with arsenopyrite-hosted gold, and located in the proximity of a major shear structure as the Hanhimaa Shear zone in Kiimakuusikko and the Kiistala Shear Zone in Iso-Kuotko (Molnár et al. 2018). Extensive drilling and abundance of the porphyries in the drill holes makes this target also very interesting regarding possible Au mineralisation in the contacts of porphyries. An inadequate feature is the narrowness of the porphyry units, making the contacts thin, where the amount of Au might be locally anomalous, but uncapable to form a mineralisation. Also the depth of the drilling programs completed in the area are shallow. To study the porphyrite gold contents more

detailed, a study focused directly to sampling the contacts would be necessary. The W and Sb enrichment and good correlation of Au-Ag and Ag-Cu makes the Kiimakuusikko target interesting example of complex hydrothermal fluid flow at the area, as the antimony occurs as stibnite inclusions in arsenopyrite and chalcopyrite, which also hosts the gold. The local redox trap theory by Pokrovski et al. (2002) is an intriguing theory of arsenopyrite creating a local redox trap, and could have potentially been affecting the other elements to precipitate in Kiimakuusikko target so intensively (Figs. 13 and 21), where especially antimony is highly enriched throughout the samples.

The Väli-Kiima samples are mostly Veikasenmaa type porphyry, with anomalously high silica composition. Hydrothermal alteration is mostly sericitation in this target, which indicates that the area was not altered as intensively as the others in the first stage of alteration occurring generally as albitisation. Two of the studied mafic metavolcanites hosting the felsic porphyries were detected to contain sulphides. Samples FIEXD117951 and FIEXD117952 from Väli-Kiima target are hydrothermally altered mafic metalavas with strong albite-, sericite and carbonate alteration, hosting a porphyry unit (sample FIEXD117952). Although there is only one example from the contact between the porphyry and mafic metavolcanites, there is distinguishable sulphidisation occurring condensed towards the contacts in the lava side. Sulphides include mainly pyrite with minor arsenopyrite. Geochemical assay for the volcanite samples show anomalous As, Sb, Cu and Ni in comparison to the porphyry, representing possible impure pyrite or arsenian pyrite in the altered mafic lavas. Väli-Kiima target is the only one showing clear proof of sulphide concentration into the contact zone of porphyry to mafic metavolcanites, with arsenopyrite and pyrite intensifying in the mafic volcanites towards the contact.

The Kiimalaki-Kellolaki-Kello North is a complex group with varying parameters, but all are unified by very proximal location at the Hanhimaa shear zone, and the intense deformation and alteration it has caused to the surrounding rocks. The group comprises of both Nyssäkoski and Veikasenmaa type porphyries, although in macroscopical perspective the samples seem very much alike due to pervasive hydrothermal alteration. Geochemical assay and especially the Jensen Cation plot and the AFM ternary plot provides confirmation of both Nyssäkoski dyke and Veikasenmaa subvolcanic porphyrite occurring at these locations. Both Kiimalaki and Kellolaki are recognised Au

mineralisation hosted by mafic metavolcanites, but the porphyries do not have any relation to gold based on the samples in this study.

8. CONCLUSIONS

Mineralogical study, geochemical analysis and plotting of the Hanhimaa area felsic porphyrites conclude in five statements:

- Felsic porphyry rocks in the gold occurrences can be correlated with both, the Nyssäkoski and Veikasenmaa types.
- Based on the types of felsic porphyry rocks and their mineralogical and geochemical features occurring in different target areas, five groups can be inferred: 1) Kiimalaki-Kellolaki-Kello N, 2) Siskeli-Kousa-Lisma, 3) Kiimakuusikko, 4) Väli-Kiima and 5) Kapsa. Of these, group 1 contains both older, rhyolitic-dacitic Veikasenmaa type subvolcanic porphyrite and younger, highly rhyolitic Nyssäkoski dyke porphyrite. Groups 2 and 3 are solely Nyssäkoski type, and group 4 Veikasenmaa type. Group 5 Kapsa type is separated from others and named as plagioclase porphyry rock with unidentified origin. Geochemically, all samples except Kapsa fit well into earlier studies of the Kittilä Suite felsic porphyrite geochemistry.
- Samples in the vicinity of the HSZ (Kiimakuusikko, Kiimalaki-Kellolaki-Kello N) are strongly hydrothermally altered with albitisation and sericitation as main alteration assemblages, and the samples further away show lesser alteration.
- Sulphidisation and possible Au mineralisation follow the intensity of alteration in the felsic porphyrites. Gold occurs scarcely and in low concentration in Kiimakuusikko and Kiimalaki; in samples belonging to both Nyssäkoski and Veikasenmaa type porphyrites. This indicates that in Hanhimaa shear zone, gold does not favour certain porphyry type.
- Occurrence and correlations of sulphides, Au and Ag show that gold occurs in typical setting of Au-Ag alloy hosted by arsenopyrite, except for Kiimakuusikko target where stibnite and chalcopyrite are present with arsenopyrite and Ag correlates with Cu, indicating atypical metal association for orogenic gold deposit.

Further, detailed work would be necessary to identify the Kapsa type more specific, including wider sampling and possible age determination study. When considering exploration, Kiimakuusikko as polymetallic Au occurrence and Lisma as arsenopyrite-hosted Au occurrence are the most interesting, when focusing on the felsic porphyrites.

9. ACKNOWLEDGMENTS

I would like to thank my supervisors Dr. Jukka-Pekka Ranta of University of Oulu and MSc., Exploration Geologist Veli-Pekka Kämäräinen of Agnico Eagle Finland Oy for all the good advices, help and support provided during the process of my thesis.

Agnico Eagle Finland Oy is thanked for providing me the most interesting topic to study, allowing access to drill cores and funding of the study. Exploration Manager Jyrki Korteniemi, Project Manager Jukka Välimaa, Senior Exploration Geologist Jari Ylinen and Exploration Geologist Johanna Paadar from Agnico Eagle Finland are thanked for all the support and excellent conversations regarding this study and geology in general. My fellow summer trainee geologists are thanked for great field days and experiences in Kittilä. The geotechnical staff at Agnico Eagle's logging hall in Pakatti is thanked for helping me track the drill cores needed for this study. Marko Moilanen and Leena Palmu from University of Oulu are thanked for the help with operating EPMA.

My warmest thanks goes to my family for all the help and encouragement during my studies.

References

Agnico Eagle Mines Limited, 2018. Detailed Mineral Reserves and Resources Data. Accessed 05.02.2020. Available at https://www.agnicoeagle.com/English/operations-and-development-projects/reserves-and-resources/default.aspx.

Davies J. F. and Whitehead R. E., 2006, Alkali-alumina and MgO-alumina molar ratios of altered and unaltered rhyolites: Exploration and Mining Geology, v. 15, p. 77-90.

Eilu, P.K., Mathison, C.I., Groves, D.I. and Allardyce, W. J. 1999. Atlas of Alteration Assemblages, Styles and Zoning in Orogenic Lode-Gold Deposits in a Variety of Host Rock and Metamorphic Settings. Geology and Geophysics Department (Centre for Strategic Mineral Deposits) & UWA Extension, The University of Western Australia, Publication 30, 50 pp.

Eilu, P., 2007. FINGOLD: Brief descriptions of all drilling-indicated gold occurrences In Finland − the 2007 data. Geological Survey of Finland, Report of Investigation 166, 35 pp.

Frost, B.R and Frost, C.D. 2014. Essentials of igneous and metamorphic petrology. Cambridge University Press, United States of America. 303 pp.

Gill, R. 2010. Igneous rocks and processes : a practical guide. Wiley-Blackwell, United Kingdom, 428 pp.

Gebre-Mariam, M., Hagemann, S.G., Groves, D.I., 1995. A classification scheme for epigenetic Archaean lode-gold deposits. Mineralium Deposita 30, 408–410.

Goldfarb, R.J., Phillips, G.N. and Nockleberg, W.J. 1998. Tectonic setting of synorogenic gold deposits of the Pacific Rim. Ore Geology Reviews, 13, 185–218.

Goldfarb, R.J., Groves, D.I. and Gardoll, S. 2001. Orogenic gold and geologic time: a global synthesis. Ore Geology Reviews 18, 1–75.

Goldfarb, R.J., Baker, T., Dubé, B., Groves, D.I., Hart, C.J.R., Gosselin, P., 2005. Distribution, character, and genesis of gold deposits in metamorphic terranes. Economic Geology 100th Anniversary, 407–450.

Goldfarb, R.J. and Groves, D.I. 2015. Orogenic gold: Common or evolving fluid and metal sources through time. Lithos 233, 2-26.

Groves, D.I. 1993. The Crustal continuum model for late-Archaean lode-gold deposits of the Yilgarn Block, Western Australia. Mineralium Deposita 28, 366–374.

Groves, D.I., Goldfarb, R.J., Gebre-Mariam, M., Hagemann, S.G. and Robert, F. 1998. Orogenic gold deposits: A proposed classification in the context of their crustal distribution and relationship to other gold deposit types: Ore geology reviews, v. 13, 7–27.

Groves, D.I., Santosh, M., Goldfarb, R.J. and Zhang, L. 2018. Structural geometry of orogenic gold deposits: Implications for exploration of world-class and giant deposits. Geoscience Frontiers, v. 9, 1163-1177

Haldar, S.K. and Tisljar, J. 2013. Introduction to Mineralogy and Petrology. Elsevier, Burlington, 328 pp.

Hanski, E., Huhma, H. and Vaasjoki, M. 2001.Geochronology of northern Finland: a summary and discussion. In: Vaasjoki, M. (ed.) 2001. Radiometric age determinations from Finnish Lapland and their bearing on the timing of Precambrian volcano-sedimentary sequences. Geological Survey of Finland, Special Paper 33, 279 pp.

Hanski, E., Huhma, H. 2005. Central Lapland Greenstone Belt. In: Lehtinen, M., Nurmi, P.A., Rämö, O.T. (eds.) Precambrian Geology of Finland – Key to Evolution of the Fennoscandian Shield. Elsevier, Amsterdam, p. 139–194.

Huhma, H., Hanski, E., Kontinen, A., Vuollo, J., Mänttäri, I. and Lahaye, Y. 2018. Sm-Nd and U-Pb isotope geochemistry of the Palaeoproterozoic mafic magmatism in eastern and northern Finland. Geological Survey of Finland, Bulletin 405, 150 pp.

Hölttä, P., Väisänen, M., Väänänen, J. and Manninen, T., 2007. Paleoproterozoic metamorphism and deformation in Central Lapland, Finland. In: Ojala, V.J. (ed.) Gold in the Central Lapland Greenstone Belt. Geological Survey of Finland, Special Paper 44, 7-56.

Irvine, T.N., Baragar, W.R.A. 1971. A guide to the chemical classification of the common volcanic rocks. Canadian Journal of Earth Sciences 8, 523–548.

Jensen, L.S. 1976. A new cation plot for classifying subalkalic volcanic rocks. Ontario Geological Survey, Miscellaneous Paper 66, 22 s.

Konnunaho, J., Halkoaho, T., Hanski, E., Törmänen, T. 2015. –Komatiite-hosted Ni-Cu-PGE deposits in Finland. In: Maier, W.D., Lahtinen, R., O'Brien, H. (eds.) Mineral Deposits of Finland, Elsevier, Amsterdam, s. 93-131.

Kuronen, U. 1980. Kapsajoki-kohteen tutkimukset vuosina 1980-1983. Lapin Malmi Oy, Report 030/2743/UOK/83/18, 9 pp.

Kämäräinen, V-P., 2014. Kittilän Kiimalaen alueen hydrotermisesti muuttuneista kivistä. Master's thesis, Department of Geology and Geography, University of Turku, 125 pp.

Köykkä, J., Lahtinen, R. and Huhma, H. 2019. Provenance evolution of the Paleoproterozoic metasedimentary cover sequences in northern Fennoscandia: Age distribution, geochemistry, and zircon morphology. Precambrian Research 331, 21 pp.

Le Bas, M. J., Le Maitre, R. W., Streckeisen, A. Zanettin, B. 1986. A chemical classification of volcanic rocks based on the total alkali–silica diagram. Journal of Petrology 27, 745–750.

Le Maitre, R. W. and International Union of Geological Sciences, 2002. Igneous Rocks: A Classification and Glossary of Terms: Recommendations of the International Union of Geological Sciences Subcommission on the Systematics of Igneous Rocks. Cambridge, U.K.: Cambridge University Press

Lehtonen, M., Airo, M-L., Eilu, P., Hanski, E., Kortelainen, V., Lanne, E., Manninen, T., Rastas, P., Räsänen, J., and Virransalo, P., 1998. Kittilän vihreäkivialueen geologia. Lapin vulkaniittiprojektin raportti. Summary: The

stratigraphy, petrology and geochemistry of the Kittilä greenstone area, Northern Finland. Geological Survey of Finland, Report of Investigation 140, 144 pp.

Luukas, J., Kousa, J., Nironen, M. and Vuollo, J., 2017. Major stratigraphic units in the bedrock of Finland, and an approach to tectonostratigraphic division. In: Nironen, M. (ed.) Bedrock of Finland at the Scale 1:1 000 000 - Major Stratigraphic Units, Metamorphism and Tectonic Evolution. Geological Survey of Finland, Special Paper 60, 90-40.

McCuaig, T.C. and Kerrich, R. 1998. P-T-t-deformation-fluid charasteristics of lode gold deposits: evidence from alteration systematics. Ore Geology Reviews, 12, 381–453.

Molnár, F., Middleton, A., Stein, H., O'Brien, H., Lahaye, Y., Huhma, H., Pakkanen, L. and Johanson, B. 2018. Repeated syn- and post-orogenic gold mineralisation events between 1.92 Ga and 1.76 Ga along the Kiistala Shear Zone in the Central Lapland Greenstone Belt, northern Finland. Ore Geology Reviews, 101, 936-959.

Mikkola, A. 2006. Kittilän vihreäkivialueen happamat porfyyrit. Master's thesis, Department of Geology, University of Oulu, 119 pp.

MS Analytical Inc. 2019. Schedule of Services. Geochemical Laboratory Services. Brochure. Available at https://msalabs.com/resources/brochures/

Nenonen, M., 2018. Mafisten ja ultramafisten vulkaniittien petrologia Kittilän alueella. Master's thesis, Oulu Mining School, University of Oulu, 151 pp.

Niiranen, T., Lahti, I., Nykänen, V. 2015. Chapter 10.2 - The Orogenic Gold Potential of the Central Lapland Greenstone Belt, Northern Fennoscandian Shield. In: Maier, W.D., Lahtinen, R., O'Brien, H. (eds.) Mineral Deposits of Finland, Elsevier, Amsterdam, s. 733-752.

Nironen, M. (ed.) 2017. Bedrock of Finland at the scale 1:1 000 000 - Major stratigraphic units, metamorphism and tectonic evolution. Geological Survey of Finland, Special Paper 60, 128 pp.

Phillips, G. & Powell, R. 2009. Formation of gold deposits: Review and evaluation of the continuum model. Earth-Science Reviews 94, 1-21.

Pirajno, F. 2009. Hydrothermal Processes and Mineral Systems. Springer, Netherlands, 1250 pp.

Pokrovski, G.S., Kara, S., and Roux, J., 2002. Stability and solubility of arsenopyrite, FeAsS, in crustal fluids. Geochimica et Cosmochimica Acta 66, 2361-2378.

Rastas, P., Huhma, H., Hanski, E., Lehtonen, M.I., Härkönen, I., Kortelainen, V., Mänttäri, I. and Paakkola, J. 2001. U-Pb isotopic studies on the Kittilä greenstone area, central Lapland, Finland. In: Vaasjoki, M. (ed.) 2001. Radiometric age determinations from Finnish Lapland and their bearing on the timing of Precambrian volcano-sedimentary sequences. Geological Survey of Finland, Special Paper 33, 279 pp.

Robb, L., 2005. Introduction to Ore-forming Processes. Blackwell Publishing, Malden, 373 pp.

Rollinson, H. R., 1993. Using geochemical data: Evaluation, presentation, interpretation. Harlow, Longman, 352 pp.

Saalmann, K. and Niiranen, T., 2010. Hydrothermal alteration and structural control on gold deposition in the Hanhimaa shear zone and western part of the Sirkka Line. Geological Survey of Finland, Report M19/2741/2010/58, 35 pp.

Stanley, C.R. 2017. Molar Element Ratio Analysis of Lithogeochemical Data: A toolbox for Use in Mineral Exploration and Mining. In: Tschirhart, V. and Thomas, M.D. (eds.) Proceedings of Exploration 17: Sixth Decennial International Conference on Mineral Exploration, pp.471-494

Sun, S.-S., McDonough, W.S. 1989. Chemical and isotopic systematics of oceanic basalts: implications for mantle composition and processes. Geological Society, London, Special Publications, 42(1), 313-345.

Wyche, N., Eilu, P., Koppström, K., Kortelainen, V., Niiranen, T. and Välimaa, J., 2015. The Suurikuusikko gold deposit (Kittilä Mine), northern Finland. In: Maier, W.D., Lahtinen, R., O'Brien, H. (eds.) Mineral Deposits of Finland. Elsevier B.V., Amsterdam, pp. 411-433.

Digital map database for bedrock geology of Finland [electronic resource], Geological Survey of Finland. (Version dated 3.5.2017, version 2.1) Available: https://hakku.gtk.fi

APPENDIX 1.

Thin section description for thesis

Sample ID	Thin section ID	Hole ID	Target	Start depth
FIEXD117951	001	HAM18011	Väli-Kiima	40.45

Altered mafic volcanic rock, primary composition tholeiitic lava. Grain sixe aphanitic with crosscutting quartz-carbonate veining. Albitisation, carbonatisation and sericitation strong. Sulphide dissemination, mainly pyrite. Host rock of felsic porphyry sample FIEXD117952 HAM002, same alteration zone with FIEXD117953 HAM003.

FIEXD117952	002	HAM18011	Väli-Kiima	44.45

Quartz-plagioclase porphyry. Matrix aphanitic and cut by alteration bands of sericite and carbonates. Phenocrysts 0.5-2.0 mm are plagioclase and quartz, shape rounded. Plagioclase grains show twinning. Sulphides as scant dissemination of pyrite.

FIEXD117953	003	HAM18011	Väli-Kiima	56.20

Altered mafic volcanic rock, primary composition tholeiitic lava. Grain size aphanitic. Same alteration zone as sample FIEXD117951, but less altered. Sulphides mainly pyrite and occur as banded dissemination and shattered grain clusters along alteration fluid flow direction.

FIEXD117954	004	HAM18007	Siskeli	50.20

Quartz-plagioclase porphyry rock. Aphanitic, phenocrysts are shattered and sized 0.2-0.5 mm. Along quartz and plagioclase porphyries the sample contain black, lineated phenocrysts of amphibole and biotite. This mineralogical composition is typical to Nyssäkoski type veins. No sulphides.

FIEXD117955 005 543-VHO-2018 Siskeli surface (trench)

Quartz-plagioclase porphyry rock. Aphanitic, quartz and plagioclase phenocrysts shattered, size 0.2-1.0 mm. Some plagioclase crystals show twinning. Contains dark lineated amphibole and biotite. This sample is the only trench sample of the study, and due to weathering and alteration, the sample is overprinted by strong rusty fe-carbonatisation. Rusting implies occurrence of sulphides that are weathered or oxidized and eroded out.

FIEXD117956 006 KTAHAM-50 Kiimakuusikko 30.60

Altered mafic volcanic rock, primary composition tholeiitic. Pervasive albitisation alteration. Abundant sulphide dissemination of cubic and hexagonal pyrite with needle-shaped arsenopyrite or arsenic-bearing pyrite and chalcopyrite as linings on other sulphide grains. Host rock of sample FIEXD117957 HAM007 with sharp contacts.

FIEXD117957 007 KTAHAM-50 Kiimakuusikko 36.60

Quartz-plagioclase porphyry rock. Texture aphanitic, colour light possibly due to alteration. Quartz and plagioclase phenocrysts shattered by alteration minerals sericite, chlorite and carbonate, grain size 0.3-1.0 mm. Moderate sulphide dissemination of euhedral pyrite.

FIEXD117958 008 KTAHAM-50 Kiimakuusikko 98.40

Quartz-plagioclase porphyry rock. Texture aphanitic, colour darker and phenocrysts more intact than sample FIEXD117957 HAM007 from same drill hole. Quartz and plagioclase phenocrysts size 0.1-3.0 mm, twinning in largest plagioclase crystals. No sulphides. Alteration minerals mainly carbonates with weak chloritisation.

FIEXD117959 009 KTAHAM-46 Kiimakuusikko 54.30

Quartz-plagioclase porphyry rock, unaltered. Texture very fine grained, matrix has visible crystals, which have not been altered to aphanitic mass as previous samples, and is very quartz-bearing. Quartz and plagioclase phenocrysts distinctively large, 2.0-7.0 mm. Plagioclase phenocrysts are rather shattered and cloudy. Sulphides occur as weak dissemination of rounded pyrite grains.

FIEXD117960 010 KTAHAM-46 Kiimakuusikko 97.95

Quartz-plagioclase porphyry rock. Matrix aphanitic and quartz-bearing, phenocrysts are rather large quartz and cloudy, altered plagioclase with some amphiboles; size 0.2-6.0 mm. Alteration minerals include chlorite, sericite and biotite. Sulphides occur as scant dissemination of subhedral, slightly rounded pyrite.

FIEXD117961 011 KTAHAM-46 Kiimakuusikko 108.40

Quartz-plagioclase porphyry rock. Aphanitic, quartz and plagioclase phenocrysts 0.1-1.0 mm. Plagioclase grains are cloudy and sericite-bearing. Sulphides occur as fine dissemination of euhedral, cubic pyrite.

FIEXD117962 012 KTAHAM-46 Kiimakuusikko 114.40

Quartz-plagioclase porphyry rock. Aphanitic, quartz and plagioclase phenocrysts 0.1-0.5 mm. Rather strong alteration throughout the thin section, only largest quartz porphyries are intact. Few shattered, deformed pyrite grains.

FIEXD117963 013 KTAHAM-52 Kiimakuusikko 10.60

Quartz-plagioclase porphyry rock. Aphanitic, matrix-bearing. Phenocrysts quartz and plagioclase, size 0.2-0.5 mm. Intensive alteration. Sulphides occur as rare grains of pyrite, which are rounded and shattered. Contains late, post-alteration thin quartz-carbonate veins.

FIEXD117964 014 KTAHAM-52 Kiimakuusikko 83.70

Quartz-plagioclase porphyry rock. Aphanitic, phenocrysts mainly altered, cloudy plagioclase sized 0.2-0.5 mm. Few pyrite grain clusters.

FIEXD117965 015 KTAHAM-52 Kiimakuusikko 88.80

Quartz-plagioclase porphyry rock. Colour more greyish in hand sample, the sample is less altered than others from same drill core KTAHAM-52 are. Aphanitic, phenocrysts size 0.2-1.0 mm. Sulphides occur as few subhedral pyrite grains.

FIEXD117966 016 KTAHAM-52 Kiimakuusikko 104.40

Quartz-plagioclase porphyry rock. Aphanitic, plagioclase and quartz phenocrysts size 0.2-5.0 mm, where the largest are quartz grains. Few subhedral, shattered pyrite grains.

no wra 017 KTAHAM-47 Kiimakuusikko 81.80

Auriferous stibnite vein in felsic porphyry rock. Only thin section and ore analysis. Contains large grains of stibnite and pyrite in quartz-carbonate vein, hosted by quartz-plagioclase porphyry rock. Stibnite has inclusions of chalcopyrite. Microscopically visible gold nuggets in stibnite.

FIEXD117967 018 KTAHAM-47 Kiimakuusikko 17.00

Quartz-plagioclase porphyry rock. Aphanitic, groundmass is quartz rich. Few larger plagioclase and quartz phenocrysts sized 1.0 – 3.0 mm. Plagioclase phenocrysts are strongly altered, some show twinning. Sulphides occur as scant dissemination of pyrite. The hand sample has stibnite as splinter bundles along fracture surface, most likely post-alteration and post-Au-mineralisation.

FIEXD117968 019 KTAHAM-47 Kiimakuusikko 85.60

Quartz-plagioclase porphyry rock. Aphanitic, phenocrysts size 0.3-3.0 mm. Twinning in plagioclase porphyries. Few fractured pyrite grains.

FIEXD117969 020 HAM16004 Väli-Kiima 151.60

Quartz-plagioclase porphyry rock. Very aphanitic, matrix is slightly lineated. Phenocrysts 1.0-4.0 mm, plagioclase phenocrysts almost completely altered to sericite. Sulphides occur as fractured pyrite and fine, scant dissemination of subhedral arsenopyrite.

FIEXD117970 021 HAM16004 Väli-Kiima 158.00

Plagioclase porphyry rock. Very aphanitic, matrix and phenocrysts strongly lineated. Contains no quartz porphyries, but the matrix is quartz-bearing. Plagioclase phenocrysts completely altered to sericite, primary mineral detected from twinning structure. Even dissemination of rounded pyrite.

FIEXD117971 022 HAM17005 Lisma 244.20

Quartz-plagioclase porphyry rock. Aphanitic with small phenocrysts of strongly altered plagioclase and quartz. Matrix is more albitised than in other targets. Hand sample colour very greenish, which shows in thin section as strong sericitation. Fine, scant dissemination of arsenopyrite.

FIEXD117972 023 HAM17005 Lisma 250.60

Quartz-plagioclase porphyry rock. Aphanitic, matrix lineated. Phenocrysts mainly plagioclase with few quartz, lineated along the matrix lineation. Fine, scant dissemination of arsenopyrite.

FIEXD117973 024 KTAHAM-25 Kellolaki 22.90

Quartz-plagioclase porphyry rock. Aphanitic, matrix-bearing, phenocrysts lineated and pervasively altered. Sulphides occur as dissemination of pyrite.

FIEXD117974 025 KTAHAM-25 Kellolaki 33.00

Quartz-plagioclase porphyry rock. Aphanitic, matrix is very quartz-rich. Phenocrysts sized 0.2-2.0 mm and less altered than previous sample FIEXD117973 HAM024. Plagioclase phenocrysts show twinning, sericitation weaker than generally, albitisation moderate and makes the hand sample very pale in colour. Dissemination of fine, rounded pyrite.

FIEXD117975 026 KTAHAM-34 Kiimalaki 12.80

Quartz-plagioclase porphyry rock. Aphanitic, phenocrysts of quartz and plagioclase sized 0.2-1.0 mm. Plagioclase shows twinning. Sericitation occurs as lineated bands. Contains thin, post-alteration quartz-calcite veins. Scant dissemination of rounded pyrite.

FIEXD117976	027	KTAHAM-34	Kiimalaki	69.50

Quartz-plagioclase porphyry rock. Aphanitic, phenocrysts sized 0.2-3.0 mm. Alteration very strong on matrix and phenocrysts; sericite and albite dominated. Contains moderate dissemination of quite large euhedral arsenopyrite and rounded, shattered pyrite.

FIEXD117977	028	KTAHAM-34	Kiimalaki	94.90

Quartz-plagioclase porphyry rock. Aphanitic, matrix-bearing, few phenocrysts of quartz, plagioclase and amphibole sized 0.2-0.5 mm. Slightly lineated alteration minerals sericite, albite and carbonate. Scant dissemination of rounded pyrite.

FIEXD117978	029	KTAHAM-29	Kiimalaki	79.40

Quartz-plagioclase porphyry rock. Aphanitic, matrix-bearing and quartz-rich. Phenocrysts of quartz and plagioclase are size 0.1-0.4 mm. Scant dissemination of rounded pyrite.

FIEXD117979	030	KTAHAM-29	Kiimalaki	88.40

Quartz-plagioclase porphyry rock. Aphanitic, matrix-bearing. Phenocrysts 0.1-0.3 mm, plagioclase shows twinning. Abundant sericited quartz vein network. Dissemination of subhedral pyrite.

FIEXD117980	031	HAM13014	Kellolaki	48.20

Quartz-plagioclase porphyry rock. Hand sample is quite dark and greenish grey in colour, which indicates weaker albitisation in comparison to typical beige-greenish strongly altered samples. Aphanitic, phenocrysts are quartz, plagioclase and lineated biotite, sized 0.2-0.5 mm. Few rounded pyrite grains.

FIEXD117981 032 HAM13013 Kellolaki 68.00

Quartz-plagioclase porphyry rock. Aphanitic, quartz and plagioclase phenocrysts 0.1-0.3 mm, slightly lineated and almost entirely replaced by alteration minerals, majorly sericite. Very weak dissemination of pyrite.

FIEXD117982 033 HAM13013 Kellolaki 89.40

Quartz-plagioclase porphyry rock. Aphanitic, phenocrysts generally 0.2-0.5 mm with one 1 cm wide plagioclase grain. Dissemination of rather large, euhedral-subhedral pyrite.

FIEXD117983 034 HAM13013 Kellolaki 96.00

Quartz-plagioclase porphyry rock. Aphanitic, phenocrysts are quartz, plagioclase and amphibole with bluish tint in crossed polars. Phenocrysts sized 0.2-0.5 mm. Fine dissemination of rounded pyrite.

FIEXD117984 035 HAM13013 Kellolaki 139.00

Quartz-plagioclase porphyry rock. Aphanitic, matrix contains abundant schists (sericite, biotite) that are lineated. Phenocrysts of quartz and plagioclase are 0.1-0.5 mm. Few rounded pyrite grains.

FIEXD117985 036 HAM17016 Kousa 114.20

Quartz-plagioclase porphyry rock. Aphanitic, matrix is lineated. Phenocrysts mainly cloudy plagioclase with minor quartz, size 0.1-0.3 mm and shape rather rounded. Few cubic pyrite grain clusters.

FIEXD117986 037 HAM17016 Kousa 122.50

Quartz-plagioclase porphyry rock. Aphanitic, more abundant quartz phenocrysts in comparison to sample FIEXD117985 HAM036, which is from same felsic porphyry vein. Alteration is also stronger in this sample. Quartz, plagioclase and amphibole phenocrysts are sized 0.2-2.5 mm. Sulphides occur as moderate dissemination of cubic pyrite and euhedral, angular arsenopyrite.

FIEXD117987 038 HAM17016 Kousa 136.05

Quartz-plagioclase porphyry rock. Sample is from same continuous felsic porphyry vein than two previous samples FIEXD117985 and -986, HAM036 and -037. Matrix is aphanitic and finer than the two upper samples from same vein. Phenocrysts are mainly large quartz, with minor plagioclase and amphibole, sized 0.3-6.0 mm. Sulphides occur as moderate dissemination of arsenopyrite and pyrite.

FIEXD117988 039 HAM17009 Kellolaki 91.00

Quartz-plagioclase porphyry rock. Aphanitic, structure is lineated by alteration minerals sericite and carbonate. Phenocrysts of quartz, plagioclase and amphibole are rather small, 0.1-0.3 mm and shattered. Pyrite occurs as banded dissemination following the sericite bands. The sample is hosted by hydrothermally altered mafic tuff and has distinctively sharp contacts to the vein.

FIEXD117989 040 HAM17009 Kellolaki 142.80

Quartz-plagioclase porphyry rock. Aphanitic, almost glassy texture. Phenocrysts of quartz and plagioclase shattered by hydrothermal alteration and size is 0.2-0.5 mm. Few euhedral, sharp arsenopyrite grains.

FIEXD117990 041 HAM17003 Lisma 78.80

Quartz-plagioclase porphyry rock. Aphanitic texture in matrix, that is quartz-bearing. Phenocrysts of quartz and plagioclase are shattered, size 0.2-0.6 mm. No sulphides. Sample is hosted by hydrothermally altered mafic tuff.

FIEXD117991 042 HAM14016 Kiimalaki 268.50

Quartz-plagioclase porphyry rock. Aphanitic texture, phenocrysts sized 0.2-0.5 mm. Contains impure carbonate inclusions, colour in hand sample is emerald green, and in thin section typical pastel calcite colour and lamellae texture. Sulphides as scant dissemination of rounded pyrite.

FIEXD117992 043 HAM14016 Kiimalaki 333.00

Quartz-plagioclase porphyry rock. Aphanitic, almost glassy texture. Phenocrysts are strongly altered and lineated. Alteration minerals include abundant amount of carbonate, in matrix and in lineated fe-carbonate layers, in comparison to typical altered vein samples. No sulphides.

FIEXD117993 044 HAM17001 Lisma 141.80

Quartz-plagioclase porphyry rock. Aphanitic, contains fair amount of quartz and plagioclase phenocrysts, sized 0.2-2.0 mm. Plagioclase crystals show twinning. Sample contains few thin, post-alteration quartz-carbonate veins that have remained intact. Contains few large grains of cubic pyrite.

FIEXD117994	045	KAP14001	Kapsa	85.90

Quartz-plagioclase-amphibole porphyry rock. Aphanitic matrix with abundant phenocrysts sized 0.2-3.0 mm. Amphibole phenocrysts are mostly hornblende, which is partially altered to biotite. Pyrite occurs as broken grains.

FIEXD117995	046	KAP14001	Kapsa	159.10

Quartz-plagioclase-amphibole porphyry rock. Matrix aphanitic, abundant phenocrysts. Amphibole phenocrysts are altered to biotite and one large grain to berlin blue chlorite. Hydrothermal alteration is stronger in this sample than the previous FIEXD117994 HAM045 from the same drill core. Sulphides are pyrite, arsenopyrite and chalcopyrite, occurring together as grain clusters.

FIEXD117996	047	KAP14001	Kapsa	175.50

Quartz-plagioclase-amphibole porphyry rock. Matrix aphanitic, abundant phenocrysts. Some amphiboles are altered to biotite and blue chlorite. Arsenopyrite, pyrite and chalcopyrite occur as shattered grain clusters.

FIEXD117997	048	KAP14004	Kapsa	62.30

Quartz-plagioclase-amphibole porphyry rock. Matrix aphanitic, abundant phenocrysts. Amphiboles altered to biotite and blue chlorite. Plagioclase phenocrysts show twinning. Alteration intensity is weaker than samples from drill hole KAP14001. Contains pyrite and minor chalcopyrite as shattered grains.

FIEXD117998	049	KAP14004	Kapsa	67.00

Quartz-plagioclase-amphibole porphyry rock. Matrix aphanitic, abundant phenocrysts. Plagioclase phenocrysts show twinning, and are more abundant than in previous sample. Sulphides are pyrite and minor chalcopyrite, as shattered grains.

FIEXD117999 050 KAP14004 Kapsa 91.10

Quartz-plagioclase-amphibole porphyry rock. Matrix aphanitic, phenocrysts rather small but they seem to form clusters, which shows in the hand sample as clumpy texture. Sulphides are mainly pyrite, occurring as fractured and shattered grains.

FIEXD118000 051 KAP14004 Kapsa 220.80

Quartz-plagioclase-amphibole porphyry rock. Matrix aphanitic, abundant phenocrysts. Plagioclase phenocrysts show twinning and also zonation structures. Amphibole phenocrysts are altered to biotite. Few tiny pyrite grains.

FIEXD143571 052 HAM14003 Väli-Kiima 155.70

Quartz-plagioclase porphyry rock. Matrix aphanitic, phenocrysts are size 0.1-5.0 mm. Sericite alteration occurs as lineated bands in the matrix. Plagioclase phenocrysts show twinning, and are shattered by alteration minerals sericite, albite and carbonates. Pyrite occurs as broken cubic grains.

FIEXD143572 053 HAM14003 Väli-Kiima 200.80

Quartz-plagioclase porphyry rock. Aphanitic, almost glassy matrix. Phenocrysts scant and strongly altered, sized 0.1-0.8 mm. Phenocrysts include few altered amphibole grains, most likely hornblende. Pyrite occurs as fine dissemination of rounded, small grains.

FIEXD143573 054 HAM18005 Siskeli 12.60

Quartz-plagioclase porphyry rock. Aphanitic, matrix-bearing. Phenocrysts are scant and rather small, 0.1-0.3 mm. Matrix has a needle-like texture in comparison to the usual rounded. Alteration minerals include fe-carbonatisation due to the shallow depth of the sample in drill core. No sulphides.

FIEXD143574 055 HAM18005 Siskeli 10.20

Quartz-plagioclase porphyry rock. Aphanitic, matrix-bearing with small phenocrysts. Needle-like texture in matrix, similar to previous sample FIEXD142573 HAM054. No sulphides.

APPENDIX 2. Whole-rock major- and trace element analyses

	Passing	Al2O3_%	BaO_%	CaO_%	Cr2O3_%	Fe2O3_%	K2O_%	MgO_%	MnO_%	Na2O_%	P2O5_%	SiO2_%	SrO_%	TiO2_%	LOI_%	Total_%	TC_%	TS_%
FIEXD117951	93	14.87	0.27	10.22	0.03	7.75	3.53	3.46	0.2	1.11	0.07	40.05	0.02	1.09	16.26	98.93	4.11	0.18
FIEXD117952		14.85	0.09	2.77	<0.01	2.49	2.19	0.9	0.05	3.79	0.08	65.69	0.03	0.32	5.38	98.63	1.11	0.03
FIEXD117953		11.63	0.06	8.42	<0.01	10.73	2.26	5.49	0.16	0.14	0.1	42.65	0.02	1.2	15	97.86	3.51	0.19
FIEXD117954		15.34	0.09	2.37	<0.01	2.39	2.71	0.97	0.04	3.9	0.09	66.02	0.02	0.35	3.91	98.2	0.56	<0.01
FIEXD117955		16.97	0.04	0.41	<0.01	2.11	1.76	0.13	0.07	6.36	0.05	69.88	0.01	0.28	2.24	100.3	0.08	<0.01
FIEXD117956		11.74	0.05	11.03	0.01	11.11	3.75	5.13	0.28	0.24	0.19	37.25	0.04	1.85	16.13	98.81	4.4	3.73
FIEXD117957		14.59	0.09	3.1	<0.01	2.63	2.31	0.89	0.07	4.02	0.08	66.53	0.05	0.31	5.23	99.9	1.15	0.13
FIEXD117958		14.17	0.06	4.86	<0.01	2.22	2.89	0.86	0.05	3.07	0.07	64.03	0.03	0.28	6.27	98.86	1.43	0.09
FIEXD117959		15.66	0.05	2.96	<0.01	2.48	0.9	1.06	0.03	5.4	0.09	69.23	0.07	0.33	3.16	101.42	0.44	0.07
FIEXD117960		15.23	0.09	2.8	<0.01	2.56	2.29	0.93	0.06	3.95	0.08	66.73	0.03	0.33	6.07	101.15	1.29	0.18
FIEXD117961		11.95	0.07	5.28	<0.01	7.9	3.31	1.45	0.23	0.45	0.06	57.57	0.01	0.26	9.53	98.08	2.34	1.65
FIEXD117962		14.32	0.05	3.02	<0.01	2.9	2.07	0.93	0.07	4.27	0.07	66.53	0.03	0.3	5.09	99.66	1.15	0.43
FIEXD117963		14.32	0.05	3.42	<0.01	2.82	2.55	0.99	0.05	3.34	0.07	64.76	0.04	0.32	5.5	98.25	1.21	0.4
FIEXD117964		14.42	0.05	3.25	<0.01	3.28	2.32	1.01	0.08	4.01	0.07	63.82	0.04	0.29	5.52	98.16	1.31	0.44
FIEXD117965		14.28	0.05	4.28	<0.01	2.87	1.66	0.74	0.05	4.41	0.07	68.01	0.05	0.28	4.37	101.13	0.93	0.54
FIEXD117966		14.65	0.08	4.33	<0.01	1.9	2.16	0.67	0.04	4.1	0.07	64.35	0.05	0.29	5.91	98.59	1.3	0.07
FIEXD117967		14.49	0.04	3.14	<0.01	2.63	2.12	1.12	0.07	4.11	0.07	64.45	0.03	0.31	5.44	98.02	1.22	0.19
FIEXD117968		15.41	0.08	3.12	<0.01	2.81	2.71	0.93	0.07	3.64	0.08	65.88	0.05	0.32	5.57	100.66	1.19	0.09
FIEXD117969		15.68	0.08	2.82	<0.01	2.28	2.35	0.91	0.09	3.43	0.09	65.67	0.03	0.34	5.74	99.49	1.11	0.08
FIEXD117970	87	14.37	0.07	3.58	<0.01	2.86	2.21	0.99	0.08	1.22	0.07	68.71	0.03	0.21	7.22	101.6	1.41	0.03
FIEXD117971		14.96	0.13	2.68	<0.01	2.48	4.05	1.19	0.05	1.69	0.06	68.41	0.01	0.24	5.7	101.67	1.02	<0.01
FIEXD117972		14.85	0.11	4.14	<0.01	2.14	2.78	1	0.05	3.87	0.06	66.53	0.02	0.24	5.56	101.32	1.19	<0.01
FIEXD117973		15.1	0.1	5.99	<0.01	4.55	2.5	2.24	0.12	3.7	0.13	55.5	0.03	0.5	9.81	100.25	2.5	0.1
FIEXD117974		13.69	0.03	8.05	<0.01	4.7	1.2	3.27	0.18	5.61	0.06	52.31	0.01	0.2	12.08	101.38	3.27	0.02
FIEXD117975		16.05	0.11	5.64	<0.01	4.29	3.3	2.11	0.17	2.62	0.12	57.12	0.02	0.5	9.38	101.44	2.27	0.04
FIEXD117976		14.97	0.09	5.25	<0.01	6.08	2.82	2.06	0.12	2.52	0.14	55.54	0.02	0.53	9.37	99.51	2.16	1.49
FIEXD117977		15.52	0.11	5.01	<0.01	4.76	3.43	1.87	0.12	1.8	0.13	57.99	0.02	0.48	9.27	100.51	2.07	0.09
FIEXD117978		13.45	0.05	1.59	<0.01	2.07	2.21	0.73	0.06	3.38	0.04	74.39	0.01	0.09	3.37	101.44	0.67	0.27
FIEXD117979		14.13	0.06	1.31	<0.01	1.61	2.14	0.55	0.05	4.06	0.04	71.12	0.02	0.09	3.24	98.4	0.57	0.09
FIEXD117980		16.07	0.17	3.34	<0.01	4.54	3.27	1.9	0.09	2.4	0.15	61.58	0.02	0.48	6.65	100.66	1.34	0.08
FIEXD117981		14.72	0.14	3.95	<0.01	2.84	3.09	1.37	0.06	1.13	0.11	63.95	0.02	0.31	7.39	99.08	1.57	0.04
FIEXD117982		15.21	0.18	5.07	<0.01	5.95	2.64	2.44	0.14	3.17	0.15	54.81	0.04	0.62	10.21	100.63	2.56	0.07
FIEXD117983		15.6	0.16	5.32	<0.01	5.94	2.35	2.35	0.13	3.37	0.16	56	0.04	0.58	9.98	101.99	2.4	0.07
FIEXD117984		15.44	0.21	4.45	<0.01	4.88	3.6	2.11	0.14	1.79	0.15	58.79	0.02	0.52	8.36	100.47	1.81	0.11
FIEXD117985		15.19	0.05	2.97	<0.01	1.82	2.42	0.53	0.04	4.82	0.06	67.18	0.02	0.29	4.02	99.42	0.84	0.15
FIEXD117986		14.31	0.03	1.34	<0.01	1.8	2.79	0.47	0.04	3.59	0.05	73.38	0.01	0.17	3.02	101	0.45	0.29
FIEXD117987		13.71	0.03	2.26	<0.01	1.87	2.74	0.55	0.06	3.28	0.05	70.93	0.02	0.17	4.08	99.74	0.76	0.22
FIEXD117988		14.84	0.07	3.66	<0.01	2.94	2.48	1.54	0.06	3.79	0.09	64.97	0.02	0.35	7.15	101.97	1.58	0.04
FIEXD117989		14.95	0.05	2.84	<0.01	2.07	2.11	1.19	0.04	4.1	0.06	66.5	0.01	0.25	5.88	100.05	1.24	<0.01
FIEXD117990	93	14.94	0.05	2.75	<0.01	2.06	2.34	1.14	0.04	4.26	0.06	67.72	0.02	0.23	5.47	101.06	1.21	0.02
FIEXD117991		12.65	0.1	9.64	0.01	7.47	3.31	4.66	0.24	0.84	0.25	43.7	0.02	1.01	17.88	101.76	4.51	0.05
FIEXD117992		14.73	0.15	4.62	<0.01	3.41	3.93	2.07	0.12	0.71	0.14	61.63	0.01	0.38	9.53	101.42	2.05	<0.01
FIEXD117993		14.52	0.08	2.85	<0.01	2.05	2.58	0.97	0.05	4.25	0.06	66.23	0.01	0.22	5.01	98.88	1	0.01
FIEXD117994		16.76	0.08	4.67	<0.01	3.96	1.51	1.89	0.05	4.66	0.11	65.81	0.1	0.45	1.84	101.88	0.05	0.11
FIEXD117995		16.51	0.07	3.98	<0.01	3.47	1.31	2.27	0.04	5.34	0.11	64.22	0.08	0.44	2.32	100.16	0.19	0.49
FIEXD117996		16.6	0.02	4.49	<0.01	3.4	0.48	2.05	0.04	5.92	0.11	64.93	0.09	0.43	2.11	100.67	0.28	0.57
FIEXD117997		16.36	0.09	3.12	<0.01	3.04	2.02	1.9	0.05	6.2	0.11	64.06	0.06	0.43	1.51	98.95	0.14	0.14
FIEXD117998		15.9	0.07	3.87	<0.01	2.99	1.61	1.92	0.04	5.27	0.11	62.27	0.03	0.42	4.54	99.02	0.77	0.28
FIEXD117999		15.82	0.07	4.42	<0.01	3.45	1.46	1.58	0.03	5.52	0.12	62.23	0.06	0.46	2.13	97.35	0.25	0.79
FIEXD118000		16.56	0.12	3.91	<0.01	3.8	1.64	1.95	0.06	4.66	0.1	65.99	0.11	0.45	1.87	101.22	0.03	0.01
FIEXD143571		14.3	0.06	3.46	<0.01	2.46	2.32	0.96	0.05	3.61	0.07	66.7	0.03	0.33	6.01	100.35	1.32	0.22
FIEXD143572		15.04	0.07	3.16	<0.01	2.44	2.66	1.3	0.1	3.41	0.09	64.82	0.04	0.38	6.49	100	1.38	0.19
FIEXD143573		15.65	0.09	0.21	<0.01	2.32	2.81	1.06	0.02	4.22	0.08	69.2	0.01	0.38	2.3	98.36	<0.01	<0.01
FIEXD143574		15.99	0.07	0.29	<0.01	1.15	2.03	0.47	0.03	6.18	0.09	70.73	0.01	0.39	1.59	99.02	0.02	<0.01

APPENDIX 2. Continue

	Ba_ppm	Ce_ppm	Cr_ppm	Cs_ppm	Dy_ppm	Er_ppm	Eu_ppm	Ga_ppm	Gd_ppm	Hf_ppm	Ho_ppm	La_ppm	Lu_ppm	Nb_ppm	Nd_ppm	Pr_ppm	Rb_ppm	Sm_ppm	Sn_ppm	Sr_ppm	Ta_ppm	Tb_ppm	Th_ppm	Tm_ppm	U_ppm	V_ppm	W_ppm	Y_ppm	Yb_ppm	Zr_ppm	As_ppm	Au_ppm	Bi_ppm	Hg_ppm	Sb_ppm	Se_ppm	Tl_ppm	Ag_ppm	Cd_ppm	Cu_ppm	Mo_ppm	Ni_ppm	Pb_ppm	Zn_ppm
FIEXD117951	2291.4	6.2	158	4.34	2.59	1.63	0.79	18.5	2.09	1.7	0.54	2.3	0.23	3	5.4	0.99	98.3	1.78	6	153.9	0.6	0.39	1.65	0.2	0.12	313	<1	13.4	1.51	31	44.9	0.0042	0.03	0.426	34.19	0.3	0.1	0.51	0.18	91.3	0.56	67	3.7	39
FIEXD117952	725.2	26.6	14	3.93	0.74	0.39	0.56	18.9	1.43	2.9	0.14	14.8	0.06	5.2	10.4	2.82	62.2	1.69	<5	238.1	0.7	0.17	2.96	0.02	2.28	33	<1	3.7	0.28	74	3.5	0.0011	0.01	0.053	1.45	<0.2	0.06	0.04	0.02	1.1	0.65	6	5.2	22
FIEXD117953	546.8	9.5	50	2.99	4.27	2.74	1.06	16.3	3.35	2.3	0.91	3.6	0.41	3.7	7.7	1.47	72	2.54	<5	114.4	0.7	0.64	1.75	0.37	0.34	318	<1	24.3	2.63	57	27.1	0.0023	0.01	0.185	28.24	0.3	0.1	0.18	0.11	78.7	0.42	52.2	0.7	63
FIEXD117954	759.8	36.2	27	0.76	1.06	0.57	0.71	20.9	1.95	3	0.2	20.3	0.07	5.3	13.4	3.71	33.1	2.12	<5	107.2	0.7	0.24	3.24	0.03	2.21	39	<1	5.7	0.41	99	10.6	0.0025	0.01	0.085	0.52	<0.2	0.03	0.03	0.07	0.9	0.36	8.7	2	18
FIEXD117955	304.6	24.2	33	0.87	2.15	1.1	1.17	18.7	2.77	2.1	0.41	19.5	0.13	4	13.1	3.5	28	2.53	<5	72.1	0.7	0.4	2.79	0.13	1.32	48	<1	14.1	0.82	64	2.4	0.0011	0.01	1.938	1.05	<0.2	0.05	0.07	0.17	40	0.75	16.7	1.8	4
FIEXD117956	395	21.3	82	1.44	5.12	3.04	1.54	18.9	4.4	3.5	1.03	9	0.39	7.7	14.1	2.98	148.9	3.87	5	271.4	0.7	0.76	1.78	0.39	1.04	350	16	27.4	2.52	98	>10000	0.167	0.62	0.013	36.19	<0.2	0.1	1.51	0.19	57.4	2.05	58.6	9.1	27
FIEXD117957	751.3	30.7	11	0.96	0.81	0.49	0.64	18.9	1.54	3	0.16	17	0.07	5	11.5	3.2	59.5	1.88	<5	364.2	0.7	0.18	3.21	0.03	2.17	33	11	4.5	0.41	99	121.8	0.0133	0.2	0.014	40.93	<0.2	0.09	0.51	0.04	33.1	0.7	6.7	10.5	7
FIEXD117958	480.9	21.3	19	1.15	0.78	0.44	0.49	18.6	1.31	2.8	0.15	11.1	0.05	4.2	8.5	2.28	75	1.42	<5	200.2	0.7	0.17	3	0.02	1.93	34	2	4.6	0.33	96	861.7	0.0469	0.06	0.07	2.82	<0.2	0.06	0.13	0.02	11.5	0.42	9.4	2.4	6
FIEXD117959	439.2	28.1	18	0.43	0.78	0.43	0.61	20.7	1.5	2.9	0.14	15.7	0.05	4.4	10.6	2.88	25.1	1.69	<5	479.9	0.6	0.18	3.08	0.02	1.6	33	6	3.9	0.31	92	5.8	0.0027	0.04	0.051	5.15	<0.2	0.03	0.13	0.04	57.7	2.82	9.8	3.9	28
FIEXD117960	737.9	28.5	15	3.98	0.7	0.41	0.6	20.4	1.48	2.8	0.14	15.6	0.05	4.9	10.7	3	68	1.7	<5	257.9	0.7	0.17	3.07	<0.01	2.26	32	5	4	0.32	87	77.6	0.0064	0.12	0.04	8.01	<0.2	0.05	0.12	0.02	29.5	1.37	7.1	2	8
FIEXD117961	554.6	21.5	17	0.86	0.96	0.54	1.07	16.9	1.43	2.2	0.18	11.8	0.06	3.8	8.7	2.35	90.8	1.61	<5	94.6	0.6	0.2	3.1	0.03	1.47	29	904	5.1	0.45	67	3963.5	0.3524	0.85	0.06	53.41	<0.2	0.06	0.22	0.06	331	4.18	11.2	2	11
FIEXD117962	398	25.7	18	0.79	0.69	0.39	0.58	18.2	1.35	2.4	0.14	14.1	0.05	4.1	9.8	2.69	61.4	1.55	<5	214.7	0.7	0.18	2.79	0.02	1.78	30	2	3.8	0.3	77	438.7	0.0281	0.25	0.087	19.34	<0.2	0.04	0.13	0.02	83.2	1.09	6.2	2.6	7
FIEXD117963	403.4	30.2	20	1.28	0.8	0.47	0.59	18.1	1.49	2.5	0.15	16.8	0.06	4.3	10.8	3.03	81.3	1.63	<5	305.8	0.7	0.19	2.31	0.03	1.98	36	4	4.6	0.36	74	282.1	0.0696	0.25	0.065	64.68	<0.2	0.07	4.43	0.1	158.4	0.75	9.9	2.6	15
FIEXD117964	426.7	27.1	15	1.01	0.76	0.4	0.56	19	1.45	2.3	0.15	14.7	0.05	4.3	10.1	2.81	80.2	1.62	<5	324.9	0.7	0.18	3.17	0.01	2	33	4	4	0.29	75	805.5	0.0192	0.33	0.017	39.34	<0.2	0.06	0.68	0.05	84.4	0.73	8.6	2.6	10
FIEXD117965	422	24.5	13	0.89	0.7	0.38	0.61	18.3	1.33	2.3	0.14	14.1	0.05	3.6	9.1	2.49	47.3	1.42	<5	358.7	0.6	0.17	2.78	0.01	1.85	33	2	4.1	0.29	69	702.4	0.0582	0.46	0.02	7.15	<0.2	0.07	0.4	<0.02	270	2.36	12.1	5.1	8
FIEXD117966	646.3	31	11	1.14	0.9	0.48	0.68	19	1.64	2.3	0.17	17	0.07	4.6	11.6	3.23	58.1	1.83	<5	337.8	0.7	0.21	3.46	0.02	2.1	30	2	5	0.38	82	209.3	0.0492	0.07	0.019	2.63	<0.2	0.05	0.06	<0.02	7.4	0.47	6.6	2.4	6
FIEXD117967	375.8	23.9	18	0.66	0.53	0.32	0.4	19.9	1.15	2.4	0.11	13.2	0.05	4.8	8.9	2.44	65.8	1.3	<5	250.9	0.7	0.12	2.27	<0.01	0.93	30	6	3	0.24	60	1454.9	0.0395	0.05	0.038	51.18	<0.2	0.07	0.76	0.08	40	0.82	9.4	4.3	14
FIEXD117968	670.1	31.5	18	0.89	0.84	0.5	0.62	19.7	1.65	2.6	0.15	17.7	0.07	4.8	11.6	3.28	61.5	1.85	<5	341.4	0.7	0.21	2.58	0.03	2.27	32	3	4.8	0.4	80	54.9	0.0068	0.11	0.051	3.26	<0.2	0.05	0.08	<0.02	13.5	0.73	5.8	2.5	7
FIEXD117969	704.7	28.6	12	2.29	0.58	0.37	0.44	20.9	1.35	2.7	0.12	15.9	0.05	5.3	10.8	3.04	62.9	1.75	<5	242.4	0.7	0.15	3.21	0.04	2.37	32	3	3.3	0.33	90	422.5	0.0642	0.06	0.033	3.32	<0.2	0.06	0.22	0.06	10.2	0.48	6.5	4.2	12
FIEXD117970	553.5	43.9	10	2.56	0.98	0.71	0.56	16.4	1.59	2.8	0.22	25.6	0.13	9.2	13.3	4.2	61.5	1.74	<5	193.4	0.9	0.21	5.73	0.07	4.04	23	1	6.7	0.71	85	3	0.0022	0.02	0.022	2.37	<0.2	0.06	0.07	<0.02	2.6	0.48	1.1	4.6	14
FIEXD117971	1099.5	35.2	25	1.18	0.78	0.44	0.77	17.5	1.7	2.4	0.14	20.3	0.06	6.1	12.1	3.46	81.9	1.95	<5	71.3	0.7	0.2	6.23	0.02	3.7	32	2	4.2	0.31	87	14.7	0.0018	0.02	0.031	0.42	<0.2	0.06	0.06	0.04	2.6	0.99	7.8	3.1	17
FIEXD117972	865.9	36.4	22	0.94	1.13	0.54	0.72	15.8	1.88	2.5	0.19	21.4	0.06	6	12.5	3.62	60	2	<5	134.7	0.7	0.23	6.66	0.02	3.53	26	1	5.4	0.35	83	151.3	0.002	<0.01	0.022	0.36	<0.2	0.06	0.04	0.03	1.4	0.3	8.3	3.1	19
FIEXD117973	881.8	45.3	19	3.07	2	1.23	0.97	17.7	2.54	2.8	0.41	25	0.17	9.5	17	4.74	53.6	2.9	<5	173.8	0.8	0.37	6.07	0.14	3.09	87	<1	11	1.07	98	6.6	0.006	0.03	0.073	3.38	<0.2	0.05	0.08	0.09	3.8	1.06	2.7	5.5	20
FIEXD117974	232.6	40.2	32	0.58	4.01	1.76	1.52	22.6	4.33	2.1	0.69	22.4	0.21	4.4	16.9	4.42	23.2	4.26	<5	98.1	0.8	0.74	4.32	0.22	1.27	39	5	16.9	1.53	73	7.7	0.0047	<0.01	0.066	1.19	<0.2	<0.02	0.03	0.08	0.5	0.35	14.3	5.3	8
FIEXD117975	927.8	30.7	27	2.57	1.65	0.99	0.83	19.3	2.22	2.6	0.32	16.3	0.13	5.5	12.6	3.28	69.5	2.35	<5	135.5	0.8	0.31	3.39	0.1	1.62	86	2	9.6	0.81	91	17.1	0.0031	0.04	0.066	1.12	<0.2	0.04	0.05	0.1	1.6	0.64	7.8	4.4	18
FIEXD117976	743.8	50.4	17	2.81	1.92	1.22	0.91	16.4	2.71	2.8	0.4	28.3	0.18	9.2	18.6	5.23	65.3	2.92	<5	130.4	0.9	0.37	5.26	0.14	2.91	91	12	11.1	1.11	89	7148.3	0.7241	0.27	0.226	8.06	<0.2	0.05	0.36	0.09	9.9	0.87	2.9	3.8	16
FIEXD117977	929.7	45.4	20	2.77	2	1.24	1.02	18.3	2.8	3	0.41	24.9	0.18	10.4	17.8	4.83	74.1	3	<5	114.7	0.9	0.38	5.84	0.14	3.18	78	8	11.4	1.12	104	35	0.0106	0.02	0.476	1.06	<0.2	0.05	0.1	0.07	2.9	0.46	2.2	4.4	17
FIEXD117978	402.7	42.7	<10	1.91	0.83	0.52	0.69	16.6	1.69	2.1	0.17	24.6	0.09	8.5	13.9	4.15	47.8	1.98	<5	87.4	0.8	0.2	5.85	0.04	3.35	11	2	5	0.52	61	28.3	0.2601	0.05	0.053	1.35	<0.2	0.04	0.11	0.04	1.7	1.77	7.9	6.2	5
FIEXD117979	461.1	44.4	<10	1.98	0.86	0.53	0.62	18.5	1.62	2.4	0.16	25.6	0.09	9.8	13.9	4.27	46.3	1.85	<5	106.6	0.9	0.19	6.4	0.03	3.47	<10	<1	5.5	0.5	69	13.9	0.0225	0.04	0.673	0.93	<0.2	0.04	0.11	0.07	1.4	1.86	2.8	4.5	8
FIEXD117980	1444.5	51.2	15	2.8	2.12	1.15	1.05	18.7	2.89	3.1	0.4	28.3	0.17	8.6	20.3	5.47	70.1	3.48	<5	144	0.8	0.37	6.59	0.16	3.24	62	<1	11.2	1.05	111	7.8	0.0018	0.03	0.052	1.49	<0.2	0.07	0.13	0.35	12.8	1.38	3.9	13.7	80
FIEXD117981	1212.7	57.3	29	1.68	1.35	0.69	0.86	17.4	2.57	3	0.23	33	0.08	10.1	19.3	5.6	68.6	2.95	<5	162.6	0.8	0.3	7.54	0.05	4.24	40	<1	6.7	0.54	113	60.3	0.0157	0.06	0.098	7.92	<0.2	0.07	0.17	0.07	13.4	1.24	12.5	3.7	15
FIEXD117982	1524.9	56.2	25	1.98	2.52	1.55	1.13	17.8	3.14	3.1	0.5	31.3	0.23	10.3	20.7	5.73	62.9	3.52	<5	265.5	0.9	0.45	7.5	0.19	3.35	119	1	14.1	1.28	109	4.9	0.002	0.01	0.09	3.77	<0.2	0.05	0.06	0.16	5.6	1.19	5.9	6.2	46
FIEXD117983	1370.8	54.5	21	2.45	2.22	1.31	1.11	19	2.86	2.8	0.46	30.7	0.19	10.5	20	5.65	59.8	3.33	<5	323.4	0.9	0.42	7.2	0.16	3.29	110	<1	13.4	1.26	113	5.3	0.0012	0.01	0.029	3.2	<0.2	0.06	0.05	0.2	5.9	1.24	2.9	7.1	43
FIEXD117984	1779.8	48	22	2.86	1.97	1.18	1.1	18.5	2.86	3	0.39	26.1	0.17	8.1	19.1	5.19	72.6	3.35	<5	156.9	0.9	0.41	5.53	0.18	3.03	77	<1	11.3	1.04	103	9.1	0.0027	0.02	0.072	1.79	<0.2	0.12	0.11	0.37	13.2	1.94	5.8	10.7	77
FIEXD117985	406.6	43.8	15	1.85	0.71	0.36	0.67	20.1	1.66	3.1	0.13	25.9	0.04	3.4	14.5	4.49	62.9	2.17	<5	120.1	0.7	0.17	2.46	0.06	3.74	25	<1	3.4	0.23	75	11.1	0.0032	0.02	0.021	1.36	<0.2	0.08	0.26	0.02	10.8	11.09	2.8	6.2	9
FIEXD117986	261.5	42.8	12	1.56	0.79	0.46	0.49	19.1	1.62	2.5	0.16	23.8	0.06	4.5	14.6	4.62	69.9	2.22	<5	87.9	0.9	0.17	2.82	0.07	5.8	18	<1	4.3	0.39	58	231.7	0.0657	0.29	0.03	1.69	<0.2	0.07	0.4	<0.02	5.4	2.28	2.4	7.4	9
FIEXD117987	245.6	44.4	10	1.33	0.88	0.44	0.53	19	1.78	2.6	0.16	24.1	0.06	4.5	15.4	4.78	70.1	2.44	<5	118.2	0.8	0.18	3.52	0.07	5.58	19	<1	4.6	0.37	62	401.1	0.0482	0.12	0.031	1.56	<0.2	0.05	0.14	0.05	2	0.47	2.5	10.9	13
FIEXD117988	571.6	48.7	40	2.14	1.43	0.75	0.91	17.4	2.25	2.9	0.27	27.6	0.09	5	17.2	5.12	63.6	2.89	<5	152.4	0.8	0.26	3.42	0.11	3.4	49	<1	7.2	0.58	83	7.7	0.0013	0.05	0.193	1.78	<0.2	0.06	0.06	0.08	20	0.99	12.1	5.1	24
FIEXD117989	406.5	34.5	26	1.67	0.99	0.47	0.63	17.2	1.71	2.4	0.18	19.8	0.06	3.5	12.2	3.7	53.1	2.01	<5	102.7	0.6	0.19	2.99	0.06	3.54	29	<1	4.8	0.35	75	58.7	0.0013	0.02	0.067	2.55	<0.2	0.07	0.09	0.04	3	0.41	8.1	2.7	10
FIEXD117990	390.1	33.8	26	0.77	0.91	0.46	0.63	17.2	1.64	2.6	0.17	20	0.05	3.7	11.6	3.51	49.8	2.1	<5	147.6	0.8	0.19	3.03	0.07	3.54	30	<1	4.6	0.35	77	75.6	0.0011	0.02	0.01	0.97	<0.2	0.05	0.08	0.04	4.4	0.47	7	4.2	10
FIEXD117991	884.4	35.9	95	1.86	3.83	2.22	1.56	16.2	4.45	3	0.78	17.1	0.3	7	19.8	4.74	72.2	4.82	<5	173.5	0.8	0.63	2.2	0.31	1.47	268	1	20	1.92	76	6.2	0.0012	0.02	0.107	2.81	<0.2	0.04	0.07	0.18	2.5	0.48	14.3	3.7	23
FIEXD117992	1297.1	73.3	34	3.88	2.21	1.1	1.32	17.8	3.46	4	0.39	41.2	0.13	9.2	26.3	7.85	92.7	4.49	<5	85	0.9	0.42	4.49	0.16	4.76	51	1	10.4	0.79	132	12.5	0.0015	0.02	0.084	6.74	<0.2	0.07	0.18	0.12	8	0.69	15.4	6.5	26
FIEXD117993	695.3	34.6	25	0.79	1.15	0.52	0.83	17.2	1.93	2.6	0.21	20.3	0.05	3.2	12.5	3.85	60.3	2.32	<5	97	0.7	0.23	3.28	0.07	3.41	28	<1	5.6	0.38	79	545.9	0.0091	0.02	0.072	1.72	<0.2	0.06	0.06	0.03	2.3	0.53	7.8	3.3	17
FIEXD117994	732.1	41.3	49	0.41	1.94	1.16	0.9	20.9	2.53	3	0.39	22.5	0.16	4.3	16.8	4.77	33.2	3.06	<5	816.7	0.8	0.33	1.86	0.18	2.64	66	<1	10.3	0.97	83	5.6	0.0039	0.05	0.012	0.29	<0.2	0.04	0.06	0.07	13.2	1.66	16.4	9	35
FIEXD117995	571.9	35.9	64	0.55	1.89	1.11	0.92	20.1	2.39	3.2	0.38	17.8	0.16	3.8	15.9	4.42	29.4	2.88	<5	675.5	0.7	0.33	1.93	0.16	2.67	72	<1	10.3	0.99	94	8	0.0028	0.13	0.015	0.42	0.2	0.05	0.1	0.07	45.2	1.45	21	7.1	36
FIEXD117996	200.3	36.8	48	0.27	1.83	1.1	0.94	20.6	2.4	3.2	0.37	19.4	0.15	4	15.9	4.4	11.9	2.82	<5	771.5	0.7	0.32	1.87	0.18	2.67	65	<1	10.2	0.98	94	8.8	0.0021	0.13	0.035	0.62	0.4	0.03	0.12	0.18	61.8	0.63	19	6.9	54
FIEXD117997	860.5	33	37	0.39	1.93	1.1	0.87	20.9	2.36	3	0.38	17.6	0.16	3.8	14.3	3.96	30.7	2.79	<5	488.6	0.8	0.32	1.88	0.18	2.39	64	<1	9.9	1	89	12.1	0.0044	0.08	0.076	0.35	<0.2	0.04	0.12	0.13	39.5	0.43	12.7	7.7	46
FIEXD117998	583.5	32.4	32	0.75	1.85	1.12	0.69	20.3	2.29	2.9	0.38	16.7	0.17	3.4	14.2	3.87	35.8	2.66	<5	257.9	0.8	0.31	1.87	0.17	2.39	64	<1	10.3	0.96	88	15.8	0.0054	0.13	0.025	0.2	<0.2	0.03	0.08	0.03	36.4	0.71	9.4	3.3	27
FIEXD117999	643.7	41.2	22	0.37	2.31	1.38	1	19.9	2.78	3	0.49	21.7	0.19	3.8	17.6	4.91	38.9	3.32	<5	486	0.7	0.4	1.79	0.19	2.46	63	<1	12.3	1.16	89	8.4	0.002	0.22	0.021	0.29	0.4	0.04	0.08	0.09	2.1	1.17	8.7	9.8	21
FIEXD118000	1028.8	32.2	31	0.9	1.88	1.14	0.9	21.7	2.33	3.3	0.39	16.7	0.16	4.3	14.6	3.91	37.3	2.88	<5	906.2	0.8	0.34	1.38	0.18	2.95	62	<1	10	0.96	83	5.1	0.0021	0.02	0.023	0.5	<0.2	0.05	0.06	0.14	15.8	1.42	12	7.9	49
FIEXD143571	492.2	28.2	13	1.39	0.99	0.5	0.5	21.4	1.52	2.5	0.18	15.3	0.06	2.8	11.3	3.21	70	2.11	<5	241.3	0.7	0.2	1.6	0.07	2.46	33	<1	4.8	0.38	63	98.2	0.0221	1.5	0.213	88.25	<0.2	0.05	2.06	1.38	137.4	0.48	5.6	2.9	245
FIEXD143572	611.6	34.8	36	2.02	1	0.45	0.64	21.7	1.71	3	0.17	19.1	0.05	3.1	13.7	3.97	72.3	2.32	<5	270.9	0.8	0.21	1.57	0.08	2.35	37	1	4.5	0.34	80	52.8	0.0537	0.05	0.034	4.38	<0.2	0.06	0.09	0.06	3.5	0.21	19.8	6.9	8
FIEXD143573	793.9	37.4	27	1.04	1.12	0.61	0.73	23	1.99	2.9	0.21	20.7	0.07	2.6	14.8	4.31	43.8	2.56	<5	96.9	0.8	0.23	1.79	0.09	2.12	40	<1	5.4	0.42	69	1.3	0.0012	0.01	0.074	0.67	<0.2	0.03	0.04	0.03	1.4	0.31	7.5	2.2	18
FIEXD143574	659.4	9	31	0.66	0.88	0.48	0.48	23.1	1.01	2.6	0.18	4.3	0.06	2.4	4.5	1.16	30.2	1.1	<5	85.7	0.7	0.14	1.94	0.08	1.95	73	1	4.4	0.43	67	0.2	0.0014	0.01	1.117	0.61	<0.2	0.02	0.04	0.05	0.3	0.3	4.7	1.9	7

APPENDIX 3. Detection limits of whole-rock major- and trace element analyses

Assayed element or oxide	Lower detection limit	Unit of measure
Al2O3	0.01	%
BaO	0.01	%
CaO	0.01	%
Cr2O3	0.01	%
Fe2O3	0.01	%
K2O	0.01	%
MgO	0.01	%
MnO	0.01	%
Na2O	0.01	%
P2O5	0.01	%
SiO2	0.01	%
TiO2	0.01	%
C	0.01	%
S	0.01	%
Ba	0.5	ppm
Ce	0.1	ppm
Cr	10	ppm
Cs	0.01	ppm
Dy	0.05	ppm
Er	0.03	ppm
Eu	0.03	ppm
Ga	0.2	ppm
Gd	0.05	ppm
Hf	0.2	ppm
Ho	0.01	ppm
La	0.1	ppm
Lu	0.01	ppm
Nb	0.1	ppm

Nd	0.1	ppm
Pr	0.03	ppm
Rb	0.2	ppm
Sm	0.03	ppm
Sn	5	ppm
Sr	0.1	ppm
Ta	0.1	ppm
Tb	0.01	ppm
Th	0.05	ppm
Tm	0.01	ppm
U	0.05	ppm
V	10	ppm
W	1	ppm
Y	0.5	ppm
Yb	0.03	ppm
Zr	2	ppm
As	0.01	ppm
Au	0.5	ppb
Bi	0.01	ppm
Hg	0.005	ppm
Sb	0.05	ppm
Se	0.2	ppm
Tl	0.02	ppm
Ag	0.01	ppm
Cd	0.02	ppm
Cu	0.2	ppm
Mo	0.05	ppm
Ni	0.2	ppm
Pb	0.5	ppm
Zn	2	ppm

APPENDIX 4. EPMA results

Thin section ID	Na2O	F	V2O3	Cr2O3	P2O5	K2O	MnO	MgO	CaO	Cl	Al2O3	FeO	BaO	SiO2	TiO2	Total
004-8	2.417	0.000	0.000	0.000	0.010	8.715	0.000	0.607	0.034	0.002	32.017	1.089	0.177	51.339	0.290	96.697
009-1	7.630	0.000	0.004	0.018	0.000	0.255	0.008	0.033	5.806	0.000	24.079	0.115	0.073	60.834	0.000	98.855
009-6	7.859	0.000	0.008	0.033	0.000	0.245	0.043	0.008	5.199	0.000	23.959	0.062	0.018	61.501	0.014	98.949
009-8	7.348	0.000	0.000	0.000	0.000	0.246	0.015	0.018	5.842	0.000	24.110	0.062	0.016	60.987	0.000	98.644
022-1	10.549	0.000	0.000	0.000	0.000	0.112	0.000	0.087	0.233	0.014	19.363	0.238	0.000	68.109	0.000	98.702
025-3	10.680	0.000	0.000	0.021	0.002	0.000	0.051	0.652	2.872	0.000	17.947	1.507	0.002	63.048	0.041	96.823
025-4	11.164	0.000	0.000	0.026	0.000	0.019	0.000	0.000	0.040	0.005	19.594	0.035	0.000	68.209	0.000	99.091
026-3	10.100	0.000	0.000	0.000	0.030	0.066	0.000	0.000	0.134	0.006	18.084	0.146	0.000	70.920	0.008	99.493

023-1	0.000	0.000	0.031	0.039	0.027	0.092	0.485	18.052	27.883	0.006	0.503	7.537	0.040	0.589	0.810	56.093
023-2	0.120	0.000	0.000	0.003	0.035	2.493	0.359	0.540	42.567	0.010	8.205	1.391	0.081	10.536	0.091	66.429
023-3	0.222	0.000	0.006	0.054	0.021	10.604	0.000	1.203	0.000	0.001	32.163	2.754	0.453	46.416	0.340	94.237
023-4	0.000	0.000	0.063	0.000	0.025	0.024	0.415	18.459	27.255	0.003	0.181	8.615	0.000	0.302	0.031	55.372
023-5	0.000	0.000	0.031	0.029	0.016	0.000	0.282	0.275	54.859	0.000	0.019	0.822	0.000	0.000	0.007	56.340
023-6	0.153	0.000	0.031	0.036	0.027	10.675	0.030	1.350	0.009	0.002	31.692	2.659	0.287	47.202	0.403	94.556
023-7	0.000	0.000	0.012	0.000	0.000	0.026	0.503	13.472	28.543	0.005	0.000	14.160	0.000	0.000	0.015	56.735
031-1	0.000	0.000	0.002	0.008	0.018	0.004	0.403	17.466	28.445	0.003	0.126	8.923	0.043	0.000	0.022	55.462
031-2	0.636	0.000	0.042	0.000	0.000	9.874	0.014	0.569	0.000	0.017	34.405	2.322	0.439	45.971	0.131	94.416
031-3	0.000	0.000	0.000	0.010	0.000	0.000	0.868	13.965	27.806	0.007	0.052	13.521	0.000	0.000	0.000	56.227
031-4	0.168	0.000	0.000	0.000	0.004	0.013	0.758	14.097	27.808	0.007	0.070	13.344	0.000	0.000	0.000	56.267
031-5	0.551	0.000	0.031	0.000	0.000	9.871	0.000	0.524	0.001	0.000	34.351	2.216	0.446	46.363	0.123	94.477
039-1	0.000	0.000	0.035	0.013	0.005	0.000	0.290	13.416	28.307	0.011	0.009	14.533	0.000	0.000	0.000	56.617
039-2	0.046	0.000	0.037	0.000	0.011	0.024	0.272	13.495	28.188	0.008	0.000	14.416	0.000	0.000	0.000	56.495
039-3	0.693	0.000	0.000	0.003	0.000	9.434	0.015	0.449	0.000	0.012	35.585	1.414	0.278	46.424	0.111	94.415
039-4	0.000	0.000	0.000	0.008	0.020	0.032	0.915	15.870	27.720	0.009	0.048	10.965	0.027	0.000	0.051	55.663
039-5	0.046	0.000	0.010	0.000	0.000	0.000	0.292	13.740	28.593	0.000	0.011	14.630	0.009	0.000	0.000	57.331
039-6	0.000	0.000	0.037	0.015	0.016	0.000	0.481	8.831	35.814	0.031	0.026	10.818	0.000	0.000	0.000	56.062
039-7	0.987	0.000	0.033	0.030	0.015	9.130	0.000	0.472	0.000	0.000	35.721	1.308	0.189	46.264	0.149	94.298
042-1	0.146	0.000	0.000	0.000	0.044	0.007	0.813	10.912	27.253	0.045	0.049	17.555	0.008	0.000	0.000	56.822
042-2	0.988	0.000	0.127	0.503	0.019	8.875	0.008	0.387	0.015	0.004	35.055	1.277	0.363	45.996	0.092	93.708
042-3	0.037	0.000	0.002	0.000	0.000	0.030	0.434	14.816	28.584	0.106	0.044	12.235	0.000	0.000	0.000	56.264
042-4	0.000	0.000	0.000	0.000	0.000	0.038	0.372	14.087	27.582	0.000	0.086	12.956	0.000	0.000	0.005	55.126
042-5	1.319	0.000	0.039	0.080	0.008	8.728	0.007	0.328	0.056	0.010	35.610	1.974	0.359	45.817	0.065	94.398
042-6	0.040	0.000	0.000	0.007	0.012	0.023	0.393	19.824	29.495	0.086	0.037	4.987	0.000	0.000	0.004	54.889
052-1	0.074	0.000	0.002	0.000	0.034	0.023	0.464	10.250	27.806	0.004	0.026	18.311	0.005	0.000	0.004	57.002
052-2	1.086	0.000	0.074	0.010	0.000	9.059	0.034	0.604	0.080	0.020	35.881	0.564	0.198	47.801	0.148	95.554
052-3	0.024	0.000	0.044	0.016	0.000	0.046	0.373	9.574	28.534	0.018	0.149	17.372	0.026	0.000	0.000	56.172
052-4	0.411	0.000	0.053	0.005	0.012	9.719	0.000	0.777	0.032	0.010	35.113	0.713	0.200	47.487	0.049	94.579
052-5	0.041	0.000	0.000	0.000	0.034	0.040	0.426	9.903	27.857	0.006	0.412	18.444	0.000	0.251	0.031	57.444
052-6	0.941	0.000	0.007	0.000	0.000	8.974	0.008	0.707	0.041	0.010	35.230	0.884	0.114	46.608	0.089	93.611
054-1	0.810	0.000	0.000	0.020	0.008	2.058	0.130	11.931	0.148	0.068	22.835	20.607	0.000	32.075	0.124	90.799
054-2	0.389	0.000	0.028	0.000	0.004	9.770	0.018	1.451	0.005	0.000	29.786	2.398	0.332	49.209	0.341	93.731
054-3	0.000	0.000	0.022	0.000	0.000	0.019	0.117	16.874	0.000	0.027	20.008	26.150	0.007	26.743	0.057	90.018
054-4	0.296	0.000	0.041	0.038	0.025	10.645	0.000	2.357	0.009	0.007	29.809	3.334	0.270	48.327	0.334	95.490
054-5	0.000	0.000	0.013	0.004	0.006	0.031	0.071	16.902	0.035	0.021	20.789	26.256	0.026	26.386	0.037	90.572
054-6	0.353	0.000	0.006	0.054	0.006	10.346	0.000	2.226	0.065	0.008	29.298	3.153	0.317	48.736	0.414	94.980
054-7	0.187	0.000	0.034	0.000	0.000	0.147	0.159	16.268	0.039	0.023	20.679	26.310	0.000	26.650	0.075	90.566
054-8	0.193	0.000	0.028	0.029	0.004	10.475	0.000	2.179	0.030	0.024	29.727	3.247	0.225	48.559	0.350	95.065
045-1	0.428	0.000	0.076	0.000	0.000	0.201	0.275	19.299	12.324	0.081	3.210	11.261	0.003	52.786	0.302	100.228
045-2	6.798	0.000	0.000	0.000	0.000	0.262	0.000	0.029	8.136	0.000	26.263	0.119	0.021	58.006	0.000	99.634
045-3	6.653	0.000	0.006	0.000	0.000	3.464	0.048	0.045	2.060	0.083	26.087	0.281	0.030	59.135	0.012	97.885
045-4	0.297	0.000	0.053	0.026	0.002	0.177	0.222	18.911	12.565	0.084	2.926	11.647	0.008	53.240	0.229	100.368
045-5	0.729	0.000	0.035	0.000	0.006	0.231	0.245	18.656	11.925	0.073	4.110	11.198	0.015	52.190	0.338	99.735
045-6	0.099	0.000	0.055	0.007	0.000	0.000	0.320	18.547	0.000	0.011	19.874	25.223	0.000	26.728	0.034	90.896
045-7	0.152	0.000	0.000	0.000	0.000	15.942	0.036	0.000	0.031	0.022	18.347	0.075	0.689	63.849	0.017	99.155
045-8	0.040	0.000	0.085	0.008	0.000	0.000	0.034	0.064	22.977	0.005	23.105	12.435	0.025	37.831	0.052	96.660
045-9	0.423	0.000	0.075	0.054	0.014	0.081	0.123	18.064	12.116	0.034	2.804	12.893	0.000	52.988	0.139	99.800
045-10	0.086	0.000	0.173	0.005	0.012	0.001	0.097	0.025	23.021	0.002	23.304	11.691	0.000	37.516	0.028	95.961
045-11	0.075	0.000	0.033	0.005	0.018	0.000	0.037	0.024	24.090	0.011	27.418	7.096	0.035	38.442	0.014	97.296
045-12	0.650	0.000	0.035	0.077	0.006	0.196	0.336	19.416	12.305	0.069	3.309	11.662	0.004	52.372	0.286	100.707
046-1	0.043	0.000	0.000	0.023	0.000	0.027	0.063	0.062	23.786	0.016	28.655	5.172	0.008	38.603	0.009	96.463
046-2	0.238	0.000	0.019	0.102	0.002	0.058	0.074	21.614	12.030	0.025	2.504	8.951	0.000	54.122	0.101	99.834
046-3	0.000	0.000	0.000	0.013	0.000	0.020	0.047	0.000	0.028	0.000	0.003	0.009	0.000	99.410	0.000	99.530
046-4	0.000	0.000	0.022	0.015	0.292	0.013	0.249	0.058	23.604	0.000	29.795	4.000	0.006	38.844	0.000	96.898
046-5	0.325	0.000	0.046	0.048	0.000	0.136	0.145	19.393	12.773	0.052	2.205	10.532	0.004	53.677	0.184	99.508
046-6	0.031	0.000	0.116	0.013	0.008	0.025	0.059	0.030	24.240	0.000	28.109	6.289	0.000	38.816	0.086	97.822
046-7	0.000	0.000	0.000	0.017	0.000	0.224	0.164	0.086	55.923	0.010	0.296	0.075	0.000	0.267	0.023	57.083
046-8	0.284	0.000	0.021	0.008	0.018	0.099	0.219	19.712	12.731	0.047	2.482	11.417	0.000	54.625	0.122	101.774
049-1	0.000	0.000	0.048	0.026	0.000	0.018	0.255	20.701	0.000	0.015	21.811	21.982	0.006	26.747	0.000	91.606
049-2	0.050	0.000	0.006	0.000	0.011	0.019	0.015	0.000	0.009	0.000	0.022	0.035	0.000	99.567	0.011	99.745
049-3	0.000	0.000	0.013	0.000	0.002	0.154	0.165	17.357	8.995	0.028	18.028	17.548	0.003	22.768	0.032	85.087
049-4	0.167	0.000	0.006	0.033	0.017	11.081	0.000	2.360	0.034	0.007	31.593	1.456	0.258	48.499	0.062	95.571
049-5	0.068	0.000	0.015	0.032	0.018	0.001	0.236	19.966	0.334	0.032	22.015	21.626	0.013	25.935	0.028	90.312
049-6	0.000	0.000	0.052	0.020	0.000	0.009	0.140	22.118	0.050	0.043	19.510	20.479	0.000	27.835	0.059	90.305
049-7	0.035	0.000	0.000	0.000	0.054	0.016	0.233	0.486	54.592	0.001	0.370	0.632	0.000	0.037	0.006	56.462
049-8	0.014	0.000	0.011	0.005	0.006	0.000	0.205	21.932	0.238	0.010	19.633	21.134	0.000	27.617	0.088	90.891
049-9	0.066	0.000	0.000	0.012	0.000	0.003	0.000	0.000	0.000	0.000	0.002	0.004	0.015	98.901	0.021	99.024
049-10	0.000	0.000	0.033	0.012	0.002	0.012	0.207	21.589	0.170	0.008	19.377	20.299	0.028	27.479	0.062	89.276

APPENDIX 5. EPMA standards

	Element	X-ray	Crystal	CH	Acc.v.	Peak	Pos.	BG_L	BG_U
1	Na	Ka	TAP	1	15.0	129.515	1.19101	5.000	5.000
2	F	Ka	LDE1	3	15.0	83.581	1.83200	6.500	4.500
3	V	Ka	LIFH	4	15.0	174.379	0.25036	5.000	5.000
4	Cr	Ka	LIFH	4	15.0	159.539	0.22897	5.000	5.000
5	P	Ka	PETH	5	15.0	197.121	0.61570	5.000	5.000
6	K	Ka	PETJ	2	15.0	119.800	0.37414	5.000	5.000
7	Mn	Ka	LIFH	4	15.0	146.488	0.21018	5.000	5.000
8	Mg	Ka	TAP	1	15.0	107.269	0.98900	5.000	5.000
9	Ca	Ka	PETJ	2	15.0	107.536	0.33584	5.000	4.500
10	Cl	Ka	PETH	5	15.0	151.437	0.47278	5.000	5.000
11	Al	Ka	TAP	1	15.0	90.346	0.83393	5.800	5.800
12	Fe	Ka	LIF	2	15.0	134.657	0.19360	4.000	4.000
13	Ba	La	PETH	5	15.0	88.974	0.27759	2.128	5.000
14	Si	Ka	TAP	1	15.0	77.078	0.71254	5.000	5.000
15	Ti	Ka	PETH	5	15.0	88.110	0.27485	1.300	4.000